

Regulation of Cartilage Tumors by Mutations in Isocitrate Dehydrogenases

by

Hongyuan Zhang

Department of Cell Biology
Duke University

Date: _____

Approved:

Benjamin A. Alman, Supervisor

Eda Yildirim

Courtney M. Karner

Donald P. McDonnell

Dissertation submitted in partial fulfillment of
the requirements for the degree of Doctor
of Philosophy in the Department of
Cell Biology in the Graduate School
of Duke University

2021

ABSTRACT

Metabolic Regulation of Cartilage Tumors

by

Hongyuan Zhang

Department of Cell Biology
Duke University

Date: _____

Approved:

Benjamin A. Alman, Supervisor

Eda Yildirim

Courtney M. Karner

Donald P. McDonnell

An abstract of a dissertation submitted in partial
fulfillment of the requirements for the degree
of Doctor of Philosophy in the Department of
Cell Biology in the Graduate School of
Duke University

2021

Copyright by
Hongyuan Zhang
2021

Abstract

Enchondroma and chondrosarcoma are common benign and malignant cartilaginous neoplasms. Mutations in isocitrate dehydrogenase 1 and 2 (*IDH1/2*) are present in the majority of these tumors. Mutant IDH enzymes gain a neomorphic function of producing D-2-hydroxyglutarate (D-2HG) from α -ketoglutarate. Expression of a mutant *Idh1* gene is sufficient for enchondroma initiation but inhibiting mutant IDH enzymes did not cause a consistent change in the tumorigenic properties of chondrosarcomas. It is unclear how mutations of isocitrate dehydrogenases regulate cartilage tumors from initiation to cancer progression and maintenance. I hypothesize that mutations in IDH enzymes could regulate cartilage tumors through changes in gene expression and cellular metabolism. To address these questions, I examined the transcriptional regulation and metabolic regulations of mutant isocitrate dehydrogenases in chondrocytes and chondrosarcomas and identified cholesterol biosynthesis and glutamine metabolism as two key pathways dictating tumor behavior.

To understand the transcriptional regulation of *IDH1* mutation in cartilage tumors, I performed RNA-sequencing analysis in chondrocytes from *Col2a1Cre;Idh1^{LSL+}* mutant animals and their littermate wildtype controls and identified that cholesterol biosynthesis pathway was upregulated. Genetic inhibition of cholesterol biosynthesis in an enchondroma mouse model and pharmacological inhibition of cholesterol

biosynthesis in human patient chondrosarcoma samples suppressed tumor development in vivo. Taken together, these data suggest that intracellular cholesterol synthesis is a potential therapeutic target for enchondromas and chondrosarcomas.

From a metabolic perspective, I found that chondrocytes and chondrosarcomas with mutations in *IDH1/2* genes had enhanced glutamine utilization for downstream metabolism. Using genetic and pharmacological approaches, I demonstrated that glutaminase-mediated glutamine metabolism played distinct roles in enchondromas and chondrosarcomas with *IDH1/2* mutations. Genetic ablation of glutaminase in chondrocytes with *Idh1* mutation increased the number and size of enchondroma-like lesions. Pharmacological inhibition of glutaminase led to decreased tumor weight of chondrosarcoma xenograft. During enchondroma development, glutamine-derived α -ketoglutarate plays important roles in regulating chondrocyte differentiation and proliferation. In chondrosarcoma, glutamine-derived non-essential amino acids are important in preventing cell apoptosis.

In summary, findings in this dissertation described transcriptional and metabolic regulations by mutations in isocitrate dehydrogenases in cartilage tumors enchondroma and chondrosarcoma and provide novel insights for developing therapies for these diseases.

Contents

Abstract	iv
List of Tables.....	x
List of Figures.....	xi
Acknowledgements.....	xiv
1. Introduction and Background.....	1
1.1 Introduction	2
1.2 Chondrocyte Differentiation in Growth Plate.....	3
1.2.1 The Process of Endochondral Ossification.....	3
1.2.2 Signaling Pathways Governing Chondrocyte Differentiation	7
1.2.2.1 Hedgehog Signaling Pathway	8
1.2.2.2 HIF Signaling Pathway	9
1.2.3 Metabolic Regulation of Chondrocyte Differentiation	12
1.2.3.1 Cholesterol Biosynthesis.....	12
1.2.3.2 Glutamine Metabolism	18
1.3 Enchondromas and Chondrosarcomas.....	26
1.3.1 Overview of Enchondromas and Chondrosarcomas.....	26
1.3.2 <i>IDH1/2</i> Mutations in Enchondromas and Chondrosarcomas	27
1.3.2.1 Normal Function of IDH enzymes.....	28
1.3.2.2 Mutations in <i>IDH1/2</i>	30
1.3.2.3 D-2HG as an “Oncometabolite”	31

1.3.3 Other Signaling Pathways and Mutations Implied in Enchondroma and Chondrosarcoma	33
1.3.3.1 Hedgehog Signaling	33
1.3.3.2 MAPK/ERK pathway	34
1.3.3.3 Retinoblastoma Protein (pRb) Pathway	35
1.3.3.4 FGF signaling pathway	36
1.3.3.5 PTEN-PI3K pathway	36
1.3.3.6 Other Mutations in Enchondroma	37
1.3.4 Progression from Enchondromas to Chondrosarcomas	38
2. Intracellular Cholesterol Biosynthesis in Enchondroma and Chondrosarcoma	40
2.1 Summary	41
2.2 Introduction	41
2.3 Results	44
2.3.1 <i>Col2a1Cre;Idh1^{LSL/+}</i> chondrocytes exhibited distinct gene expression profiles...44	
2.3.2 <i>Col2a1Cre;Idh1^{LSL/+}</i> chondrocytes had increased intracellular cholesterol levels, which was likely due to increased cholesterol biosynthesis.....46	
2.3.3 Deleting <i>Scap</i> postnatally did not alter growth plate phenotype.....48	
2.3.4 Deleting <i>Scap</i> reduced enchondroma-like lesion formation in <i>Col2a1Cre;Idh1^{LSL/+}</i> animals.....50	
2.3.5 Pharmacological inhibition of cholesterol synthesis reduced chondrosarcoma growth in vitro and in vivo.....52	
2.4 Discussion.....57	
3. Glutamine Metabolism in Enchondroma and Chondrosarcoma	61

3.1 Summary	61
3.2 Introduction	62
3.3 Results.....	65
3.3.1 Glutaminase is upregulated in IDH1/2 ^{Mut} human patient chondrosarcomas and IDH1 ^{Mut} murine chondrocytes.....	65
3.3.2 Chondrocytes and chondrosarcomas with mutations of IDH1/2 enzymes exhibited increased glutamine contribution to anaplerosis and non-essential amino acids production.....	67
3.3.2.1 IDH1 ^{Mut} murine chondrocytes had increased glutamine contribution to anaplerosis and non-essential amino acids production.....	67
3.3.2.2 IDH1/2 ^{Mut} human patient chondrosarcoma cells had increased glutamine contribution to anaplerosis and non-essential amino acids production	70
3.3.3 Glutamine is the primary source for D-2-hydroxyglutarate production in IDH1 ^{Mut} murine chondrocytes.....	72
3.3.4 <i>Gls</i> is the primary isoform of glutaminase in chondrocytes.....	74
3.3.4.1 <i>Gls</i> is the primary isoform of glutaminase expressed by chondrocytes.....	74
3.3.4.2 Conditional deletion of <i>Gls</i> in chondrocytes significantly reduced glutaminase activity.....	75
3.3.5 Deleting <i>Gls</i> in <i>Col2a1Cre;Idh1^{LSL/+}</i> chondrocytes affected chondrocyte differentiation	76
3.3.6 Deleting <i>Gls</i> in <i>Col2a1Cre;Idh1^{LSL/+}</i> chondrocytes increased cell proliferation and did not induce cell apoptosis.....	80
3.3.7 Deleting <i>Gls</i> in <i>Col2a1Cre^{ERT2};Idh1^{LSL/+}</i> chondrocytes increased the number and size of enchondroma-like lesions.....	81
3.3.8 Glutaminase regulated the differentiation of chondrocytes with <i>Idh1</i> mutation through downstream metabolite α -ketoglutarate	84
3.3.8.1 α -ketoglutarate level was lower in IDH1 ^{Mut} chondrocytes.....	84

3.3.8.2 GLS inhibition reduced α -ketoglutarate levels in IDH1/2 ^{WT} and IDH1 ^{Mut} chondrocytes	84
3.3.8.3 Exogenous cell permeable dimethyl- α -KG restored chondrocyte differentiation in <i>Col2a1Cre;Gls^{fl/fl};Idh1^{LSL/+}</i> animals.....	87
3.3.9 Inhibiting GLS induced apoptosis in IDH1/2 ^{Mut} chondrosarcomas and led to reduced tumor weight.....	88
3.3.10 Glutaminase regulated apoptosis in IDH1/2 ^{Mut} chondrosarcoma cells through production of non-essential amino acids.....	92
3.4 Discussion.....	96
4. Methods and Materials:	101
5. Conclusion and Future Directions:	117
5.2 Cholesterol in Cancer.....	119
5.2 α -KG and Chondrocyte Differentiation	124
5.3 Non-Essential Amino Acids in Cancer.	128
5.3.1 Glutathione and Reactive Oxygen Species.....	128
5.3.2 “Essential” Non-Essential Amino Acids upon GLS Inhibition	131
5.4 Divergent Roles of D-2HG in Tumor Initiation and Cancer Maintenance in Cartilage Tumors.....	133
5.5 HIF Signaling in Cartilage Tumors.....	138
Appendix A	141
Appendix B.....	143
References	144
Biography.....	171

List of Tables

Table 1 Antibodies	143
Table 2 qPCR Primers	143
Table 3 Mouse Strains	143

List of Figures

Figure 1: Endochondral ossification in developing limbs.	7
Figure 2 Regulation of chondrocyte differentiation by IHH and PTHLH	9
Figure 3 Cholesterol Biosynthesis Pathway	14
Figure 4 Glutamine Metabolism	22
Figure 5: Enchondroma of a patient.....	26
Figure 6: Development of benign enchondroma and its progression to malignant chondrosarcoma.....	27
Figure 7: The functions of wildtype and mutant IDHs.	29
Figure 8 RNA sequencing revealed distinct gene expression profile in <i>Col2a1Cre;Idh1^{LSL/+}</i> chondrocytes.....	45
Figure 9 Genes in cholesterol biosynthesis pathway were significantly upregulated in <i>Col2a1Cre;Idh1^{LSL/+}</i> chondrocytes.....	47
Figure 10 Cholesterol levels were higher in <i>Col2a1Cre;Idh1^{LSL/+}</i> chondrocytes.	48
Figure 11 Deleting Scap postnatally did not cause a noticeable phenotype in the growth plate chondrocytes.....	50
Figure 12 Representative Safranin O staining of tibia and femur growth plates of mice .	51
Figure 13 Quantification of enchondroma-like lesions in animals of indicated genotypes.	52
Figure 14 Lovastatin inhibited chondrosarcoma viability in vitro.	53
Figure 15 Illustration for patient-derived xenograft experiment.	55
Figure 16 Lovastatin inhibited chondrosarcoma growth in vivo.	55
Figure 17 Lovastatin suppressed proliferation of chondrosarcoma cells in vivo.	56

Figure 18 Lovastatin caused increased apoptosis in some IDH1 mutant chondrosarcomas.	57
Figure 19: Expression of <i>Gls</i> in IDH1/2 ^{WT} and IDH1/2 ^{Mut} chondrosarcoma tumors.	65
Figure 20 Glutaminase activity was upregulated in IDH ^{Mut} murine chondrocytes.	66
Figure 21 Graphic Depiction of tracing glutamine metabolism using ¹³ C ₅ -Glutamine.	68
Figure 22 Percentage of ¹³ C labeling contribution to downstream metabolites in IDH1/2 ^{WT} and IDH1 ^{Mut} murine chondrocytes.	69
Figure 23 Percentage of ¹³ C labeling contribution to downstream metabolites in human chondrosarcoma cells with wildtype <i>IDH1/2</i> , <i>IDH1</i> mutation, and <i>IDH2</i> mutations.	71
Figure 24 Glutamine is the primary source for D-2HG production in IDH1 ^{Mut} murine chondrocytes.	73
Figure 25 Gene expression of <i>Gls</i> and <i>Gls2</i> in chondrocytes.	74
Figure 26 Deletion of <i>Gls</i> was efficient in <i>Col2a1Cre;Gls^{fl/fl}</i> chondrocytes.	75
Figure 27 Expression of different chondrocyte markers.	79
Figure 28 Proliferation and apoptosis in embryonic growth plate.	81
Figure 29 Safranin O staining of the growth plate cartilage and enchondroma-like lesions.	83
Figure 30 GLS inhibition led to suppressed hypertrophic differentiation and reduced α -KG levels.	86
Figure 31 Exogenous cell permeable dimethyl- α -KG (DM- α -KG) restored chondrocyte differentiation and proliferation in <i>Col2a1Cre;Gls^{fl/fl};Idh1^{LSL/+}</i> animals.	88
Figure 32 Inhibiting glutaminase reduced tumor weight and induced apoptosis in chondrosarcomas with <i>IDH1/2</i> mutations.	91
Figure 33 Glutaminase and transaminases regulated cell viability of chondrosarcomas with <i>IDH1/2</i> mutations.	93

Figure 34 Glutaminase regulated chondrosarcoma apoptosis through non-essential amino acids.....	95
Figure 35 Mineralization in metatarsal organ culture.....	141
Figure 36 HIF-1 α signaling is activated in <i>Idh1</i> -mutant chondrocytes.....	142

Acknowledgements

It has been my great fortune, honor, and pleasure to pursue my Ph.D. training with my supervisor Dr. Benjamin Alman at Duke University. Dr. Alman has mentored me with invaluable advice, tremendous support, and omnipresent patience. With his guidance, I learned to think critically, be innovative, and follow the data relentlessly. He always encourages me to come up with my own ideas and to disagree with him, which is critical for me to develop independent thinking skills as well as self-confidence. In the past six years, he provided me with every support and help I needed for my academic success. With his support, I was able to travel around the world for conferences, collaborate with renowned scientists, and participate in various collaborative projects. His training has made me into an independent scientist and prepared me for the next stage of my career. Dr. Alman's mentorship and support are not limited to scientific guidance, but also in every aspect of my life. From him, I learned to lead, to solve conflicts, to always welcome challenges, and to accept failure. He is a role model for me as a scientist, a mentor, and a leader. He is the best mentor I could ever imagine.

I would express my sincere gratitude to my committee members: Dr. Courtney Karner, Dr. Donald McDonnell, and Dr. Eda Yildirim for their invaluable guidance and constructive feedback. I am especially thankful for Dr. Courtney Karner, who has provided me with tremendous amount of mentorship, support, and patience. He

welcomed me to his lab and mentored me as if I was his own student. He shared great scientific insights and expertise with me, and helped me patiently with my research projects, academic presentation, and career advancement. He also kindly invited me to participate in his own research projects. His mentorship is essential for my academic success. He always inspired with his scientific rigor and enthusiasm. I look up to him as my role model. I am grateful for all faculty who have taught, guided, and helped me, especially Drs. Colleen Wu and Matthew Hilton in the Orthopaedic Surgery Department, and Drs. Drs. Kenneth Poss, David Sherwood, Blanche Capel, Debra Silver, and Terry Lechler from my home program Developmental and Stem Cell Biology.

I would like to deliver special thanks for my collaborators Dr. Guofang Zhang from Duke Molecular Physiology Institute, Dr. Ivan Spasojevic and Ping Fan from Duke Cancer Institute, Dr. Gooden from the Department of Chemistry at Duke, and Dr. David Corcoran from Genomic Analysis and Bioinformatics Shared Resource at Duke. Their collaboration is critical for the success my research.

I would like to thank all the members of the Alman lab, my peers in the Department of Orthopaedic Surgery, the program of Developmental and Stem Cell Biology, the Department of Cell Biology at Duke, and all my friends for their company through this journey. In particular, I would like to thank Vijitha Puviindran and Puviindran Nadesan in the Alman lab for their mentorship, technical support, and constant encouragement. I would like to thank Drs. Hidetoshi Tsushima, Yasuhito

Yahara, and Ga I (Joy) Ban for sharing their scientific expertise and helpful advice. I would like to thank my friends and peers, Xiruo Ding, Fei Sun, Yihan Liao, Dr. Leyao Shen, Dr. Yilin Jiang, Jingyi Tian, Dr. Yuning Jackie Tang, Dr. Junjie Bao, Dr. Yoon Hae Kwak, Dr. Zeyu Huang, Dr. Claire Hsu, Wendi Guo, Dr. Yinshi (Rene) Ren, Dr. Chike Cao, Dr. Deepika Sharma, Dr. Guoli Hu, Corey Bunce, Jason Long, Abigail Leinroth for their company, support, and encouragement. I would like to thank Dr. Qingxia Wei, Sinthu Pathmanapan, Raymond Poon, Anthony Mirando, Dr. Bin Li, Dr. Michael Cook, Yilin Yu for their technical support.

Last but not least, I want to express my gratitude to my parents for their unconditional love, support, and care. This dissertation would not be possible without them.

1. Introduction and Background

Part of this work has been published:

H Zhang and B Alman (2021). *Enchondromatosis and Growth Plate Development*. Current Osteoporosis Reports. 2021 Feb;19(1):40-49. doi: 10.1007/s11914-020-00639-7.

1.1 Introduction

Long bones develop via endochondral ossification, a process through which a bone forms from a cartilage template. During this process, chondrocytes in the growth plate differentiate through different stages and finally undergo apoptosis or transdifferentiate into osteoblasts [1, 2]. In human, growth plates usually close after puberty and the chondrocytes are no longer present. Precise regulation of chondrocyte differentiation during endochondral ossification is critical for proper development of long bones [1]. Deregulation of chondrocyte differentiation can cause persistence of growth plate chondrocytes in bones and development of enchondromas [3, 4].

Enchondromas are benign cartilaginous neoplasms that develop within the medullary space of bones [5, 6]. When enchondromas occur as multiple lesions, they have a high chance to undergo malignant transformation to form chondrosarcomas [7, 8].

Mutations in isocitrate dehydrogenases 1 and 2 are the most common genetic variations in enchondroma and chondrosarcomas [9-11]. Wildtype IDH1/2 enzymes convert isocitrate to α -ketoglutarate (α -KG). Mutant IDH1/2 enzymes convert α -KG to D-2-hydroxyglutarate (D-2HG). Inhibiting the function of these mutant enzymes did not affect tumorigenic behaviors consistently in chondrosarcomas [7, 12]. Mutations of these genes are reported to cause changes in gene expression and metabolic reprogramming in other types of tumors [13]. The focus of this dissertation is to understand the transcriptional and metabolic regulations in chondrocytes and chondrosarcomas with

mutations in *IDH1/2*. I identified that mutation of these genes led to upregulated gene expression of genes in the cholesterol biosynthesis pathway and increased glutamine metabolism.

In this chapter, I reviewed the process of chondrocyte differentiation in the growth plate and introduced enchondroma and chondrosarcoma. For the process of chondrocyte differentiation, I focused on the key regulatory pathways that are relevant to this dissertation. For enchondromas and chondrosarcomas, I introduced the current knowledge of *IDH1/2* mutations as well as other known mutations and dysregulated signaling pathways implied in these pathological conditions.

1.2 Chondrocyte Differentiation in Growth Plate

1.2.1 The Process of Endochondral Ossification

Endochondral ossification is a process where a long bone forms from a cartilaginous template (Fig 1). The process starts when undifferentiated mesenchymal cells condense, differentiate to chondrocytes, and form a cartilage primordia that is rich in type II collagen and the proteoglycan aggrecan [1]. During skeletal development, chondrocyte proliferation and maturation are restricted near the ends of long bones, which is called the growth plate [14]. Growth plate chondrocytes differentiate through

resting, proliferating, prehypertrophic, hypertrophic stages, and eventually undergo apoptosis or transdifferentiate into osteoblasts [2, 14, 15].

In the hindlimbs of mice, endochondral ossification starts as mesenchymal stem cells condense and commit into the chondrogenic lineage at embryonic day (E)11.5. Then the cells differentiate into early resting chondrocytes. SRY-Box transcription factor 9 (SOX9) is the master chondrogenic transcription factor. It is essential for mesenchymal condensation and chondrogenesis [16, 17]. SOX9 is also required for the expression of SRY-Box transcription factor 5 (*Sox5*) and SRY-Box transcription factor 6 (*Sox6*) [17]. SOX5, SOX6, and SOX9 function together in governing chondrocyte differentiation through activating and regulating expression of different chondrocyte marker genes. Together they are called “Sox Trio” [17-21].

Resting chondrocytes secrete an extracellular matrix rich in type II collagen (encoded by *Col2a1*) and aggrecan (encoded by *Acan*). From there, the maturation process starts. In this process, resting chondrocytes first become highly proliferative and adopt a columnar shape. As these chondrocytes exit from cell cycle, they enlarge in size and differentiate to prehypertrophic, hypertrophic, and late hypertrophic chondrocytes. Prehypertrophic chondrocytes are marked by the expression of parathyroid hormone 1 receptor (encoded by *Pth1r*). Prehypertrophic and hypertrophic chondrocytes both express and secrete type X collagen (encoded by *Col10a1*). As hypertrophic chondrocytes continue to mature, they express and secrete matrix metalloproteinase 13 (encoded by

Mmp13) to remodel the cartilage matrix and produce vascular endothelial growth factors (VEGFs) to attract blood vessels. The invasion of blood vessels into the hypertrophic cartilage in the center of the long bone is responsible for bringing osteoblasts and osteoclasts to form the bone and remodel the cartilage matrix [1, 22].

The fate of hypertrophic chondrocytes has been a long debate. It was once commonly accepted that hypertrophic chondrocytes would undergo programmed cell death after terminal differentiation despite that several groups observed that hypertrophic chondrocytes could differentiate to osteoblasts, express osteogenic markers, and secrete bone matrix in vitro [1, 23-26]. The theory of chondrocyte-to-osteoblast differentiation lacked in vivo evidence before the availability of lineage tracing techniques. With the advancement of technologies, several groups have demonstrated that chondrocytes do contribute to the osteoblast population during development and fracture repair in the past few years.

To examine the fate of chondrocytes, independent research groups used Cre- or inducible CreER recombination systems to label the progeny of chondrocytes by crossing chondrocyte-specific Cre/CreER mice to reporter mice. Type X collagen is a specific marker expressed by prehypertrophic and hypertrophic chondrocytes, but not by osteochondral progenitors in the perichondrium and periosteum. In 2014, Yang et al. showed that *Col10a1*Cre and *Col10a1*CreERT-labeled hypertrophic chondrocytes gave rise to early osteoblasts that express Osterix (*Osx*) and mature osteoblasts that express

type I collagen (*Col1a1*) both during prenatal development and after birth [2]. Later in the same year, Zhou et al. showed that progeny of *Agc1*CreERT2 and *Col10a1*Cre-labeled chondrocytes contributed to prenatal and postnatal bone formation as well as fracture repair [15]. Zhou et al.'s data suggested that more than half of the osteoblasts were derived from hypertrophic chondrocytes during embryonic development and early postnatal development (~2 weeks). In animals at 13 weeks old, *Agc1*CreERT2 labeled chondrocytes barely contributed to osteoblasts in uninjured mice [15]. A follow up study suggested chondrocyte-derived osteoprogenitors existed at the chondro-osseous junction. These cells were actively proliferating and expressing stem-cell typical genes *CD34*, *Sca1*, *Sox2* and *c-myc* [27].

Growth plates are responsible for the length of long bones. In humans, growth plates usually close after puberty. The process of chondrocyte differentiation is tightly regulated by multiple transcription factors, extracellular signaling molecules, and metabolic processes in a coordinated manner. Deregulated growth plate chondrocyte differentiation leads to pathological conditions such as skeletal dysplasia and the development of enchondromas [28]. In the following paragraphs in this chapter, I will discuss the signaling and metabolic pathways that are relevant to the scope of this study.

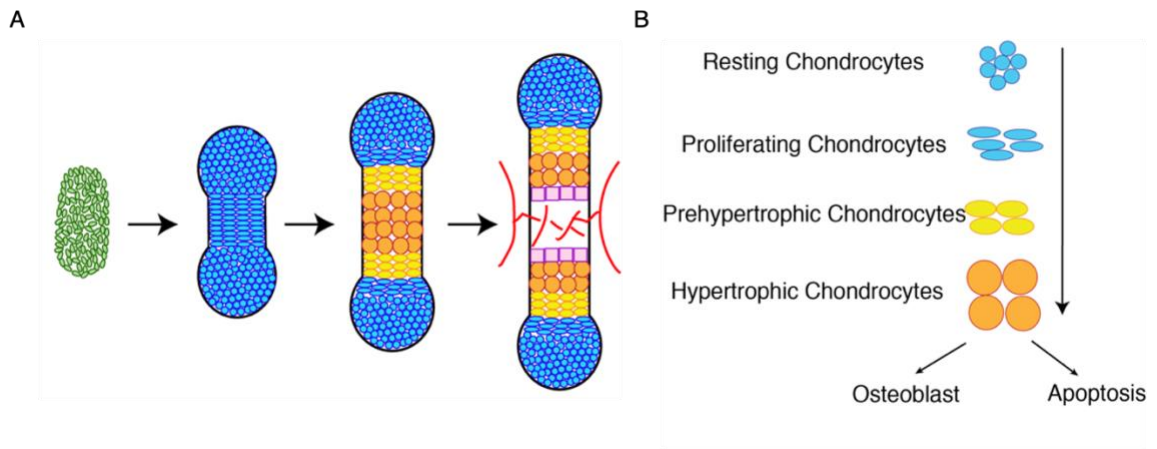


Figure 1: Endochondral ossification in developing limbs.

(A) Graphical illustration of endochondral ossification. The process starts from mesenchymal condensation. After that, mesenchymal progenitor cells differentiate to chondrocytes. Chondrocytes produce and secrete cartilage matrix and undergo hypertrophic differentiation. After that, vasculature invades into the cartilage template and brings in osteoprogenitors. (B) The process of chondrocyte differentiation. During endochondral ossification, early resting chondrocytes first become highly proliferative and adopt a columnar structure. Proliferative chondrocytes then exit the cell cycle and undergo hypertrophic differentiation. Hypertrophic chondrocytes would either undergo apoptosis or transdifferentiate into osteoblasts.

1.2.2 Signaling Pathways Governing Chondrocyte Differentiation

Chondrocyte differentiation in growth plates is strictly regulated by various signaling pathways in a coordinated manner. Mutations of genes in these pathways have been identified in different pathological conditions of the bone. In this section, I reviewed the role of hedgehog signaling and hypoxia inducible factor (HIF) signaling in chondrocyte differentiation because of their relevance in the context of enchondromas and chondrosarcomas.

1.2.2.1 Hedgehog Signaling Pathway

Hedgehog signaling is an important pathway that regulates endochondral ossification. In initial studies of the regulation of growth plate chondrocyte differentiation, it was found that parathyroid hormone like hormone (PTHrP) and Indian hedgehog (IHH) regulated chondrocyte hypertrophy in a negative feedback loop (Fig 2). *Pthlh* is expressed at high levels in perichondral cells [29-31]. Mouse genetic studies showed that PTHrP signaling suppressed chondrocyte hypertrophy [32-37]. *Ihh* is expressed by prehypertrophic and early hypertrophic chondrocytes [30]. IHH stimulates the expression of *Pthlh* by the perichondral cells, which in turn suppresses the expression of *Ihh* [30]. IHH also promotes chondrocyte differentiation independently of PTHrP by regulating zinc finger protein GLI transcription factors [22, 38]. When PTHrP signaling activity was remained at constant level, overexpression of *Ihh* still increased the length of the columnar zone in the growth plate, suggesting IHH could promote the transition of resting chondrocytes to proliferating chondrocytes independent of PTHrP signaling [38]. *Ihh* mutant mice displayed reduced chondrocyte proliferation and early onset of hypertrophic differentiation, and ablation of *Gli3* in *Ihh* mutant mice restored such changes, showing that IHH could regulate chondrocyte differentiation by inhibiting the repressor activity of GLI3 [39] (Fig 2). PTHrP could also regulate chondrocyte differentiation independent of IHH through protein kinase A and GLI transcription factors. Mau et al. showed that PTHrP inhibited hypertrophic

differentiation of chondrocytes in the presence of IHH blockade cyclopamine, but the effects were blunted upon *Gli3* deletion, suggesting PTHLH regulated chondrocyte differentiation via GLI3 [40] (Fig 2).

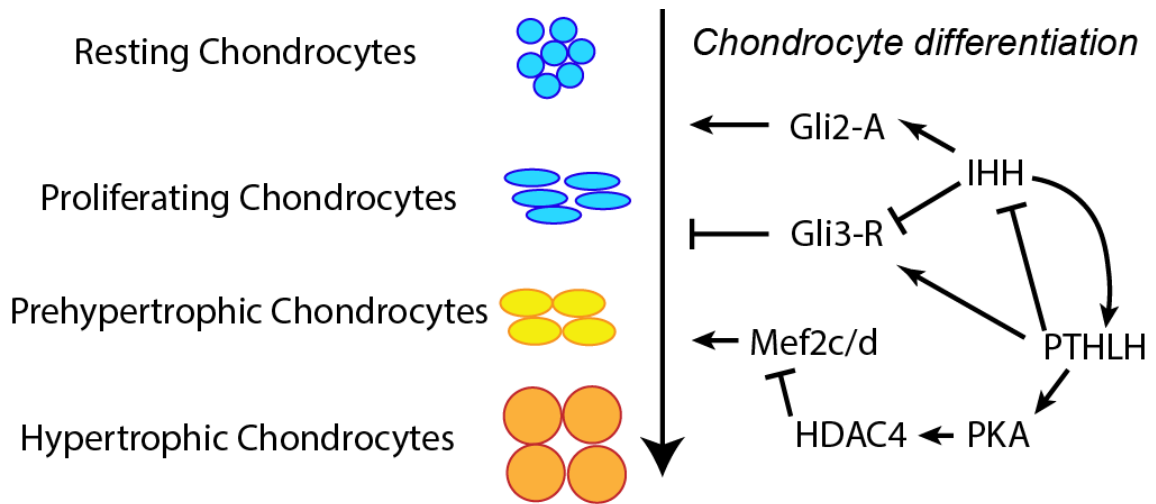


Figure 2 Regulation of chondrocyte differentiation by IHH and PTHLH

IHH and PTHLH form a feedback loop in regulating chondrocyte differentiation. IHH secreted by prehypertrophic chondrocytes stimulates perichondral cells to secrete PTHLH, which inhibits hypertrophic differentiation and the expression of *Ihh*. IHH could promote chondrocyte differentiation by inhibiting the repressor function of GLI3 and activating the activator function of GLI2 in a manner that is independent of PTHLH. PTHLH could also suppress hypertrophic differentiation independent of IHH through regulating GLI3 repressor function and promoting protein kinase A (PKA). PKA signaling leads to activation of histone deacetylase 4 (HDAC4), which inhibits Mef2 function.

1.2.2.2 HIF Signaling Pathway

The growth plate cartilage is a hypoxic avascular mesenchymal tissue and chondrocytes are capable of surviving and differentiating in the hypoxic environment partially through the regulation by hypoxia inducible factor (HIF) signaling. HIFs are

heterodimeric transcription factors composed of HIF- α and HIF- β subunits. Both subunits are constitutively expressed, but only HIF- β subunits are stabilized constitutively whereas HIF- α subunits are degraded at normal O₂ tension (normoxia). When O₂ is sufficient, the proline residues in HIF- α subunits are hydroxylated by prolyl hydroxylases domain-containing (PHD) proteins. These hydroxylated proline residues are recognized and ubiquitinated by the von Hippel Lindau (pVHL) E3 ubiquitin ligase, and subsequently undergo proteasomal degradation. Under hypoxic conditions, PHD enzymes could not hydroxylate HIF- α subunits due to the lack of O₂. Non-hydroxylated HIF- α subunits accumulate and translocate to the nucleus to dimerize with HIF- β subunits. The heterodimer transcription factors would bind to hypoxia-responsive elements (HREs) and regulate expression of downstream target genes [41].

Previous studies demonstrated chondrocytes' differentiation and viability were mediated through HIF signaling pathway. HIF-1 α is necessary in maintaining cell viability of growth plate chondrocytes as massive cell death was observed in *Hif1 α ^{-/-}* growth plate [42]. HIF-1 α regulates aerobic and anaerobic glycolysis, ATP production, synthesis of VEGF, as well as production of type II collagen in chondrocytes [43]. The cell death phenotype in *Hif1 α* -deficient chondrocytes was partially rescued by inhibiting mitochondrial respiration or over expressing the HIF-1 α target gene *Vegfa*, suggesting HIF-1 α signaling could regulate chondrocyte apoptosis through regulating mitochondrial respiration and vasculature invasion [44-47]. Conditionally deleting *Hif1 α*

in mesenchymal stem cells did not affect mesenchymal condensation, but significantly impaired early chondrogenesis and terminal differentiation of chondrocytes likely through its regulation of the master chondrogenic transcription factor *Sox9* [48, 49]. HIF-2 α could form a heterodimer with HIF-1 β subunit and function as a transcription factor. Heterozygous deletion of *Epas1* (*Epas1*^{+/-}, the gene encoding for HIF-2 α), or conditionally deleting it in mesenchymal progenitors only caused a transient and mild delay in endochondral ossification [50, 51], suggesting HIF-2 α might be dispensable for endochondral bone development.

Genetically disrupting other components of HIF signaling in limb bud mesenchyme or chondrocytes also led to disrupted chondrocyte differentiation in growth plates. PHD enzymes hydroxylate HIF- α subunits and target them for proteasomal degradation. Cheng et al. reported that conditional deleting *Phd2*, the major PHD isoform expressed in chondrocytes, in *Col2a1*-expressing chondrocytes led to upregulated HIF signaling, higher bone mass through increased bone formation, and decreased bone length in long bones at postnatal 4-5 weeks [52, 53]. Later, Stegen et al. reported similar findings that *Col2a1*Cre;*Phd2*^{fl/fl} mice exhibited increased bone mass and shorter bone length, but they did not observe a change in bone formation [54]. Instead, they proposed that the increased bone mass was caused by enhanced collagen hydroxylation, which rendered the collagen resistant to proteasomal degradation [54]. They found that elevated HIF signaling upregulated glutamine metabolism and

increased level of α -ketoglutarate (α -KG) [54]. α -KG served as a substrate for collagen prolyl hydroxylases and collagen lysine hydroxylase, promoted the activity of these enzymes, and increased collagen hydroxylation [54]. VHLH is the E-3 ubiquitin ligase that degrades hydroxylated HIF- α subunits. When *Vhlh* was conditionally deleted in mesenchymal progenitors or chondrocytes using *Prx1Cre* or *Col2a1Cre*, the mice had reduced chondrocyte proliferation and severe dwarfism [55, 56]. Moreover, deleting *Vhlh* in mesenchymal progenitors caused delayed terminal differentiation of chondrocytes since E13.5 and led to the formation of a cartilage remnant in the bone marrow postnatally [56], which phenotypically resembled enchondroma lesions in human patients.

1.2.3 Metabolic Regulation of Chondrocyte Differentiation

In addition to signaling pathways, recent studies have shown that metabolic regulation also plays critical roles in governing chondrocyte differentiation during endochondral ossification. In this section, I reviewed the role of cholesterol biosynthesis and glutamine metabolism in chondrocyte differentiation and endochondral bone development.

1.2.3.1 Cholesterol Biosynthesis

Cholesterol is a sterol, a type of lipid that shares a four-fused-ring structure and 3 β -hydroxyl group [57]. Cholesterol is an essential component for cell membrane, and a

critical precursor for other biomolecules such as oxysterols, steroid hormones, Vitamin D, bile acids, etc. [58, 59]. Cholesterol is also a key regulator of hedgehog signaling [60-63], a well-known pathway that regulates chondrocyte differentiation during endochondral ossification. Cholesterol could modify the hedgehog ligands and the signaling transducer Smoothed [60, 64]. Cholesterol biosynthesis is a complex pathway consisting of multiple steps (Fig 3). For the first part of cholesterol biosynthesis, acetyl-Coenzyme A (acetyl-CoA) is used to produce lanosterol in a multi-step pathway, mevalonate pathway (Fig 3A). After that, lanosterol is converted to cholesterol through either Bloch pathway or Kandutsch–Russell pathway (Fig 3B) [57, 58]. Defects in the process of cholesterol biosynthesis are implicated in multiple diseases characterized by skeletal disorders. On the other hand, disruption of the regulation of cholesterol biosynthesis could cause impaired chondrocyte differentiation, suggesting that cholesterol biosynthesis plays a critical role in regulating chondrocyte differentiation. In this subsection, I will discuss current knowledge about the role of cholesterol biosynthesis in skeletal development and pathologies.

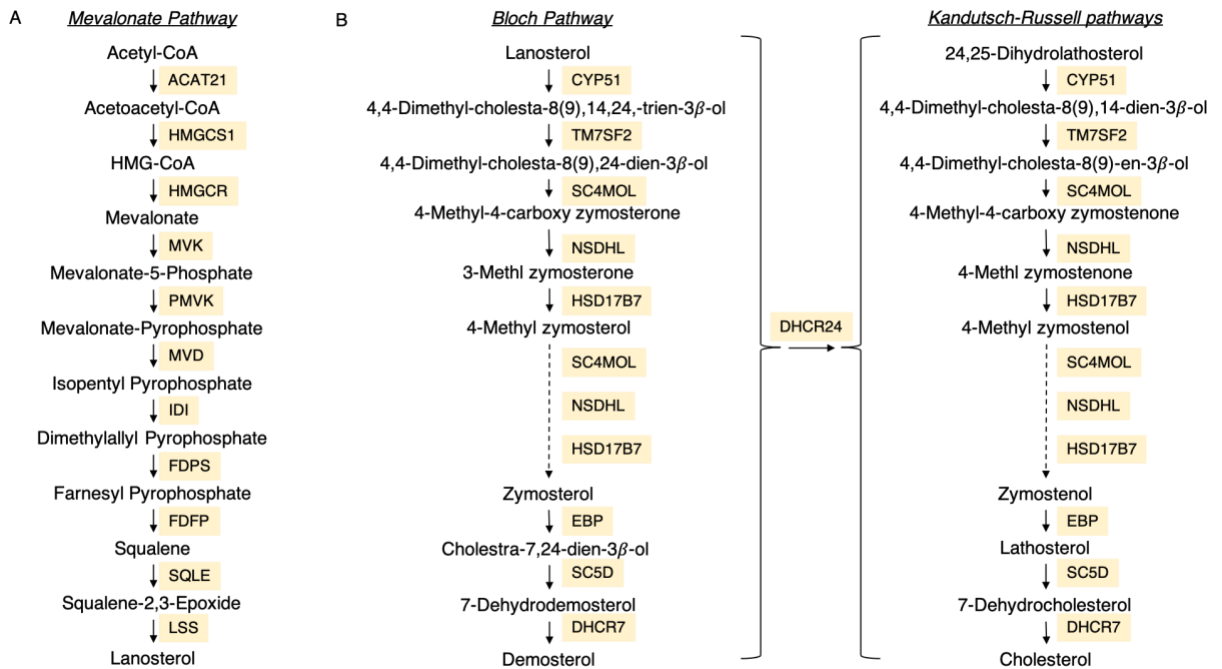


Figure 3 Cholesterol Biosynthesis Pathway

(A) Mevalonate Pathway. (B) Bloch pathway and Kandutsch–Russell pathway.

3-Hydroxy-3-Methylglutaryl-CoA Reductase (HMGR) converts HMG-CoA to mevalonate. This is the rate-limiting step in the mevalonate pathway. HMGR could be inhibited by a family of drugs called statins [59]. In a zebrafish model, when *hmgrb* was mutated, or when HMGR was inhibited by atorvastatin, the animals displayed reduced or lack of cartilage growth [65]. The authors proposed that the phenotype might be caused by dampened hedgehog signaling based on reduced expression of the Hh effector *Gli1* [65]. In a mouse model of achondroplasia caused by a gain-of-function mutation of fibroblast growth factor receptor type III gene (*Fgf3*), treatment with rosuvastatin restored the defects in bone growth [66]. In the same study, it was also

reported that statin treatment restored cartilage formation ability of the induced pluripotent stem cells (iPSCs) derived from patients with thanatophoric dysplasia type I and achondroplasia [66].

Lanosterol 14 α -demethylase (encoded by *CYP51A1*) catalyzes conversion from lanosterol to 4,4-dimethylcholesta-8(9),14,24-trien-3- β -ol. Impaired activity of lanosterol 14 α -demethylase was reported in Antley-Bixler-Syndrome, a disease with skeletal defects [67]. Genetic deletion of *Cyp51a1* caused prenatal lethality at E14.5-E15.5 [67]. At E14.5, the animals deficient in *Cyp51a1* displayed skeletal abnormalities, including shortened forelimbs and hindlimbs, bowed radius and tibia, absence of distal phalanges, etc. [67].

Lamin-B receptor (LBR) and 14-dehydrocholesterol reductase (DHCR14, encoded by *TM7SF2*) catalyzes the reduction of the C14-unsaturated bond of lanosterol, a step in the cholesterol biosynthesis pathway. Mutation of *LBR* was identified in patients with Hydrops-ectopic calcification-“moth-eaten” (HEM) or Greenberg skeletal dysplasia, a rare condition characterized by fetal hydrops, dwarfism, abnormal chondro-osseous ossification [68]. When *Tm7sf2* and/or *Lbr* was deleted (*Dhcr14 Δ 4-7/ Δ 4-7, Lbr $^{+/-}$; Dhcr14 Δ 4-7/ Δ 4-7, Lbr $^{-/-}$), mice displayed disorganized hypertrophic zone [69]. Cartilage remnant was present in *Lbr $^{-/-}$* mice [69].*

NAD(P) Dependent Steroid Dehydrogenase-Like (NSDHL) decarboxylates 4,4-dimethylcholesta-8,24-dien-3 β -ol in the process of cholesterol synthesis. Mutation of this

gene was identified in patients with Congenital Hemidysplasia, Ichthyosiform erythroderma, Limb Defects (CHILD syndrome) [70], a disease characterized by unilateral ichthyosiform skin lesions and ipsilateral limb reduction defects [71]. Heterozygous *Nsdhl* mutant mice (bare patches [*Bpa*] mice) displayed skeletal dysplasia that was associated with chondrodysplasia punctata [72].

Sterol-C5-Desaturase (encoded by *SC5D*) converts lathosterol to 7-dehydrocholesterol (7-DHC). This is the second last step in cholesterol biosynthesis. A homozygous mutation of *SC5D* was identified in a patient with lathosterolosis [73], a condition characterized by growth retardation, microcephaly, limb anomalies, calvarial defects, etc. [74]. *SC5D* deficient mice (*Sc5d^{-/-}*) displayed skeletal defects including short, malformed forelimbs and hindlimbs, gracile ribs, etc., suggesting a critical role of *Sc5d* in endochondral ossification [73]. In two cases of lathosterolosis, simvastatin effectively reduced plasma lathosterol levels and improved the patient's neurodevelopmental profile and liver function respectively [74, 75]. These findings suggested the accumulation of lathosterol, instead of deficiency of 7-DHC or cholesterol, was the major cause for some defects in these patients.

7-Dehydrocholesterol Reductase (DHCR7) converts 7-DHC to cholesterol and 7-dehydrodesmosterol to desmosterol. Mutations of this gene were identified in patients with Smith-Lemli-Opitz syndrome (SLOS), a disease characterized by microcephaly, cleft palate, craniosynostosis, mental retardation, and limb anomalies (shorter thumbs,

polydactyly, syndactyly), etc. [76]. Limb abnormalities were not observed in *Dhcr7*^{-/-} animals [77]. When rats were treated with a DHCR7 inhibitor AY 9944, they exhibited reduced growth plate height and chondrocyte proliferation [78].

The expression of most genes in the cholesterol synthesis pathways is regulated by the transcription factors sterol regulatory element-binding proteins (SREBPs) [79-81]. Cleavage and activation of SREBPs are regulated via a negative feedback loop. When sterol levels are high in the endoplasmic reticulum (ER), full-length SREBPs are retained in the ER membrane through a complex with SREBP cleavage-activating protein (SCAP) and insulin induced gene 1 and 2 protein (INSIG1/2). INSIG1/2 binding to SCAP leads to its retention in the ER membrane. When sterol levels are low in the ER, SCAP dissociates from INSIG1/2, and translocates to the Golgi with SREBPs. SREBPs are cleaved in the Golgi by site-1 protease (S1P) and S2P, and then homodimerize and translocate to the nucleus to activate transcription of their target genes, including the ones encoding for enzymes in the cholesterol biosynthesis pathway [59].

Besides enzymes in the process of cholesterol biosynthesis pathway, genes that regulate this pathway also regulate chondrocyte differentiation and endochondral ossification. When *Scap* was deleted in murine mesenchymal progenitor cells (*Prx1Cre;Scap*^{fl/fl}), the forelimbs and hindlimbs in the mice were significantly shortened. These *Scap*-deficient mesenchymal progenitor cells failed to undergo chondrogenesis in the micromass culture, and expression of chondrogenic markers in the micromass was

significantly reduced when compared to their littermate control [82]. When *Scap* was deleted in chondrocytes (*Col2a1Cre;Scap^{fl/fl}*), the mice developed severe dwarfism and the growth plates were disorganized [82]. When *Insig1* and *Insig2* were deleted in mesenchymal stem cells (*Prx1Cre; Insig1^{fl/fl}; Insig2^{-/-}*), the mice also developed dwarfism [82]. These data suggest that cholesterol needs to be at an optimal level to ensure proper chondrogenesis and chondrocyte differentiation as either upregulating or downregulating its biosynthesis led to disrupted chondrocyte differentiation. Furthermore, Hedgehog signaling was dampened in *Scap*-deficient chondrocytes and overactivated in *Insig1/2*-deficient mice [82]. Forced activation of Hedgehog signaling by overexpressing *Gli2* in chondrocytes (*Col2a1Cre;Scap^{fl/fl};Gli2^{OE}*) rescued the phenotype of *Scap* deletion [82], suggesting intracellular cholesterol biosynthesis may regulate chondrocyte differentiation partially through Hedgehog signaling.

1.2.3.2 Glutamine Metabolism

Glutamine is the most abundant non-essential amino acids in circulation [83]. Glutamine can be uptake by cells through amino acid transporters including ASCT2, SNAT1, SNTAT2 (encoded by *Slc1a5*, *Slc38a1*, *Slc38a2* respectively), and then metabolized in cells [84-87]. Glutamine metabolism starts when glutaminase (GLS) deaminates glutamine to glutamate and releases the ammonium ion (Fig 4). Two genes of glutaminase, kidney-type glutaminase (encoded by *Gls*) and liver-type glutaminase (encoded by *Gls2*), are expressed by human and mice [88]. Expression of *Gls* was found

to be ubiquitous in different tissues and expression of *Gls2* was reported to be restricted to livers [89]. There are two splicing isoforms of kidney-type glutaminase. They differ at the C-terminus. The longer isoform is called kidney-type glutaminase (KGA) and the shorter isoform is called glutaminase C (GAC) [90].

Glutaminase could be regulated at gene transcription level, protein level, via posttranslational modification, and allosterically. The proto-oncogene c-Myc promotes *Gls* expression through repression of miRNA -23a/b [91]. Interferon- α activates *Gls* expression through phosphorylation and activation of STAT1 [92]. The E3 ubiquitin ligase APC/C could negatively regulate KGA through ubiquitination. Once ubiquitinated, KGA would be targeted for degradation [93]. GAC could be degraded by mitochondrial Lon protease upon diphenylarsinic acid treatment [94]. Epidermal growth factor (EGF) mediated MEK-ERK pathway regulates KGA activity post-translationally through phosphorylation [95]. In breast cancer cells, Rho GTPase enhanced glutaminase activity independent of its protein expression through the transcription factor NF- κ B, probably by regulating expression of proteins that could modulate glutaminase phosphorylation [96]. Later, the same group found that NF- κ B could regulate GAC phosphorylation through the kinase PKC ϵ in non-small cell lung cancer [97]. Inorganic phosphate could activate KGA and GAC allosterically [98].

Glutamate is used for biosynthesis of other molecules. It is a key precursor for glutathione (GSH), a tripeptide (glutamate-cysteine-glycine) that modulates cellular

redox homeostasis [85]. Glutamate could be used in exchange for cystine (the dimer of cysteine) through the antiporter xCT (encoded by *Slc7a11*) and to produce glycine through transamination, thus contributing to the production of glutathione indirectly [85, 99]. Glutamate could be further metabolized to α -ketoglutarate (α -KG) through glutamate dehydrogenase (GDH) or transaminases (Fig 4) [85]. When GDH deaminates glutamate to α -KG, it converts NAD(P)⁺ to NAD(P)H (Fig 4), which could be used for other metabolic reactions that consume reducing agent, such as nucleotide synthesis [100]. When a transaminase generates α -KG from glutamate, it transfers the amino group from glutamate to other keto acids and produce non-essential amino acids (Fig 4) [85]. Glutamate-pyruvate transaminases (GPT) transfer the amino group from glutamate to pyruvate and produce alanine and α -KG. Glutamate-oxaloacetate transaminases (GOT) transfer the amino group from glutamate to oxaloacetate to produce aspartate and α -KG. Phosphoserine aminotransferase 1 (PSAT1) transfers the amino group from glutamate to 3-phosphohydroxypyruvate to produce phosphoserine and α -KG, which is an important step in serine synthesis [85].

α -KG (also known as 2-oxoglutarate) serves as a cofactor for a superfamily of enzymes called 2-oxoglutarate-dependent oxygenases. [101]. These enzymes include procollagen hydroxylases, prolyl hydroxylase domain (PHD) enzymes, protein demethylase, ten-eleven translocation (TET) methylcytosine dioxygenases, etc. [101]. Through these enzymes, α -KG regulates collagen synthesis and maturation, HIF

signaling, histone methylation, and DNA methylation, respectively [101]. Other metabolites, such as succinate, fumarate, 2-hydroxyglutarate, could compete with α -KG for binding to these 2-oxoglutarate-dependent oxygenases and inhibit their enzymatic functions [102].

α -KG could enter the TCA cycle and contribute to anaplerosis (Fig 4). When an α -KG molecule is oxidized through the TCA cycle, the oxidative reactions would generate one molecule of GTP, two molecules of NADH, and one molecule of FADH₂. The reducing agent NADH and FADH₂ could feed into the electron transport chain to generate ATP through oxidative phosphorylation [88]. α -KG could also enter the TCA cycle through reductive carboxylation and be converted to citrate through isocitrate dehydrogenase 2 (IDH2) (Fig 4) [85]. The TCA cycle intermediates derived from glutamine could be further utilized to generate other biomolecules. For example, ATP citrate lyase (ACLY) converts citrate to acetyl-CoA (Fig 4), which is used as a substrate for fatty acid synthesis and cholesterol biosynthesis [88]. Transaminases convert oxaloacetate to aspartate (Fig 4), which could be utilized for nucleotide biosynthesis [103, 104]. Malic enzyme produces pyruvate from malate and generates NADPH (Fig 4) [100, 105]. Pyruvate could be converted to alanine through transaminases. NADPH could be used to support lipogenesis and restore reduced form of glutathione (GSH) from the oxidized form (GSSG) in order to maintain cellular redox homeostasis [88].

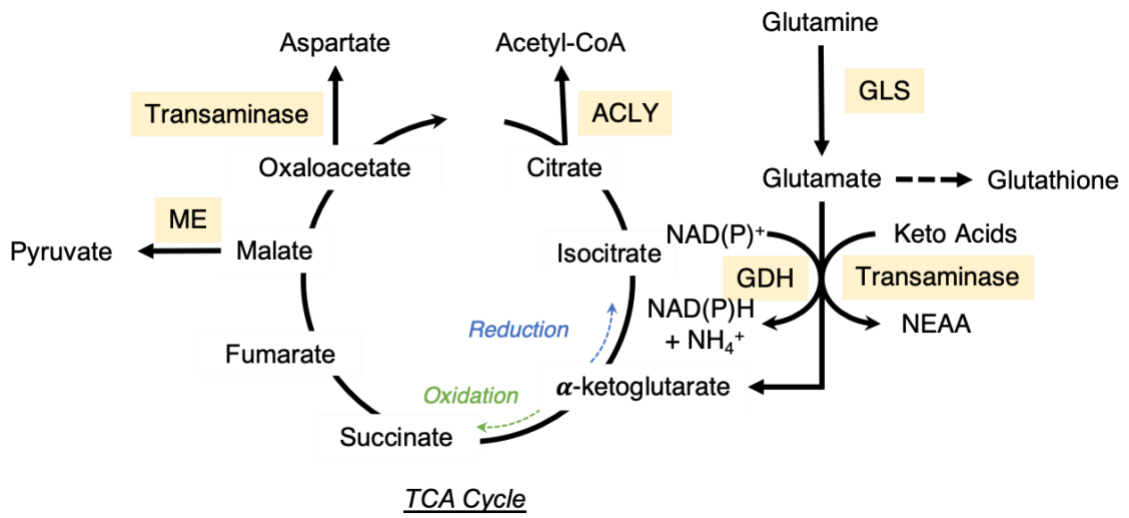


Figure 4 Glutamine Metabolism

Glutamine metabolism starts when glutaminase (GLS) deaminates glutamine to glutamate. Glutamate could be used to produce glutathione, a critical regulator for cellular redox homeostasis. Glutamate could be converted to α -ketoglutarate (α -KG) by glutamate dehydrogenase (GDH) or transaminases. When transaminases convert glutamate to α -KG, they transfer the amino group from glutamate to other keto acids and produce other non-essential amino acids (NEAA). α -KG could enter the tricarboxylic acid (TCA) cycle either through oxidative decarboxylation (green dashed arrow) or reductive carboxylation (blue dashed arrow). TCA intermediates could be further utilized to generate other metabolites. Malic Enzyme (ME) converts malate to pyruvate. Glutamic-oxaloacetic transaminases (e.g., GOT1) converts oxaloacetate to aspartate. ATP-citrate lyase (ACLY) produces acetyl-CoA from citrate.

Glutamine has been reported to be important for the proper function and differentiation of chondrocytes. In 1978, Speight et al. reported that glutamine supported glycosaminoglycan synthesis in chondrocytes as an amino group donor [106]. In 1980, the same group demonstrated that addition of exogenous glutamine to the cell culture promoted glycine incorporation into acid-insoluble protein and acetate incorporation into glycosaminoglycan in chondrocytes [107]. Recently, Stegen et al. reported that

expression of *Gls* was regulated by the master chondrogenic transcription factor SOX9 [108]. Deleting *Gls* in chondrocytes caused reduced bone growth from postnatal (P) day 3 to P14. Such phenotype could be rescued by injecting cell permeable dimethyl- α -KG (DM- α -KG) [108]. They observed that histone acetylation and expression of chondrogenic genes were suppressed upon GLS inhibition and could be rescued with supplementation of exogenous acetate or α -KG. As acetate could be used to generate acetyl-CoA, the authors proposed that glutamine metabolism controlled chondrogenic gene expression via histone acetylation through acetyl-CoA synthesis [108]. The authors also observed that deleting or inhibiting glutaminase caused reduced biosynthesis and increased cell death in chondrocytes, which could be reversed by addition of exogenous aspartate and glutathione ethyl ester respectively [108]. The same group also reported that GLS acted downstream of HIF-1 α signaling in regulating collagen hydroxylation in chondrocytes [54]. They observed that the protein level and functional activity of GLS as well as the concentration of glutamine-derived α -KG were increased when HIF-1 α signaling was inappropriately activated by *Phd2* deletion in chondrocytes [54]. Increased α -KG promoted collagen hydroxylation in wildtype animals [54]. Blocking GLS corrected inappropriate collagen hydroxylation caused by *Phd2* deletion [54]. Glutamine was also reported to promote chondrocyte differentiation during fracture repair [109]. Fracture repair usually involves both endochondral ossification and intramembranous ossification [110]. During endochondral repair, mesenchymal progenitors differentiate

into chondrocytes, and chondrocytes differentiate through hypertrophic stages and transdifferentiate to osteoblasts [15, 110]. Polat et al. observed that when fractured rats were injected with L-glutamine/L-alanyl solution, the development of cartilage callus was quicker and more regular when compared to vehicle control group [109]. In the glutamine treatment group, chondrocytes in the callus were organized in rows and were hypertrophic and calcified. Whereas in the vehicle control group, chondrocytes in the callus were disorganized and had not undergone hypertrophy, suggesting glutamine might promote chondrocyte hypertrophic differentiation during fracture repair [109]. Together, these historic studies suggest glutamine metabolism is a key regulator to ensure proper chondrocyte differentiation.

Glutamate regulates chondrocyte differentiation as a signaling molecule and through regulating redox homeostasis. Besides its metabolic function, glutamate also serves as a signaling molecule in cells in both neural and non-neural tissues [111, 112]. Glutamate signaling machinery involves several steps – signal release via sodium-independent glutamate transporters (to export glutamate), signal reception via glutamate receptors, and signal termination via sodium-dependent excitatory glutamate transporters (to uptake glutamate) [112]. Glutamate receptors could be further classified as ionotropic receptors, which are ion-gated cation channels activated by glutamate, and metabotropic receptors, which belong to the family of G protein receptors [112]. Yoneda's group showed that rodent chondrocytes expressed a fully functional

glutamate signaling machinery including ionotropic (iGluR) and metabotropic glutamate receptors (mGluR), excitatory amino acid transporters, vesicular glutamate transporter, and cystine/glutamate antiporter [113-116]. Using murine metatarsal organ culture and primary rat costal chondrocytes, they observed that agonists of group II and group III metabotropic glutamate receptors, but not ionotropic glutamate receptors, abolished chondrocyte mineralization and reduced the expression of osteopontin gene [115]. The group also showed that treating metatarsals with high concentrations ($\geq 500 \mu\text{M}$) of glutamate had similar effects of inhibiting mineralization, which could be partially rescued by addition of mGluR antagonist, glutathione, cystine, or inhibitor of glutamate / cystine antiporter [114]. High concentration of glutamate treatment could induce apoptosis, which could be rescued by exogenous glutathione, cystine, or inhibitor of glutamate / cystine antiporter, but not by mGluR antagonist [114]. These data suggest that exogenous glutamate could regulate chondrocyte differentiation through a signaling mechanism and regulating redox homeostasis, and its effects on inducing cell apoptosis were mainly through disrupting redox homeostasis. In another study, Piepoli et al found that ionotropic glutamate receptor *N*-methyl-d-aspartate (NMDA) regulated chondrocyte proliferation in the human chondrosarcoma cell line SW1353 and primary rat articular chondrocytes [117]. They found that knocking down the expression of a subunit of NMDA or blocking NMDA in SW1353 and primary rat articular chondrocytes led to significantly reduced cell proliferation [117].

1.3 Enchondromas and Chondrosarcomas

1.3.1 Overview of Enchondromas and Chondrosarcomas

Cartilage tumors as a group are the most common neoplasms affecting the bone [118]. They include benign tumors such as enchondromas (Fig 5) and osteochondromas as well as malignant cancers such as chondrosarcomas [6].



Figure 5: Enchondroma of a patient.

Enchondroma is one of the most common benign bone tumors and is estimated to affect 3% of the population [119, 120]. They are mostly present in appendicular bones, uncommon in flat bones, and rarely occur in craniofacial bones [5]. Enchondromas arise from dysregulated growth plate chondrocytes that fail to undergo terminal differentiation and remain at the end of the bone (Fig 6) [6, 8]. They occur within the

medullary bone as a single lesion or as multiple lesions (enchondromatosis) in conditions termed Ollier disease and Maffucci syndrome [6]. Upon secondary events, they could progress into malignant chondrosarcomas (Fig 6). Multiple enchondromas in Maffucci syndrome are associated with up to 50% chance of undergoing malignant transformation to form chondrosarcomas [7, 8]. Chondrosarcoma is the second most common malignant primary bone tumor and is resistant chemotherapy and radiation therapy [121].

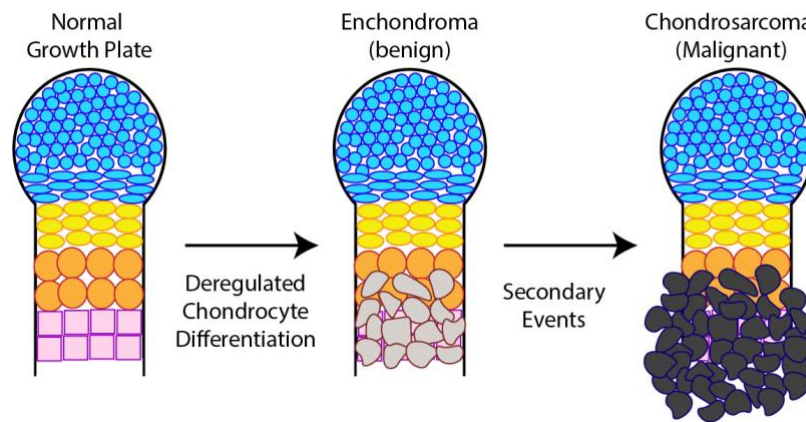


Figure 6: Development of benign enchondroma and its progression to malignant chondrosarcoma.

1.3.2 *IDH1/2* Mutations in Enchondromas and Chondrosarcomas

Somatic mutations in *isocitrate dehydrogenase 1 and 2* (*IDH1 / IDH2*) frequently occur in enchondromas and chondrosarcomas. Most of enchondromas (~70 – 80%) and more than half of chondrosarcomas harbor mutations in either *IDH1* or *IDH2* [10, 11]. Furthermore, in a genetically modified mouse model, postnatally inducing expression of mutant *IDH1*^{R132Q}, a mutation identified in a human chondrosarcoma sample, in

chondrocytes was sufficient to initiate enchondroma-like lesion formation in mice [4]. Animals expressing IDH1^{R132Q} in chondrocytes during embryonic development showed disrupted growth plate structure and defects in chondrocyte mineralization and cartilage remodeling, supporting that expression of mutant IDH1^{R132Q} caused defects in chondrocyte terminal differentiation [4].

1.3.2.1 Normal Function of IDH enzymes

IDH genes encode for isocitrate dehydrogenases, which catalyze the conversion from isocitrate to α -ketoglutarate [122]. There are three different isocitrate dehydrogenases [123] (Fig 7). IDH1 is localized in the cytoplasm and peroxisomes. IDH2 and IDH3 are localized in the mitochondria. IDH1 and IDH2 are highly homologous to each other (structurally, functionally, and evolutionarily similar), but are distinct from IDH3. IDH1 and IDH2 are both homodimeric enzymes that catalyze the reversible redox reaction, namely oxidative decarboxylation of isocitrate to α -ketoglutarate (α -KG) with production of reduced nicotinamide adenine dinucleotide phosphate (NADPH) from nicotinamide adenine dinucleotide phosphate (NADP⁺) as well as the reverse reductive carboxylation reaction (Fig 7). IDH3 is a heterotrimeric enzyme that irreversibly converts isocitrate to α -KG while producing NADH from NAD⁺ in the TCA cycle (Fig 7). Despite structural similarities, IDH1 and IDH2 have distinct functions in cellular metabolism. IDH1 promotes cytoplasmic and nuclear dioxygenases that require α -ketoglutarate as a cofactor [124]. It generates non-mitochondrial NADPH, which could be used for lipid

synthesis and maintaining redox homeostasis [124]. IDH1 could also catalyze the carboxylation of α -ketoglutarate to make isocitrate, a metabolite could be further utilized for lipid synthesis [124]. IDH2 regulates the relative abundance of isocitrate and α -ketoglutarate in the mitochondria. When mitochondrial α -ketoglutarate level is high, IDH2 converts it to isocitrate, which could feed into the TCA cycle or be converted to citrate for fatty acid biosynthesis [124]. IDH2 also generates mitochondrial NADPH that is important for protecting cells from mitochondrial reactive oxygen species (ROS) [124].

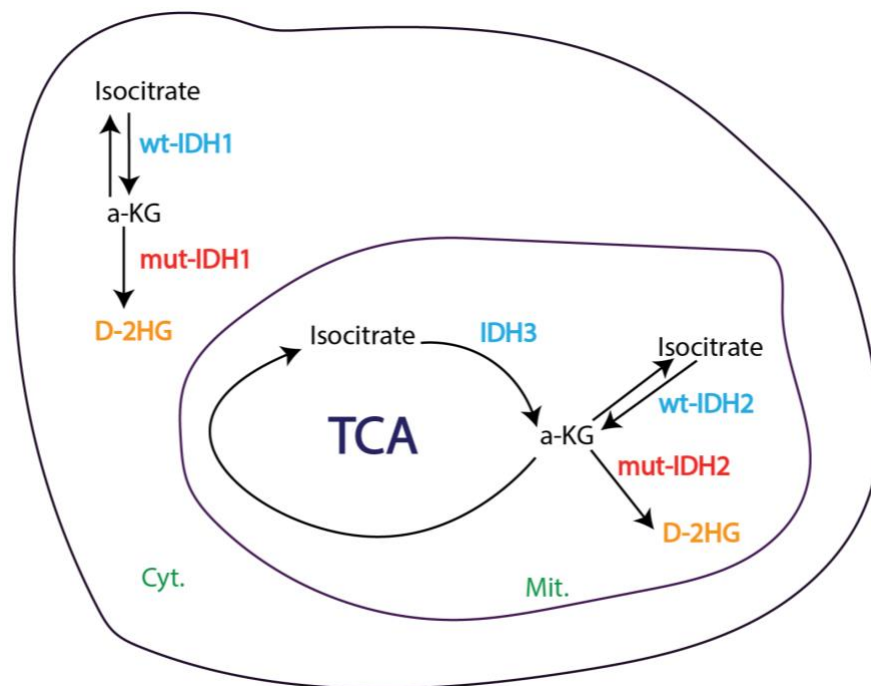


Figure 7: The functions of wildtype and mutant IDHs.

Wildtype IDH1 and IDH2 catalyzes the reversible conversion between isocitrate to α -KG in the cytoplasm and mitochondria. IDH3 converts isocitrate to α -KG irreversibly in the TCA cycle. Mutant IDH1 and IDH2 converts α -KG to D-2HG irreversibly in the cytoplasm and mitochondria.

1.3.2.2 Mutations in *IDH1/2*

A wide range of mutations in *IDH1* (*IDH1* R132C, R132G, R132H, etc.) and *IDH2* (*IDH2* R172M, R172C, R172K, etc.) genes are found in different tumor types such as glioblastoma, acute myeloid leukemia (AML), chondrosarcomas, and enchondromas, etc. The mutations were initially reported in glioblastomas from whole-genome exon-sequencing analysis, and later in AML [125-127]. As patients with enchondromas have an increased chance of developing AML and glioma, researchers investigated the frequency of *IDH1/2* mutations in cartilage tumors and found that these mutations in *IDH1* and *IDH2* also occurred in the majority of enchondromas and chondrosarcomas [9-11].

Somatic mutations in *IDH1* and *IDH2* occur at specific arginine residues in the active sites of these enzymes: *IDH1*-R132 and *IDH2*-R140, -R172 [123]. They are mostly missense mutations and cause an amino acid substitution. The percentage of different point mutations differs by tumor types. Chondrosarcoma has a broader range of *IDH1* mutations than previously identified in other tumor types [4]. *IDH1*^{R132C} is the most frequent mutation in enchondromas and chondrosarcomas [9-11]. Mutant *IDH* enzymes have impaired activity of producing α -ketoglutarate and NADPH as well as the reverse reductive carboxylation. They acquire a neomorphic activity that reduces α -ketoglutarate to D-2-hydroxyglutarate (D-2HG) in a manner that consumes NADPH [126, 128-130] (Fig 7).

1.3.2.3 D-2HG as an “Oncometabolite”

The mechanism by which mutant IDH1/2 regulate enchondroma biology are incompletely understood. Studies of other cancers suggest mutant IDH1/2 regulate cells via the putative “oncometabolite” D-2-hydroxyglutarate (D-2HG). D-2HG is a metabolite that is normally present in cells at low levels and recycled back to α -ketoglutarate by 2-HG dehydrogenases [131]. Administration of D-2HG or transfection of mutant *IDH1/2* was sufficient to increase a wide range of histone methylation in different cell types [132-134]. D-2HG potently inhibited Jumonji-domain-containing family of histone demethylase such as lysine demethylases 2A, 3A, 4A, and 4C [132, 133]. *IDH1/2* mutations were also associated with DNA hypermethylation in gliomas and AML [133, 135, 136]. Introduction of *IDH1/2* mutations was sufficient to cause DNA hypermethylation in normal human astrocytes, 293T cells, hematopoietic progenitor cells, and human mesenchymal stem cells [135-137]. This was thought to occur through D-2HG competitively inhibiting ten-eleven translocation (TET) family 5-methylcytosine hydroxylase [133, 135-137]. D-2HG is believed to exert its effects by competitively inhibiting enzymes that require α -ketoglutarate as a cofactor because its chemical structure is similar to α -ketoglutarate. In almost all the tumors with *IDH1/2* mutations, D-2HG production exceeds its elimination and could accumulate up to millimolar concentrations [129, 138, 139].

In the context of chondrocyte differentiation and cartilage neoplasia, mutant IDH1 is believed to regulate chondrocyte and osteoblast differentiation via mechanisms dependent and independent of D-2HG. Jin et al. showed that expressing mutant IDH1^{R132C} in human mesenchymal stem cells enhanced chondrocyte-related genes' expression and suppressed osteogenic genes' expression through histone modifications [137]. The induction of IDH1^{R132C} in mesenchymal stem cells caused significant increases in active histone modification marker H3K4me3 in the promoter region of chondrocyte-related genes SRY-Box transcription factor 9 (*SOX9*) and collagen type II alpha 1 chain (*COL2A1*) and suppressive histone modification marker H3K9me3 in the promoter of the osteoblast-related gene alkaline phosphatase (*ALPL*) [137]. The changes were associated with defects in human mesenchymal stem cells' ability of forming cartilage pellet and disturbed mineralization after osteogenic induction [137]. D-2HG treatment induced similar defects in osteogenic differentiation in human mesenchymal stem cells, suggesting *IDH1* mutation might suppress osteogenesis via D-2HG production [140]. However, D-2HG treatment did not cause consistent effects on chondrocyte differentiation, suggesting *IDH1* mutation might regulate chondrocyte differentiation via mechanisms other than D-2HG production [140].

There is conflicting data on the ability of pharmacologic blockade of 2-HG production to suppress the neoplastic phenotype in established cartilage tumors. One study using two cell lines found that pharmacologic inhibition of 2-HG production

inhibited chondrosarcoma cell viability [12], but a second study found that while pharmacologic targeting mutant IDH1 enzymes did lower 2-HG levels, it did not affect chondrosarcoma cell viability *in vitro* [7]. Importantly, some patients with chondrosarcoma have been treated with IDH inhibitors. The results to date have been variable, showing at best stabilization of the disease [141], supporting the notion that pharmacologic inhibition may not be effective in established cartilage tumors.

1.3.3 Other Signaling Pathways and Mutations Implied in Enchondroma and Chondrosarcoma

In the past few decades research has unraveled our understanding of the regulation of chondrocyte maturation and growth plate development. Disruption of some of these regulatory pathways leads to defects of chondrocyte differentiation, and sometimes formation of enchondroma-like lesions in mice. In this section, I will discuss some signaling pathways and mutations that are implied in these cartilage tumors.

1.3.3.1 Hedgehog Signaling

Hedgehog signaling pathway is constitutively active in some cases of enchondromas [142]. Independent studies have identified distinct mutations in *PTHR1* gene from enchondroma tumors. One of the mutations (R150C) was a hypermorphic mutation, and three other mutations (G121E, A122T, R255H) caused loss-of-function [3, 6, 143]. Animals expressing mutant *R150C PTHR1* in chondrocytes developed abnormal

cellular cartilage islands in the proximity of growth plate cartilage, which resembled patient enchondromas. Studies in mice showed that the mutant *R150C PTHR1* caused constitutive active Hedgehog signaling. Overexpression of the Hedgehog regulated transcriptional factor *Gli2* led to the formation of similar cartilage lesions [3]. Recently, Deng et al. showed that activating Hedgehog signaling pathway by deleting patched 1 (*Ptch1*) gene in mesenchymal stem cells also induced formation of enchondromas in mice. In addition to Hedgehog signaling, *Ptch1* deletion also led to activated Wnt (Wingless/integrated) / β -catenin signaling pathway and pharmacological inhibition of Wnt/ β -catenin *in vivo* suppressed tumor formation. Together these data suggested Wnt/ β -catenin could be downstream of Hedgehog activation in enchondromas and Wnt/ β -catenin signaling could be a potential therapeutic target for enchondromas [144].

1.3.3.2 MAPK/ERK pathway

Multiple groups have demonstrated that Mitogen-activated protein kinase / extracellular-signal-regulated kinase (MAPK/ERK) signaling pathway plays important roles in regulating chondrocyte differentiation. In 2014, Chen et al. showed that conditionally deleting *Erk2* in *Osx*-expressing cells in *Erk1^{-/-}* mice caused expanded hypertrophic zone during development and formation of enchondroma-like lesions after birth [145]. The effects were not present when the authors conditionally deleted *Erk2* in *Col1a1*-expressing cells. As *Osx* is expressed by hypertrophic chondrocytes and osteoblasts and *Col1a1* is only expressed by mature osteoblasts, these data suggested that

the phenotypes were resulted from defects in terminal differentiation of hypertrophic chondrocytes due to the loss of *Erk1* and *Erk2* in chondrocytes [145]. The authors suggested that *Erk1/2* regulated chondrocyte terminal differentiation through the transcription factor early growth response 1/2 (*Egr1/2*) [145]. The tyrosine phosphatase Src homology region 2 domain-containing phosphatase-2 (SHP2), encoded by the *Ptpn11* gene, is a ubiquitously expressed non-receptor protein tyrosine phosphatase that is characterized by a Src-homology-2 domain. SHP2 is known to activate ERK1/2 pathway as deletion of *Ptpn11* resulted in reduced level of phospho-ERK1/2, but the precise targets remain controversial [146, 147]. Bowen et al. showed that deleting *Ptpn11* in chondrocytes postnatally disrupted the organization of growth plate and induced formation of enchondroma-like lesions in the mice [148]. In 2017, Wang et al. demonstrated that ablating *Ptpn11* in *Co10a1*-expressing hypertrophic chondrocytes impaired transdifferentiation of chondrocytes to osteoblasts via enhanced *Sox9* expression [149].

1.3.3.3 Retinoblastoma Protein (pRb) Pathway

The tumor suppressor retinoblastoma protein pRB is important for proper chondrocyte development. pRB, p107, and p130 are members of the pocket protein family [150]. They regulated proliferation via interactions with E2F family of transcription factors [150]. Conditionally deleting *Rb* in *p107^{-/-}* mesenchymal stem cells caused defects in long bone development [151]. Embryos of these *Rb^{CKO};p107^{-/-}* animals

had expanded and disorganized proliferating and hypertrophic zones at E17.5 [151]. These animals developed enchondroma-like lesions at 6 months [151]. The enchondroma phenotypes of these animals were mediated through *E2f3a* or *E2f3b* [151]. Along the same line, it was reported that combinatorial deletion of *p107* and *p130* resulted in deregulated chondrocyte proliferation and defects in hypertrophic chondrocyte differentiation [152, 153].

1.3.3.4 FGF signaling pathway

In 2015, Zhou et al. showed that fibroblast growth factor receptor 3 (*Fgfr3*) deficiency in chondrocytes led to dysregulation of growth plate chondrocytes and formation of enchondromas and osteochondromas [154]. These cartilage lesions displayed impaired MAPK signaling activation and enhanced *Ihh* and *Pthlh* expression [154]. Smoothened inhibitor treatment significantly reduced chondroma formation in the *Fgfr3*-deficiency mice, further suggesting that FGFR3 might regulate chondrocyte maturation and chondroma formation partially via overactivation of Hedgehog signaling [154].

1.3.3.5 PTEN-PI3K pathway

The tumor suppressor phosphatase and tensin homolog (PTEN) also has a regulatory role in chondrocyte maturation. Targeted deletion of *Pten* in chondrocytes caused severe dyschondroplasia and formation of cartilage lesions, however, these neoplasms disappeared at 6 months of age [155]. The authors showed that *Pten*

deficiency was associated with increased ER stress and activation of Hif-1 α signaling [155].

1.3.3.6 Other Mutations in Enchondroma

In addition to mutations in *IDH1/2* genes and genes in the Hedgehog signaling pathway, other mutations have also been reported in enchondroma tumors. Using whole-genome sequencing and target exon sequencing, Totoki et al. reported that 13 / 41 (31.7%) of enchondroma samples harbored somatic missense mutation of *COL2A1*, a gene encoding alpha 1 chain of type II collagen, an essential component for the cartilage extracellular matrix [156]. They also found that 2.4% of the enchondroma tumors had a non-sense somatic mutation in *YEATS2*, a gene encoding for a subunit of an acetyltransferase complex [156]. Somatic missense mutations in *ACVR2A*, a gene encoding a type II receptor for activin / bone morphogenic protein (BMP) signaling, were found in 7.3% of enchondroma cases [156]. In 2019, Saiji et al. identified a germline missense mutation of the tumor suppressor gene serine/threonine kinase 11 (*STK11*) in a patient with enchondromatosis [157]. As previous studies showed that mice lacking *Stk11* in chondrocytes failed to terminal differentiate and could develop enchondroma-like lesions, this study suggested *STK11* could play a similar role in tumorigenicity of enchondromatosis in human [158, 159].

1.3.4 Progression from Enchondromas to Chondrosarcomas

When enchondromas occur as multiple lesions, they have a high chance to progress to malignant central chondrosarcoma. Disrupted signaling pathways that are implied in enchondromas also play roles in chondrosarcomas.

Active Hedgehog signaling is reported in chondrosarcomas. Whole-exome sequencing revealed that 18% of chondrosarcoma tumors harbored mutations in the IHH signaling pathway resulting in IHH activation [160]. Suppressing Hedgehog signaling decreased proliferation, cellularity, and tumor size of chondrosarcomas [142]. Deleting *p53* in *Gli2* overexpressing chondrocytes predisposed the mice to develop larger cartilage lesions that resembled malignant chondrosarcomas [161]. Deficiency in *p53* and overactivation of *Gli2* mediated apoptosis in neoplastic chondrocytes via insulin growth factor (IGF) signaling [161]. Furthermore, *Igf2* deficiency resulted in fewer cartilage lesions in *Gli2* overexpressing mice [161]. Although preclinical studies showed that active Hedgehog signaling was critical for chondrosarcoma tumor growth, Hedgehog pathway antagonists (IPI-926 and GDC-0449) did not reach the clinical endpoints in two independent clinical trials for chondrosarcomas [162, 163].

Mutations in *IDH1/2* are present in about 50% of chondrosarcoma tumors [10, 11]. Li et al. found that knocking out mutant *IDH1* in chondrosarcoma cells suppressed tumorigenicity in vitro and in vivo [164]. The authors showed that deleting mutant *IDH1* caused downregulation of multiple integrin genes. Blocking integrin $\alpha5\beta1$ and $\alpha\nu\beta5$ in

IDH1 mutant chondrosarcoma cells decreased cells' migration in vitro. Hence they speculated that mutant *IDH1* might regulate the cell – extracellular matrix interaction of chondrosarcomas by altering integrin gene expression [164]. Integrin signaling has been shown to be important for chondrocyte differentiation, hence it may also be a potential mechanism regulating enchondroma formation [165]. Increased glutamine metabolism is another potential mechanism by which *IDH* mutations regulate tumorigenicity [166]. Glutamine was shown to be the primary carbon source for D-2HG production in chondrosarcoma [167]. Chondrosarcomas were reported to rely on glutamine metabolism for viability [166]. The expression level of glutaminase was significantly higher in high-grade chondrosarcomas when compared to enchondromas and low-grade chondrosarcomas, suggesting glutamine metabolism might play different roles at different stages of tumor development [166]

2. Intracellular Cholesterol Biosynthesis in Enchondroma and Chondrosarcoma

Part of this work has been published:

Zhang, H., Wei, Q., Tsushima, H., Puviindran, V., Tang, Y. J., Pathmanapan, S., Poon, R., Ramu, E., Al-Jazrawe, M., Wunder, J., & Alman, B. A. (2019). Intracellular cholesterol biosynthesis in enchondroma and chondrosarcoma. *JCI insight*, 5(11), e127232.

<https://doi.org/10.1172/jci.insight.127232>

2.1 Summary

Enchondroma and chondrosarcoma are the most common benign and malignant cartilaginous neoplasms. Mutations in isocitrate dehydrogenase 1 and 2 (*IDH1/2*) are present in the majority of these tumors. We performed RNA-seq analysis on chondrocytes from *Col2a1Cre;Idh1^{LSL/+}* animals and found that genes implied in cholesterol synthesis pathway were significantly upregulated in the mutant chondrocytes. We examined the phenotypic effect of inhibiting intracellular cholesterol biosynthesis on enchondroma formation by conditionally deleting SCAP (sterol regulatory element-binding protein cleavage-activating protein), a protein activating intracellular cholesterol synthesis, in IDH1 mutant mice. We found fewer enchondromas in animals lacking SCAP. Furthermore, in chondrosarcomas, pharmacological inhibition of intracellular cholesterol synthesis significantly reduced chondrosarcoma cell viability in vitro and reduced tumor burden in vivo. Taken together, these data suggest that intracellular cholesterol synthesis is a potential therapeutic target for enchondromas and chondrosarcomas.

2.2 Introduction

Cartilage tumors as a group are the most common neoplasms affecting the bone [118]. They include benign tumors such as enchondromas or osteochondromas and malignant cancers such as chondrosarcomas [6]. Enchondromas arise from dysregulated growth plate chondrocytes that fail to undergo terminal differentiation and remain at

the end of the bone [6, 8]. They can occur within the medullary bone as a single lesion or as multiple lesions (enchondromatosis) in conditions termed Ollier disease and Maffucci syndrome [6]. Multiple enchondromas in Maffucci syndrome are associated with up to 50% chance of these lesions undergoing malignant transformation to form chondrosarcomas [7, 8]. Chondrosarcoma is the second most common malignant primary bone tumor and is resistant to chemotherapy and radiation therapy [121]. Somatic mutations in the isocitrate dehydrogenase 1 and 2 (*IDH1* and *IDH2*) genes are identified in the majority of enchondromas, and about half of chondrosarcomas [9-11]. Expression of a mutant *Idh1* in chondrocytes is sufficient to initiate enchondroma formation in mice by disrupting chondrocyte differentiation [4]. When the mutant *Idh1* was expressed in chondrocytes during development, the mice displayed severe defects in chondrocytes differentiation and could not survive after birth. When the mutant *Idh1* was expressed in chondrocytes postnatally, the mice developed enchondromatosis [4]. D-2-hydroxyglutarate (D-2HG), a commonly believed “oncometabolite”, is produced from mutant IDH enzymes at high levels. However, inhibition of D-2HG production did not alter cell viability of chondrosarcomas, suggesting mutant IDH enzymes may promote tumor growth via other mechanisms [7].

Intracellular cholesterol biosynthesis plays a crucial role in chondrocyte development. This process is regulated by the protein SCAP (sterol regulatory element-binding protein cleavage-activating protein). When intracellular cholesterol level is low,

SCAP cleaves and activates the transcription factors SREBPs (sterol regulatory element-binding proteins) [59]. After cleavage, SREBPs are further processed and translocate to the nucleus to activate genes responsible for cholesterol biosynthesis [59]. Genetic deletion of *Scap* in chondrocytes affected their differentiation and viability [82]. In addition, pharmacological inhibition of cholesterol synthesis by statin drugs caused reduced endochondral bone growth and decreased height of the growth plate [78]. Furthermore, statin drugs rescued chondrocyte differentiation and bone length in models of achondroplasia [66].

Deregulation of cholesterol homeostasis has been identified in multiple cancer types and is believed to be an important contributing factor to cancer progression [168]. Upregulation of cholesterol synthesis pathway is associated with decreased patient survival in sarcoma, acute myeloid leukemia, and melanoma [168]. Serum and intracellular cholesterol levels may not always be directly related, and studies suggest that intracellular cholesterol homeostasis may have a more important role in cancers than the serum cholesterol [168]. Despite this information, the role of cholesterol in cartilage tumors is not known.

Here, I investigated the role of cholesterol biosynthesis using a genetic mouse model that expressed mutant IDH1^{R132Q} and primary human patient chondrosarcoma samples. I identified that genes encoding for enzymes in the intracellular cholesterol biosynthesis were significantly upregulated in the IDH1^{R132Q} murine costal chondrocytes.

Upon deleting a positive regulator of cholesterol biosynthesis, formation of enchondromas was reduced. In human chondrosarcoma samples, patients with mutations in *IDH1* had higher levels of cholesterol in their tumors. Upon pharmacological inhibition of cholesterol biosynthesis, cell viability of chondrosarcoma cells was reduced in vitro, and tumor growth of patient-derived chondrosarcoma xenografts was suppressed in vivo. Together, these data suggested intracellular cholesterol biosynthesis was critical for the formation and growth of enchondroma and chondrosarcoma

2.3 Results

2.3.1 *Col2a1Cre;Idh1^{LSL/+}* chondrocytes exhibited distinct gene expression profiles.

We generated a mouse expressing IDH1^{R132Q} in chondrocytes by crossing a mouse expressing a conditional *Idh1*- R132Q knock-in allele [169] with a mouse expressing Cre recombinase driven by regulatory elements of the type two collagen gene (*Col2a1*-Cre) [170] To determine how *Idh1* mutation regulates chondrocyte differentiation, I performed an unbiased RNA-sequencing analysis on primary costal chondrocytes isolated from *Col2a1Cre;Idh1^{LSL/+}* animals and *Idh1^{LSL/+}*, *Col2a1Cre* littermate controls. RNA sequencing revealed distinct gene expression profiles between *Col2a1Cre;Idh1^{LSL/+}* chondrocytes and the two control groups ([GSE123130](#)) (Fig 8).

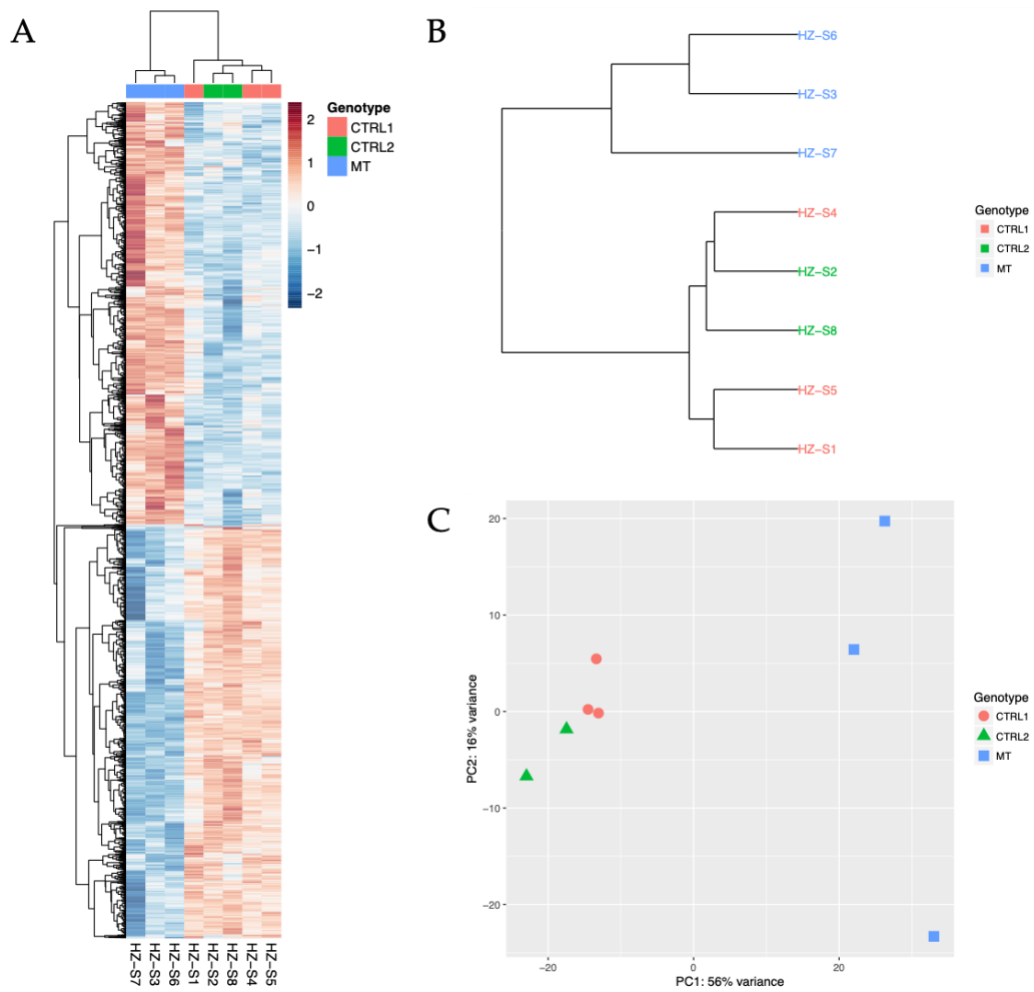


Figure 8 RNA sequencing revealed distinct gene expression profile in *Col2a1Cre;Idh1^{LSL/+}* chondrocytes.

Heatmap (A), hierarchical clustering (B), and principal component analysis (C) of RNA sequencing on costal chondrocytes from *Col2a1Cre;Idh1^{LSL/+}* (MT, $n = 3$), *Col2a1Cre* (CTRL1, $n = 3$), and *Idh1^{LSL/+}* (CTRL2, $n = 2$) mice at E18.5. Littermates were used for the analysis.

2.3.2 *Col2a1Cre;Idh1^{LSL/+}* chondrocytes had increased intracellular cholesterol levels, which was likely due to increased cholesterol biosynthesis.

Gene set enrichment analysis (GSEA) showed that genes regulating cholesterol biosynthesis pathway were significantly upregulated in *Col2a1Cre;Idh1^{LSL/+}* chondrocytes (Fig 9A). Enzymes in the mevalonate pathway (Fig 9B), which is an essential process for cholesterol synthesis, were consistently upregulated in *Col2a1Cre;Idh1^{LSL/+}* chondrocytes (Fig 9C). *Srebf2*, the gene encoding for the transcription factor that activates cholesterol synthesis, was significantly upregulated (Fig 9C). We confirmed the upregulation of genes in the pathway such as *Hmgcr*, the rate limiting enzyme in the mevalonate pathway, by qPCR (Fig 9D).

To determine whether mutation in *Idh1* led to changes in cholesterol levels, we performed filipin staining on primary costal chondrocytes isolated from *Col2a1Cre;Idh1^{LSL/+}* animals and their *Col2a1Cre* littermate controls. Filipin is a highly fluorescent chemical compound that binds to cholesterol specifically. When we treated chondrocytes with filipin, we found significantly higher levels of filipin staining intensity in *Col2a1Cre;Idh1^{LSL/+}* chondrocytes compared to chondrocytes from control animals (Fig 10A, B). Together, these data suggest cholesterol level was significantly increased in chondrocytes expressing mutant *Idh1*, which might be due to upregulation of intracellular cholesterol biosynthesis.

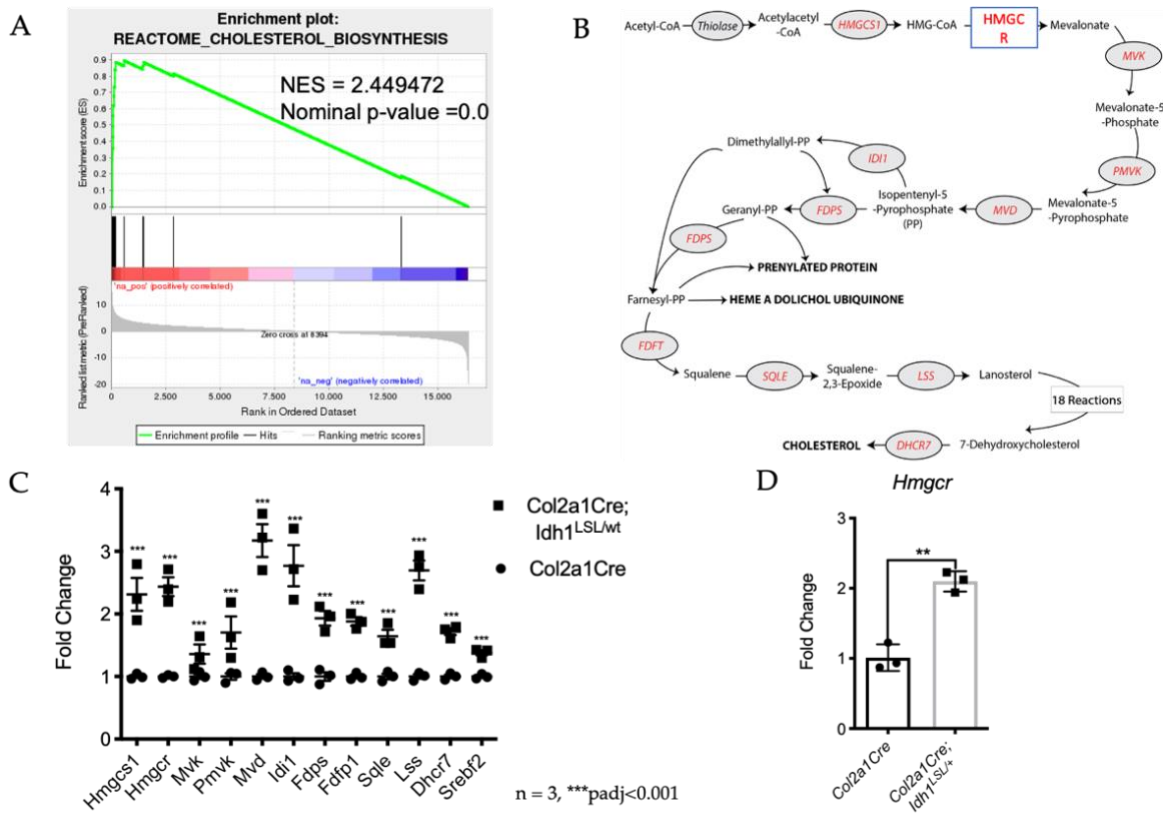


Figure 9 Genes in cholesterol biosynthesis pathway were significantly upregulated in *Col2a1Cre;Idh1^{LSL/+}* chondrocytes.

(A) Gene set enrichment analysis of the cholesterol biosynthesis pathway from RNA-sequencing. (B) The metabolic pathway of intracellular cholesterol biosynthesis. (C) Relative fold change of genes regulating and involved in intracellular cholesterol biosynthesis pathway ($n=3$), $***padj<0.001$. Padj was calculated to control for multiple hypothesis testing. (D) qPCR of *Hmgcr* of costal chondrocytes isolated from *Col2a1Cre* and *Col2a1Cre;Idh1^{LSL/+}* animals at E18.5 ($n = 3$). $**P < 0.01$, unpaired, 2-tailed

Student's *t* test. Mean \pm 95% confidence intervals are shown.

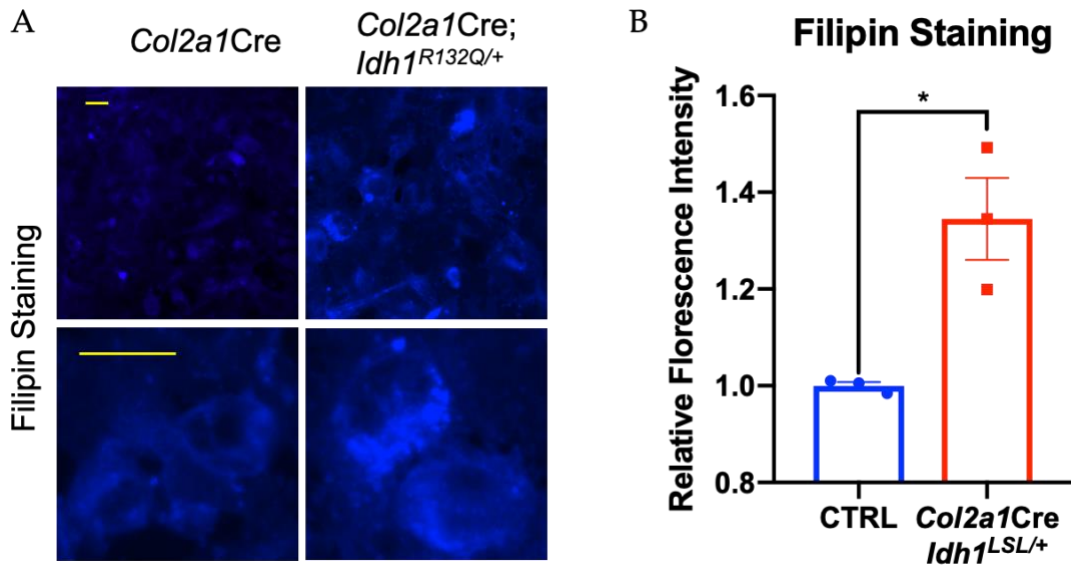


Figure 10 Cholesterol levels were higher in *Col2a1Cre;Idh1^{LSL/+}* chondrocytes.

(A) Representative filipin staining of costal chondrocytes isolated from *Col2a1Cre* and *Col2a1Cre;Idh1^{LSL/+}* mice at E18.5. (B) Quantification of the filipin staining intensity. The control group included one *Col2a1Cre* animal and two wild-type animals. Littermates were used for the analysis. Scale bars: 25 μ m. $n = 3$. * $P < 0.05$, unpaired, 2-tailed Student's *t* test. Mean \pm 95% confidence intervals are shown.

2.3.3 Deleting *Scap* postnatally did not alter growth plate phenotype

To examine the role of cholesterol biosynthesis in chondrocytes, we genetically deleted SCAP (sterol regulatory element-binding protein cleavage-activating protein) in chondrocytes postnatally. SCAP is a positive regulator of intracellular cholesterol biosynthesis. It activated the pathway by cleaving and activating transcription factors SREBPs (sterol regulatory element-binding proteins) [59]. During embryonic development, deleting *Scap* in mesenchymal stem cells or chondrocytes led to severe defects in endochondral ossification [82].

We generated *Col2a1*Cre^{ERT2};*Scap*^{*fl/fl*} (*Scap*-CKO) mice where *Scap* was conditionally deleted in *Col2a1* expressing cells upon tamoxifen administration at four weeks. Recombination was confirmed by PCR. The phenotype of the growth plate cartilage in *Scap*-CKO mice was examined at 6-month-old. Histological evaluation by safranin O did not reveal an obvious phenotype in the growth plate cartilage of *Scap*-CKO mice (Fig 11A). The presence of early-stage chondrocytes in the growth plate was not altered, as shown by immunohistochemistry of SOX9 (Fig 11B). Hypertrophic differentiation of growth plate chondrocytes was not affected by *Scap* deletion, as shown by immunohistochemistry of type X collagen (Fig 11C). Deletion of *Scap* did not cause abnormal cell proliferation, as shown by immunohistochemistry of Ki67 (Fig 11D). Together these data suggest growth plate chondrocytes in adult mice were not affected by *Scap* deletion under physiological condition.

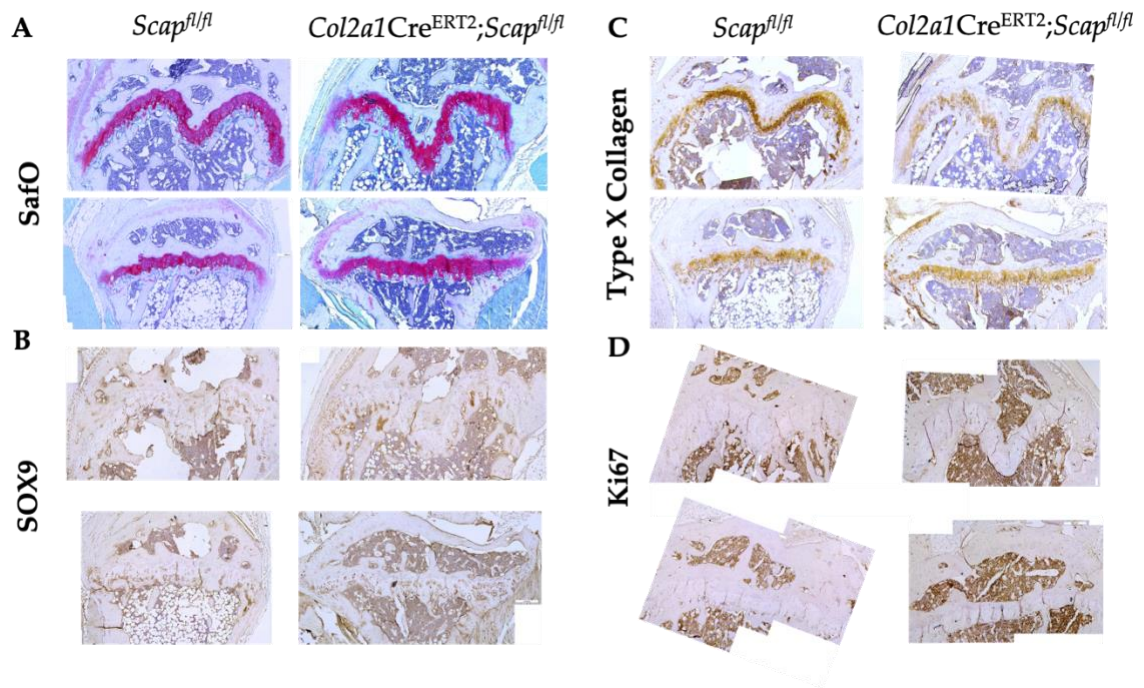


Figure 11 Deleting *Scap* postnatally did not cause a noticeable phenotype in the growth plate chondrocytes.

SafraninO (A) and immunohistochemistry of SOX9 (B), type X collagen (C), and Ki67 (D) did not reveal any differences between the growth plates from *Scap*-CKO animals and their *Scap*^{fl/fl} littermate control animals.

2.3.4 Deleting *Scap* reduced enchondroma-like lesion formation in *Col2a1Cre;Idh1*^{LSL/+} animals.

Next, I examined the role of intracellular cholesterol biosynthesis during enchondroma formation. We generated *Col2a1Cre*^{ERT2}; *Scap*^{fl/fl}; *Idh1*^{LSL/+} mice where *Scap* deletion and mutant *Idh1* expression were simultaneously induced by tamoxifen administration in *Col2a1* expressing cells.

I observed that in the absence of *Scap*, mice still developed enchondroma-like lesions (Fig 12). However, when I quantified the number and volume of these lesions, I

noticed that the number and size of enchondroma-like lesions were significantly reduced in *Col2a1Cre^{ERT2};Idh1^{LSL/+}* animals lacking *Scap* (Fig 13). These data show that inhibiting cholesterol synthesis reduced enchondroma-like lesion formation in *Col2a1Cre^{ERT2};Idh1^{LSL/+}* mice, suggesting cholesterol biosynthesis could be a potential drug target for patients with enchondromas.

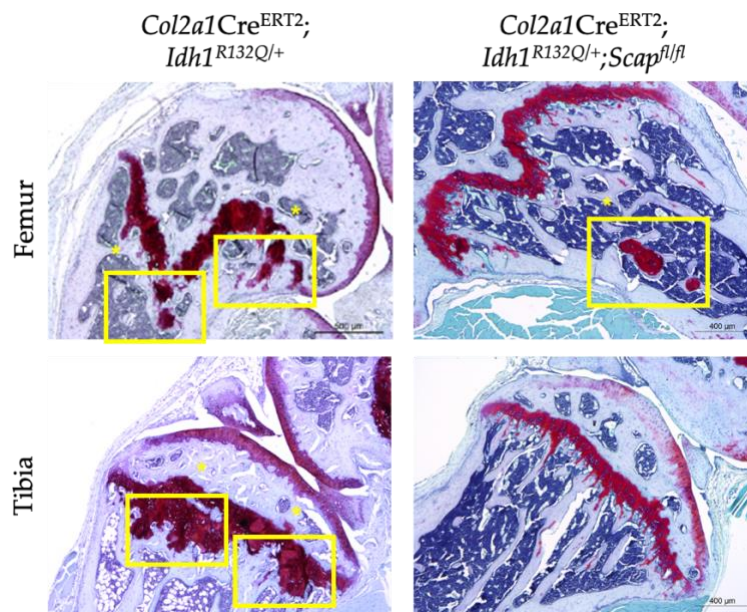


Figure 12 Representative Safranin O staining of tibia and femur growth plates of mice

Enchondroma like-lesions were marked by asterisks and squares.

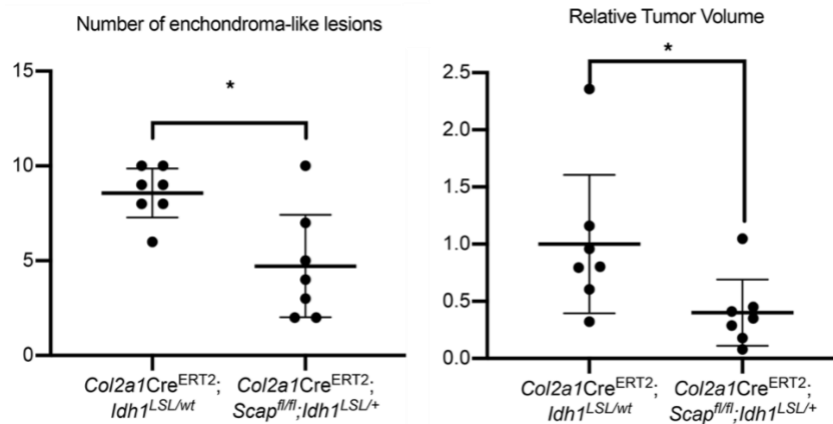


Figure 13 Quantification of enchondroma-like lesions in animals of indicated genotypes.

Number and volume of enchondroma-like lesions. Each data point represents one animal. n = 7. *p < 0.05, unpaired, 2-tailed Student's t test. Mean ± 95% confidence intervals are shown.

2.3.5 Pharmacological inhibition of cholesterol synthesis reduced chondrosarcoma growth in vitro and in vivo.

Enchondromas can progress into malignant chondrosarcomas. To examine the role of intracellular cholesterol in chondrosarcoma, we first evaluated cholesterol levels in chondrosarcomas with or without *IDH* mutations. We measured cholesterol levels in cryopreserved primary chondrosarcoma tissues from patients with wild type or mutant *IDH1* enzymes. Chondrosarcoma tumors with mutant *IDH1* had significantly higher cholesterol levels than the tumors with wildtype *IDH1/2* (Fig 14A). To modulate cholesterol synthesis in chondrosarcoma, we treated primary chondrosarcoma cells derived from five different patients with lovastatin, which inhibits HMG-CoA reductase, the rate limiting enzyme in cholesterol biosynthetic pathway [59]. One of the five patient

samples was wildtype for *IDH1/2* and the other four samples had *IDH1* mutation.

Treatment of chondrosarcoma cells with lovastatin caused a significant reduction of cell viability in vitro (Fig 14B). We also treated chondrosarcoma explants that were derived from the five patients with lovastatin in vitro. The proliferation rate in chondrosarcoma explants was significantly reduced as shown by immunohistochemistry of Ki67 (Fig 14C, D). Chondrosarcoma thus joins other tumor types that cholesterol synthesis inhibition reduced their cell viability [171].

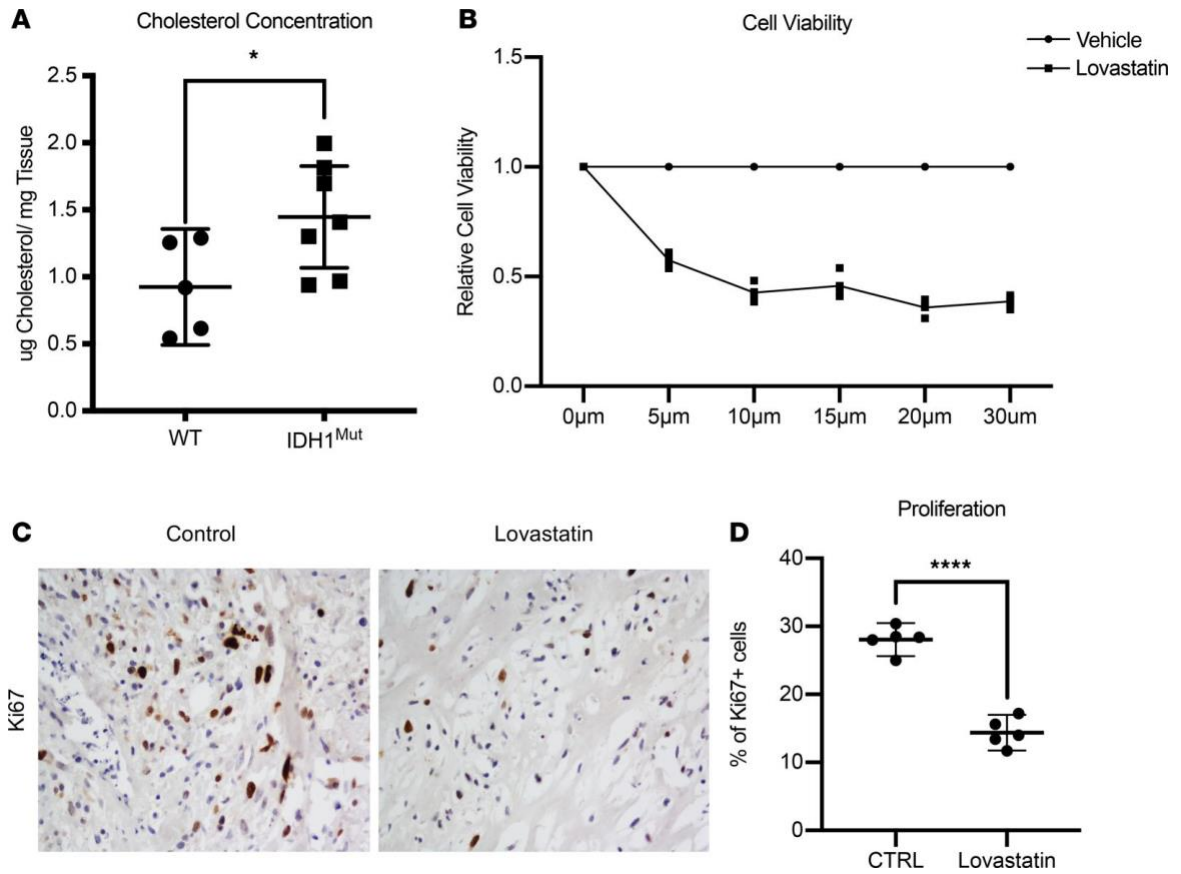


Figure 14 Lovastatin inhibited chondrosarcoma viability in vitro.

(A) Cholesterol concentration in primary chondrosarcoma tumors with wild-type *IDH1/2* (n = 5) or mutant *IDH1* (n = 7). (B) Relative cell viability of chondrosarcoma cells after lovastatin treatment for 48 hours at indicated concentrations in vitro (n = 5). (C) Representative immunohistochemistry for Ki67 on chondrosarcoma explants treated with vehicle control or lovastatin (original magnification, ×200). (D) Quantification of the percentage of Ki67-positive cells in C (n = 5). For A, B, and D, each data point represents a chondrosarcoma sample from an individual patient. *P < 0.05, ****P < 0.0001, unpaired, 2-tailed Student's t test. Mean ± 95% confidence intervals are shown.

To examine the effects of lovastatin on chondrosarcoma growth in vivo, we generated patient-derived xenografts of chondrosarcomas in NOD-scid-gamma mice as previously described [172]. We examined tumor growth in xenografts established from five different patient tumors. Each patient derived chondrosarcoma was xenografted to ten animals. Five animals were treated with vehicle control and five animals were treated with lovastatin. The treatment started when the tumor became palpable. For each individual human xenograft, control and lovastatin treatments were started at the same time. In sample #1, *IDH1* and *IDH2* were wildtype. Sample #2, #3, #4, and #5 harbor mutations in *IDH1*. After 4 weeks of treatment, tumor weight was measured (Fig 15).

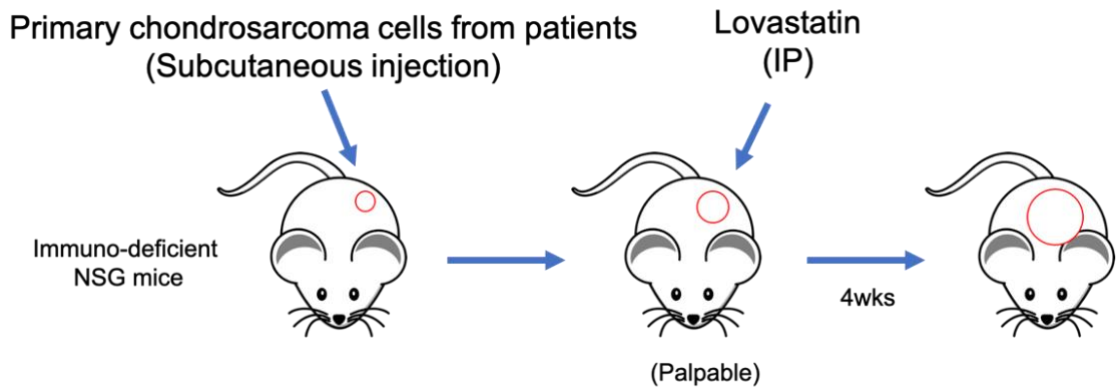


Figure 15 Illustration for patient-derived xenograft experiment.

We normalized the tumor weight of each tumor to the average tumor weight of the control group derived from the same patient because there was a high degree of variation among tumor weights from different patients. On average, the mice in the lovastatin group displayed 30% reduction in tumor weight after 4 weeks of treatment (Fig 16).

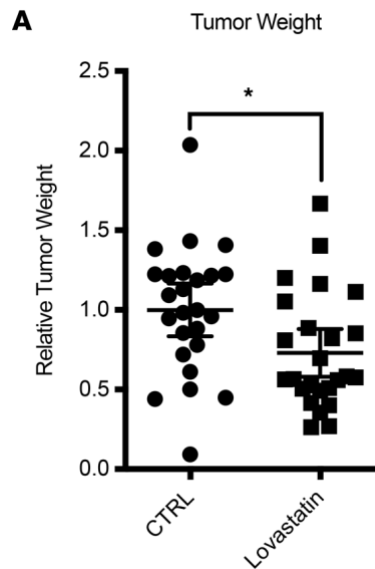


Figure 16 Lovastatin inhibited chondrosarcoma growth in vivo.

Relative tumor weight of chondrosarcoma xenografts after vehicle or lovastatin treatment. $n = 25$. * $p < 0.05$, unpaired, 2-tailed Student's t test. Mean \pm 95% confidence intervals are shown.

Proliferation rate of the xenografted chondrosarcoma tumors was examined by immunohistochemistry of BrdU. Lovastatin reduced proliferation in all five patient derived tumor xenografts (Fig 17). Apoptosis was examined by immunohistochemistry of cleaved caspase 3. For four of five patient-derived xenografts, the average apoptosis rates were increased by lovastatin treatment. For Sample #1 (IDH1/2-wt), the percentage of cleaved caspase 3 positive cells was not altered by lovastatin treatment (Fig 18), suggesting apoptosis in IDH1/2-wt chondrosarcomas might not be affected by inhibition of intracellular cholesterol biosynthesis in vivo.

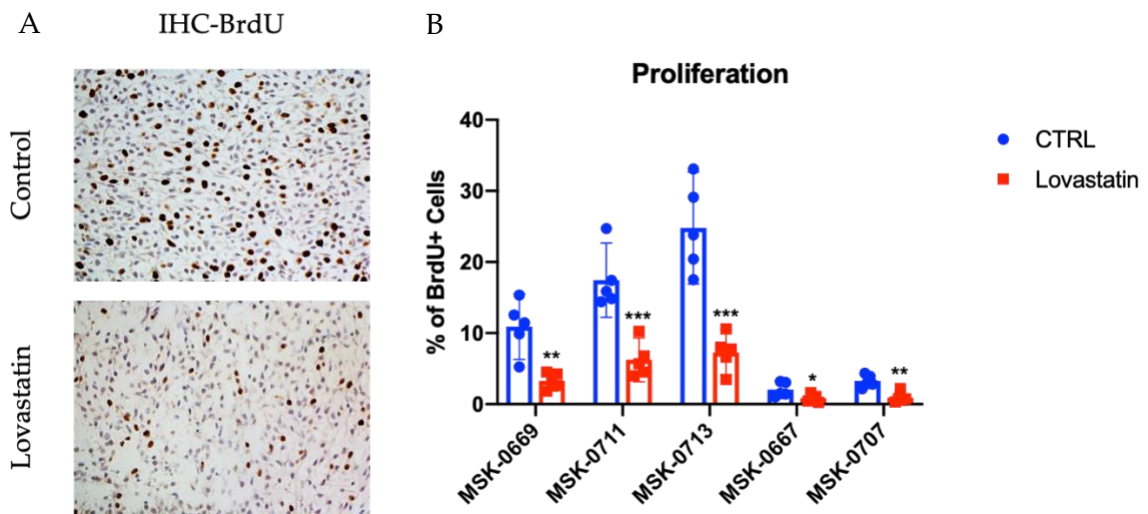


Figure 17 Lovastatin suppressed proliferation of chondrosarcoma cells in vivo.

(A) Representative images of BrdU staining on xenografted tumors (original magnification, $\times 200$). (B) Percentage of BrdU positive cells in the control group and lovastatin treatment group of five different patient derived tumor xenografts. For each

patient-derived xenograft, n=5. *p<0.05, **p<0.01, ***p<0.001. p-value was determined by unpaired, two-tailed student t test. Means ±95% confidence intervals were shown.

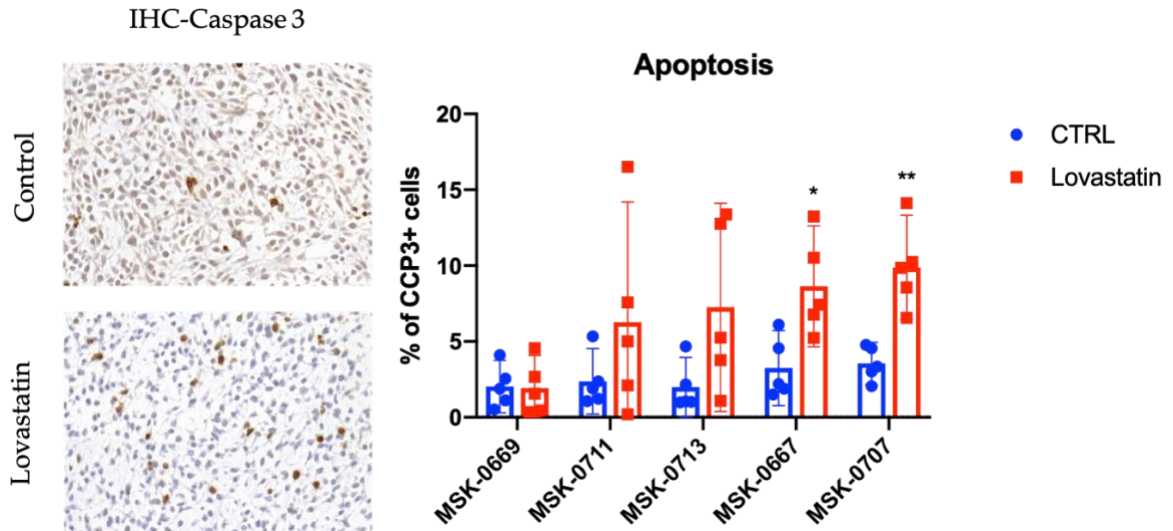


Figure 18 Lovastatin caused increased apoptosis in some IDH1 mutant chondrosarcomas.

(A) Immunohistochemistry of cleaved caspase-3 on xenografted tumors (original magnification, ×200). (B) Percentage of cleaved caspase 3 positive cells in the control group and lovastatin treatment group of five different patient derived tumor xenografts. For each patient-derived xenograft, n=5. *p<0.05, **p<0.01. p-value was determined by unpaired, two-tailed student t-test. Means±95% confidence intervals were shown.

2.4 Discussion

IDH1/2 are the most commonly mutated genes in enchondromas and chondrosarcomas. Mutation of *Idh1* in chondrocytes causes defects in their terminal differentiation and results in the formation of enchondroma-like lesions. In this study, we found that *Idh1* mutation in chondrocytes increased intracellular cholesterol biosynthesis, which was important in regulating the number and size of enchondroma-

like lesions, the viability of chondrosarcoma cells, and the tumor growth of chondrosarcomas.

At the time of analysis, some enchondroma-like lesions had grown separate from the growth plates and some remained attached to the growth plates in both *Col2a1Cre^{ERT2};Idh1^{LSL/+}* and *Col2a1Cre^{ERT2};Scap^{fl/fl};Idh1^{LSL/+}* animals. In human patients with enchondromatosis, the tumors are located attached to the growth plates initially and stay in this location after the growth plates close. Because the growth plates never close in mice, the enchondroma-like lesions that formed later during growth would usually remain attached to the growth plate throughout life.

Intracellular cholesterol regulates chondrocyte differentiation under various conditions. During development, genetic deletion of regulators of cholesterol synthesis disrupted the hypertrophic differentiation of chondrocytes and resulted in shortening limbs by altering hedgehog signaling [82]. In an achondroplasia model with FGFR3 gain-of-function mutation, statins restored chondrocyte differentiation and caused significant bone recovery, suggesting cholesterol could regulate chondrocyte differentiation via crosstalk with FGF signaling [66]. In addition, it was reported abnormal cholesterol levels were associated with the development of osteoarthritis [173].

The mechanisms of which cholesterol biosynthesis regulates tumor growth of enchondromas and chondrosarcomas are not fully elucidated. However, deregulation of cholesterol biosynthesis is known to contribute to cancer growth of other cancer types

via multiple mechanisms [168]. In prostate cancer, upregulation of cholesterol via PI3K/AKT/mTOR signaling promoted cancer aggressiveness and bone metastases [168, 174]. In hepatocellular carcinoma and colon cancer, increased mitochondrial cholesterol content induced resistance to apoptosis [168, 175]. Statins have been used alone or combined with other drugs for multiple types of cancers over the past few decades. They have shown to be especially effective in the treatment of mesenchymal-like cancer cells [168, 176].

Previous studies showed expression of wildtype and mutant *Idh1* is activated by SREBP1 and SREBP2 (encoded by *Srebf1* and *Srebf2*) in livers as well as multiple cancer cell lines [79, 177, 178], and our study demonstrated mutant *Idh1* upregulated *Srebf2*. Since expression of mutant IDH1 has been previously shown to affect histone modification and DNA methylation [134, 135], it may be possible that expression of *Srebf2* in *Idh1* mutant chondrocytes could be altered via epigenetic changes. Mutant IDH1 is also known to cause metabolic reprogramming, such as changing redox states [179], which could also be a potential mechanism that regulates intracellular cholesterol biosynthesis.

In conclusion, our study demonstrated intracellular cholesterol synthesis was upregulated in *Col2a1Cre;Idh1^{LSL/+}* chondrocytes. Genetic and pharmacological inhibition of intracellular cholesterol synthesis suppressed growth in enchondroma-like lesions and chondrosarcoma. Our study identified cholesterol synthesis pathway as a potential

therapeutic target in enchondroma and chondrosarcoma, which currently do not have any universally effective therapeutics. As *IDH1/2* are also frequently mutated in other cancers such as glioblastoma and acute myeloid leukemia, our data suggested statin drugs could be a potential therapeutic for these cancers as well.

3. Glutamine Metabolism in Enchondroma and Chondrosarcoma

3.1 Summary

Enchondromas and chondrosarcomas are common benign and malignant cartilage neoplasms. The majority of these tumors harbor mutations of *IDH1* or *IDH2*. Glutamine metabolism has been implied as a critical regulator of tumors with *IDH1/2* mutations. Chondrocytes and chondrosarcomas with mutations in *IDH1/2* genes showed enhanced glutamine utilization for downstream metabolism. Using genetic and pharmacological approaches, we demonstrated that glutaminase-mediated glutamine metabolism played distinct roles in enchondromas and chondrosarcomas with mutations in *IDH* genes. Genetic ablation of glutaminase in chondrocytes with *Idh1* mutation increased the number and size of enchondroma-like lesions. Pharmacological inhibition of glutaminase led to decreased tumor weight of chondrosarcoma xenograft. Mechanistically, glutamine regulated the differentiation, proliferation, and apoptosis in these tumors differently through different downstream metabolites. During enchondroma development, glutamine-derived α -ketoglutarate promoted hypertrophic chondrocyte differentiation and restricted chondrocyte proliferation. In chondrosarcoma, glutamine-derived non-essential amino acids prevented cell apoptosis.

3.2 Introduction

Cartilage tumors as a group are the most frequent tumors affecting the bone [118]. Enchondroma is one of the most common benign cartilaginous neoplasia and is estimated to be present in 3% of the total population [119, 120]. These tumors develop from dysregulated chondrocyte differentiation in the growth plate and are mostly present in the metaphysis of long bones [6]. In patients with multiple enchondromatosis (more than one enchondroma lesions) such as Maffucci syndrome and Ollier disease, the risk of malignant transformation from enchondroma to chondrosarcoma is reported to be up to 60% [118]. Chondrosarcoma is the second most common primary malignancy of the bone [118]. They arise de novo or develop from preexisting benign tumors including enchondromas [118]. High-grade chondrosarcomas have high metastatic potential and poor prognosis after surgical resection [180]. Currently, no universally effective therapies are available for enchondromas or chondrosarcomas.

Somatic mutations of isocitrate dehydrogenase 1 and 2 (IDH1/2) are the most frequent genetic variations in enchondromas and chondrosarcomas [9-11, 181, 182]. They are present in 56% - 90.5% of enchondroma tumors [9, 10], and in about 50% of chondrosarcoma tumors [11, 181]. Although *IDH1/2* mutations underlie enchondromas and chondrosarcomas, it is not known whether these tumors share similar metabolic requirement for cell viability and tumor growth. Expression of mutant IDH1 enzyme in chondrocytes is sufficient to initiate enchondroma development in mice through

disrupted chondrocyte differentiation [4]. Wildtype IDH1 and IDH2 enzymes catalyze reversible conversion between isocitrate to α -ketoglutarate (α -KG) in the cytoplasm and the mitochondria respectively. Mutant IDH1/2 enzymes lost their original function and gains a neomorphic function that converts α -KG to D-2-hydroxyglutarate (D-2HG) [128-130]. D-2HG is considered as a putative “oncometabolite” in various cancers with mutations in *IDH1/2* as it competitive inhibits α -KG-dependent enzymes [132-137, 183]. Interestingly, pharmacological inhibition of mutant IDH1 enzyme did not alter chondrosarcoma tumorigenesis despite effective reduction of D-2HG synthesis, suggesting mutant IDH1/2 enzymes may be able to regulate cartilage tumor through mechanisms in addition to D-2HG production [7]. Recently, an investigation of the metabolomes in chondrosarcomas showed global alterations in cellular metabolism in *IDH1/2*^{Mut} chondrosarcomas, suggesting such alteration might be potential targets for cancers with *IDH1/2* mutations [184].

Glutamine metabolism is an important metabolic pathway that is critical for the survival of various cancers as well as proper proliferation and differentiation of different cell types [85, 108, 185-189]. Glutamine metabolism starts when glutaminase (GLS) deaminates glutamine to glutamate. Glutamate could be further used to generate α -ketoglutarate (α -KG), glutathione, other non-essential amino acids, and nucleotides, etc. Through different downstream metabolites, glutamine regulates cancer behaviors by modulating bioenergetics, biosynthesis, redox homeostasis, etc. [85]. In cancers with

IDH1/2 mutations, glutamine is utilized as the primary source for D-2HG production [129, 167, 190]. In addition, some tumors with *IDH1/2* mutations, such as glioma, acute myeloid leukemia (AML), and chondrosarcoma, are reported to be dependent on glutamine metabolism for tumor growth or cell viability [166, 191-193]. In non-cancerous cells, glutamine metabolism regulates cell differentiation mainly through the downstream metabolites α -KG and acetyl-CoA due to their roles in regulating histone modifying enzymes [108, 188].

In the context of cartilage tumors, it is unknown how glutamine regulates tumor development in enchondroma and chondrosarcoma. We therefore investigated these questions using a genetically modified mouse model of enchondroma and primary patient samples of chondrosarcoma. We found that *GLS* was upregulated in both the benign enchondroma and the malignant chondrosarcoma. However, deleting *Gls* in enchondroma mouse model led to increased number and size of these benign tumor-like lesions and delayed chondrocyte differentiation, whereas inhibiting *GLS* in *IDH1/2^{Mut}* chondrosarcoma led to reduced tumor weight and cell viability likely through compromised production of non-essential amino acids.

3.3 Results

3.3.1 Glutaminase is upregulated in IDH1/2^{Mut} human patient chondrosarcomas and IDH1^{Mut} murine chondrocytes

To understand the role of glutaminase in IDH1/2^{Mut} chondrosarcoma, we first examined the expression level of *Gls* in human patient chondrosarcoma tumors. We observed that expression of *Gls* was upregulated in chondrosarcomas with *IDH1* or *IDH2* mutations from a published mRNA profiling ([E-MTAB-7264](#)) of chondrosarcoma tumors from more than 100 patients (Fig 19) [194].

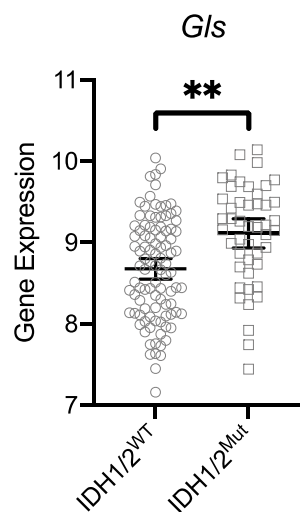


Figure 19: Expression of *Gls* in IDH1/2^{WT} and IDH1/2^{Mut} chondrosarcoma tumors.

Expression of *Gls* in IDH1/2^{WT} and IDH1/2^{Mut} chondrosarcoma tumors. **FDR < 0.01, Benjamin & Hochberg adjustment. Mean \pm 95% confidence intervals are shown.

Next, we determined if expression of mutant *Idh1* led to a change in GLS function in murine chondrocytes. Primary costal chondrocytes were isolated from postnatal day (P) 3 mice expressing the conditional IDH1^{R132Q} knock-in allele and then

transduced with adenovirus GFP (IDH1/2^{WT}) or adenovirus Cre (IDH1^{Mut}). GLS converts glutamine to glutamate. To determine the enzymatic activity of GLS in these chondrocytes, I cultured them with radioactive ³H-glutamine and measured the amount of ³H-glutamate and ³H-glutamine in the cells based on their radioactivity after eluting them out with positively charged HCl and uncharged H₂O respectively. GLS activity was determined by dividing the amount of ³H-glutamate by the sum of the amount of ³H-glutamate and ³H-glutamine (Fig 20A). Relative fold change of GLS activity was determined by normalizing the GLS activity of each sample to the average GLS activity of IDH1/2^{WT} chondrocytes. In primary chondrocytes expressing mutant *Idh1*, GLS activity was significantly upregulated by about 2.5-fold (Fig 20B).

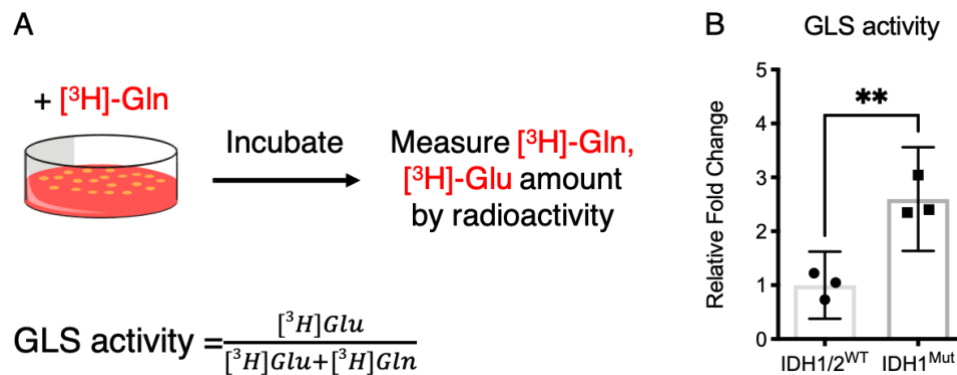


Figure 20 Glutaminase activity was upregulated in IDH^{Mut} murine chondrocytes.

(A) Experimental design for glutaminase (GLS) activity measurement. (B) GLS activity in IDH1/2^{WT} and IDH1^{Mut} murine chondrocytes. **p < 0.01, unpaired, 2-tailed Student's *t* test. Mean ± 95% confidence intervals are shown.

3.3.2 Chondrocytes and chondrosarcomas with mutations of IDH1/2 enzymes exhibited increased glutamine contribution to anaplerosis and non-essential amino acids production.

3.3.2.1 IDH1^{Mut} murine chondrocytes had increased glutamine contribution to anaplerosis and non-essential amino acids production

To investigate how chondrocytes with wildtype and mutant IDH1 enzymes utilize glutamine, we conducted ¹³C tracing experiment in them. Briefly, IDH1/2^{WT} and IDH1^{Mut} chondrocytes were cultured in glutamine-free high glucose DMEM media supplemented with 4mM ¹³C₅-glutamine. ¹³C contribution to downstream metabolites was determined by measuring the isotope-labeling pattern. If a metabolite is derived from ¹³C₅-Glutamine, it would be labeled with ¹³C, and thus has a heavier molecular weight when compared to the same molecule that was not derived from ¹³C₅-Glutamine. M+0, M+1, ..., M+n refers to the isotopologues containing n heavy atoms in a molecule. The stable isotope distribution of individual metabolites was measured by GC-MS. I cultured the chondrocytes for three hours and analyzed the ¹³C labeling in different metabolites. This was the time point when ¹³C labeling in the TCA cycle intermediates reached steady state in these chondrocytes.

To be utilized by cells, glutamine was first deaminated to glutamate through glutaminase. After that, glutamate could be converted to α -ketoglutarate (α -KG), which could enter the tricarboxylic acid (TCA) cycle. α -KG is a key metabolite in the TCA cycle (Fig 21). It could enter the TCA cycle either through oxidative decarboxylation and be converted to succinate, or through reductive carboxylation and be converted to isocitrate

(Fig 21). When α -KG is directly derived from $^{13}\text{C}_5$ -glutamine, all five carbons of α -KG would be labeled with ^{13}C (Fig 21). If $^{13}\text{C}_5$ - α -KG enters TCA cycle through oxidative decarboxylation, $^{13}\text{C}_5$ - α -KG would be converted to $^{13}\text{C}_4$ -succinate (Fig 21). If $^{13}\text{C}_5$ - α -KG enters TCA cycle through reductive carboxylation, it would be converted to $^{13}\text{C}_5$ -citrate (Fig 21). $^{13}\text{C}_4$ -succinate and $^{13}\text{C}_5$ -citrate could then cycle in the TCA cycle and give rise to other downstream TCA cycle intermediates with distinct isotope labeling patterns.

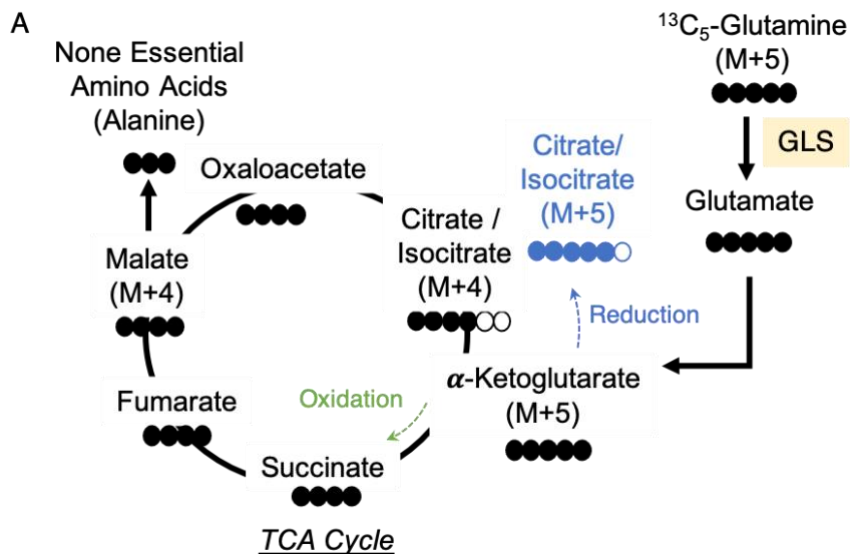


Figure 21 Graphic Depiction of tracing glutamine metabolism using $^{13}\text{C}_5$ -Glutamine.

Glutaminase deaminates glutamine to glutamate, which could be further metabolized to α -KG. Glutamine-derived $^{13}\text{C}_5$ - α -KG could enter the TCA cycle through oxidative decarboxylation (became M+4 succinate) or reductive carboxylation (became M+5 citrate). Filled circles indicate ^{13}C and open circles indicate ^{12}C . Green dashed line indicates the direction of oxidative decarboxylation and blue dashed line indicates the direction of reductive carboxylation.

After three hours of tracing, more than 60% of glutamate and α -KG in IDH1/2^{WT} and IDH1^{Mut} chondrocytes were labeled with ^{13}C (Fig 22 A, B), suggesting glutamine is

the primary carbon source for the production of glutamate and α -KG in chondrocytes with or without *Idh1* mutation. In IDH1^{Mut} chondrocytes, the percentage of ¹³C labeling in glutamate (Fig 22 A), α -KG (Fig 22 B), other TCA cycle intermediates (Fig 22 C-F), and the non-essential amino acid alanine (Fig 22 G) was significantly increased when compared to IDH1/2^{WT} chondrocytes, suggesting expression of mutant IDH1 enzyme led to increased utilization of glutamine for the production of downstream metabolites. This finding was consistent with our observation that IDH1^{Mut} chondrocytes had increased GLS activity (Fig 20).

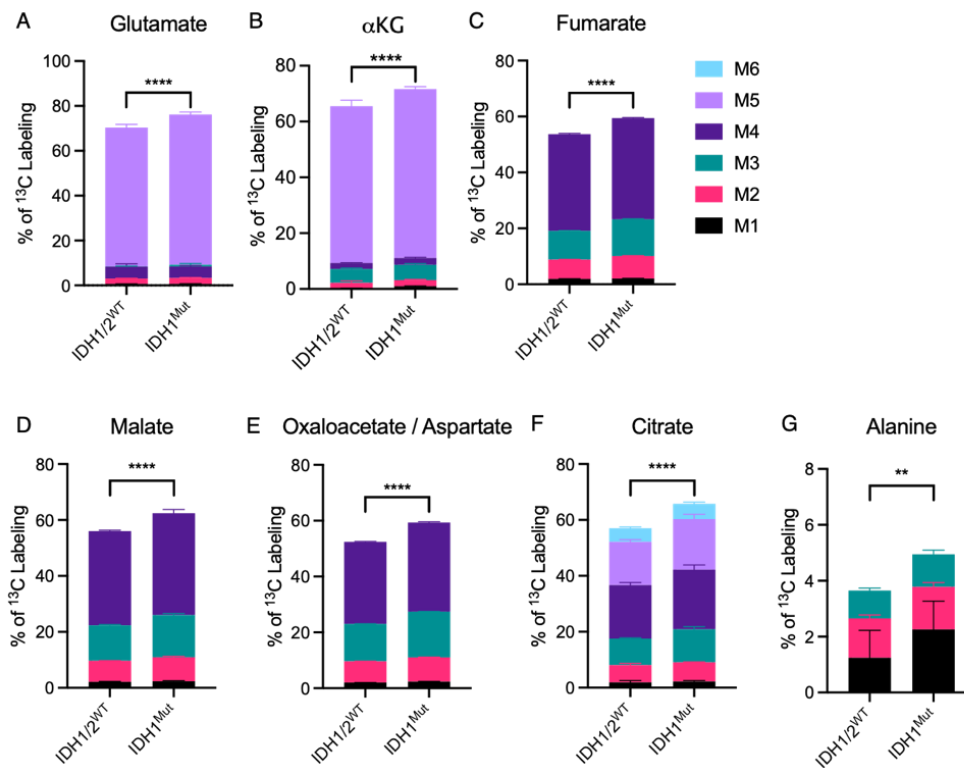


Figure 22 Percentage of ¹³C labeling contribution to downstream metabolites in IDH1/2^{WT} and IDH1^{Mut} murine chondrocytes.

Percentage of $^{13}\text{C}_5$ -glutamine contribution to glutamate (A), α -ketoglutarate (B), fumarate (C), malate (D), oxaloacetate / aspartate (E), citrate (F), and alanine (G). M1, M2, M3, M4, M5 indicate that 1, 2, 3, 4, 5 carbon atoms in the molecules were labeled with ^{13}C . mean \pm SD are shown. ** $p < 0.01$, **** $p < 0.0001$ statistical significance was determined by two-way ANOVA.

3.3.2.2 $\text{IDH1/2}^{\text{Mut}}$ human patient chondrosarcoma cells had increased glutamine contribution to anaplerosis and non-essential amino acids production

In order to understand how chondrosarcomas with wildtype or mutant IDH1/2 enzymes utilize glutamine, we performed carbon tracing experiment in chondrosarcoma cells with wild type IDH1/2 , IDH1 mutation, and IDH2 mutation. Briefly, chondrosarcoma cells of different genotypes were cultured in glutamine-free MEM- α media supplemented with 2mM $^{13}\text{C}_5$ -glutamine for three hours, a time point when ^{13}C labeling in the TCA cycle intermediates reached steady state in these chondrosarcoma cells. ^{13}C contribution to downstream metabolites was determined by measuring the isotope-labeling pattern. As expected, a significant amount of glutamate in chondrosarcomas of different genotypes was labeled with ^{13}C . Importantly, the labeling of ^{13}C in glutamate was significantly higher in $\text{IDH1/2}^{\text{Mut}}$ chondrosarcomas when compared to chondrosarcoma cells with wildtype IDH1/2 enzymes (Fig 23A). This trend was consistent with the abovementioned observations in murine chondrocytes with wildtype or mutant IDH enzymes, but the difference was more substantial. We also examined the ^{13}C labeling pattern in the tricarboxylic acid (TCA) cycle intermediates and non-essential amino acids. Chondrosarcomas with IDH1/2 mutations had significantly higher carbon contribution to all TCA cycle intermediates (Fig 23 B-G) and some non-

essential amino acids such as Alanine (Fig 23H). Together these data suggested that IDH1/2^{Mut} chondrosarcomas were more efficient in converting glutamine to its downstream metabolites when compared to IDH1/2^{WT} chondrosarcomas.

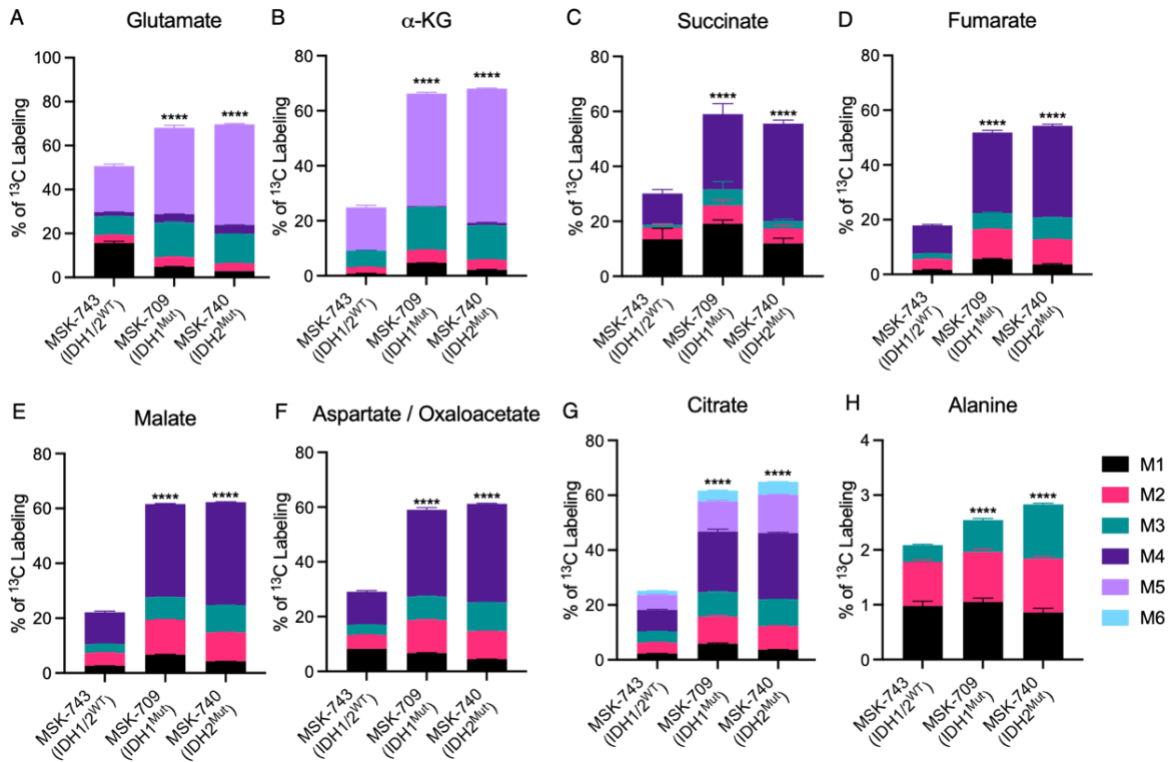


Figure 23 Percentage of ¹³C labeling contribution to downstream metabolites in human chondrosarcoma cells with wildtype IDH1/2, IDH1 mutation, and IDH2 mutations.

Percentage of ¹³C₅-glutamine contribution to glutamate (A), α-ketoglutarate (B), succinate (C) fumarate (D), malate (E), oxaloacetate / aspartate (F), citrate (G), and alanine (H). M1, M2, M3, M4, M5 indicate that 1, 2, 3, 4, 5 carbon atoms in the molecules were labeled with ¹³C. mean±SD are shown. ****p<0.0001, statistical significance was determined by two-way ANOVA.

3.3.3 Glutamine is the primary source for D-2-hydroxyglutarate production in IDH1^{Mut} murine chondrocytes

Glutamine has been shown to be the primary source for the production of D-2-Hydroxyglutarate (D-2HG) in several human cancers with *IDH1/2* mutations including chondrosarcoma [129, 167, 190]. To examine whether glutamine is the primary source for D-2HG production in the IDH1^{Mut} murine chondrocytes, we cultured these chondrocytes in glutamine-free media supplemented with ¹³C₅-Glutamine and examined the percentage of ¹³C-labeling in D-2HG at different time points. After 10 hours, more than 80% of the D-2HG was labeled with ¹³C, confirming glutamine was the primary source for D-2HG in IDH1^{Mut} murine cells (Fig 24 A, B).

Next, we investigated whether inhibiting GLS could reduce the production of D-2HG in IDH1^{Mut} chondrocytes. We treated IDH1/2^{WT} and IDH1^{Mut} chondrocytes with a specific small molecule inhibitor Bis-2-(5-phenylacetamido-1,3,4-thiadiazol-2-yl)ethyl sulfide (BPTES) for GLS [195] for 48 hours. We measured glutamate concentration in IDH1/2^{WT} and IDH1^{Mut} chondrocytes. Relative glutamate levels were determined by normalizing the glutamate concentration in each sample to the average glutamate concentration of IDH1/2^{WT} chondrocytes treated with vehicle control. We found that BPTES significantly reduced glutamate levels in IDH1/2^{WT} and IDH1^{Mut} chondrocytes (Fig 24 C), confirming the drug effectively inhibited GLS. As expected, D-2HG was only detected in IDH1^{Mut} chondrocytes. When glutaminase was inhibited, the D-2HG concentration in the cell culture media was significantly reduced (Fig 24 D). Taken

together, these data suggested that glutamine was used for the production of D-2HG in IDH1^{Mut} murine chondrocytes.

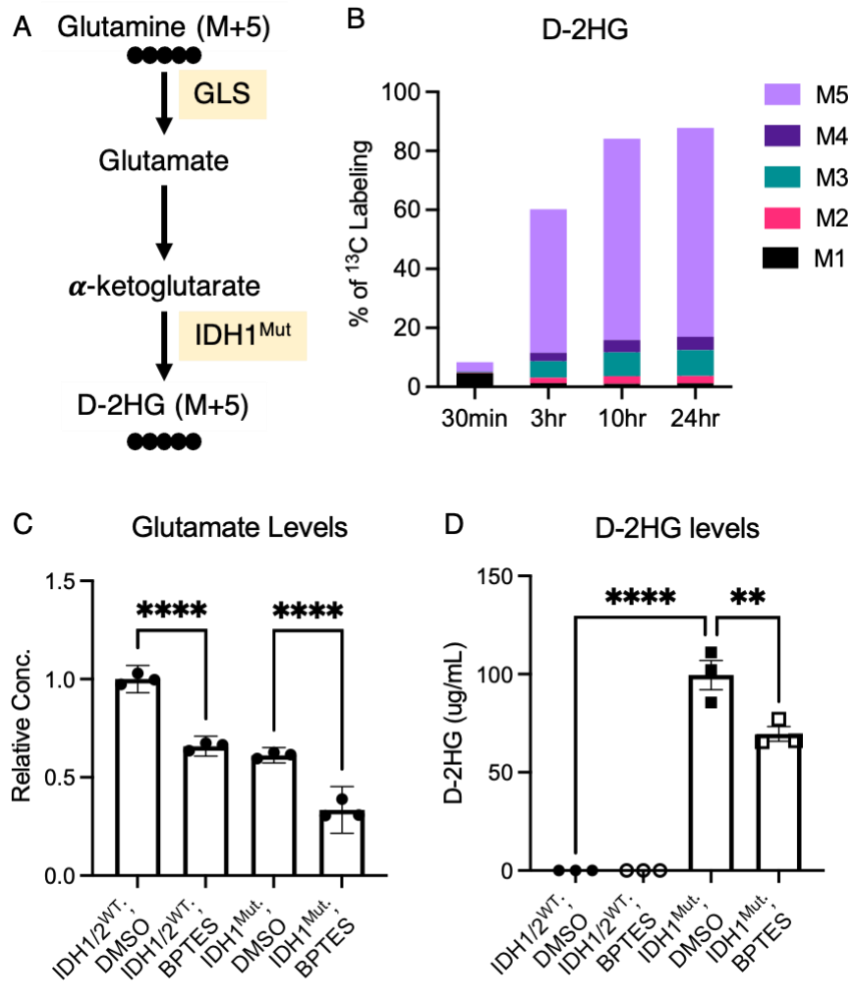


Figure 24 Glutamine is the primary source for D-2HG production in IDH1^{Mut} murine chondrocytes.

(A) Schematic illustration of carbon tracing using ¹³C₅-glutamine. Black filled circles indicate ¹³C. (B) Percentage of ¹³C labeling in D-2HG. M1, M2, M3, M4, M5 indicate that 1, 2, 3, 4, 5 carbon atoms in the molecules were labeled with ¹³C. (C) Relative glutamate levels in chondrocytes with indicated genotypes and treatment conditions. (D) D-2HG concentrations in the cell culture media of chondrocytes. **p<0.01, ****p<0.0001. One-way ANOVA. Mean \pm 95% confidence intervals are shown.

3.3.4 *Gls* is the primary isoform of glutaminase in chondrocytes.

3.3.4.1 *Gls* is the primary isoform of glutaminase expressed by chondrocytes.

Glutaminase (GLS) is the primary enzyme that catabolizes glutamine to glutamate. Two isoforms of glutaminase, kidney-type glutaminase (encoded by *Gls*) and liver-type glutaminase (encoded by *Gls2*) are expressed by mice and human. RNA sequencing analysis revealed that *Gls* was expressed at a much higher level than *Gls2* in primary chondrocytes of both *Col2a1Cre*; and *Col2a1Cre;Idh1^{LSL/+}* animals (Fig 25, GSE123130). In addition, the expression level of *Gls2* was negligible, suggesting the glutaminase activity in chondrocytes was mainly catalyzed by kidney-type glutaminase (GLS).

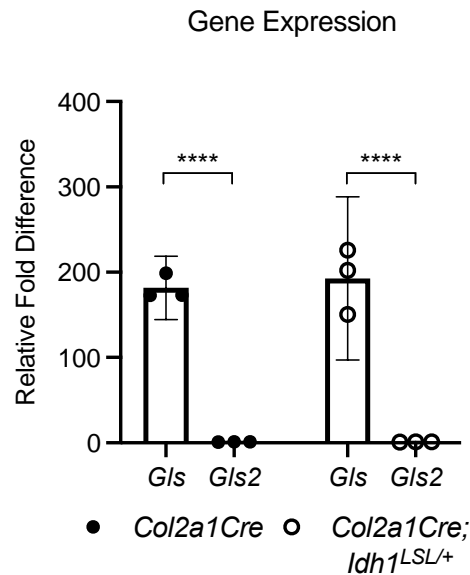


Figure 25 Gene expression of *Gls* and *Gls2* in chondrocytes.

Gene expression of *Gls* and *Gls2* in chondrocytes. ****p<0.0001, unpaired, 2-tailed Student's *t* test was used to determine statistical significance. Mean ± 95% confidence intervals are shown.

3.3.4.2 Conditional deletion of *Gls* in chondrocytes significantly reduced glutaminase activity.

Next, we conditionally deleted *Gls* in chondrocytes by crossing a conditional null allele of *Gls^{fl}* to a chondrocyte specific *Col2a1Cre* mouse [170, 196]. Deletion of *Gls* in chondrocytes was sufficient as shown by q-RT-PCR and western blot (Fig 26 A, B). In addition, deleting *Gls* significantly reduced conversion from ³H-glutamine to ³H-glutamate (Fig 26 C) and suppressed uptake of ³H-glutamine from the cell culture media (Fig 26 D). These data confirmed that *Gls* encodes for the primary glutaminase isoform in chondrocytes and deleting *Gls* significantly reduced the functional activity of glutaminase.

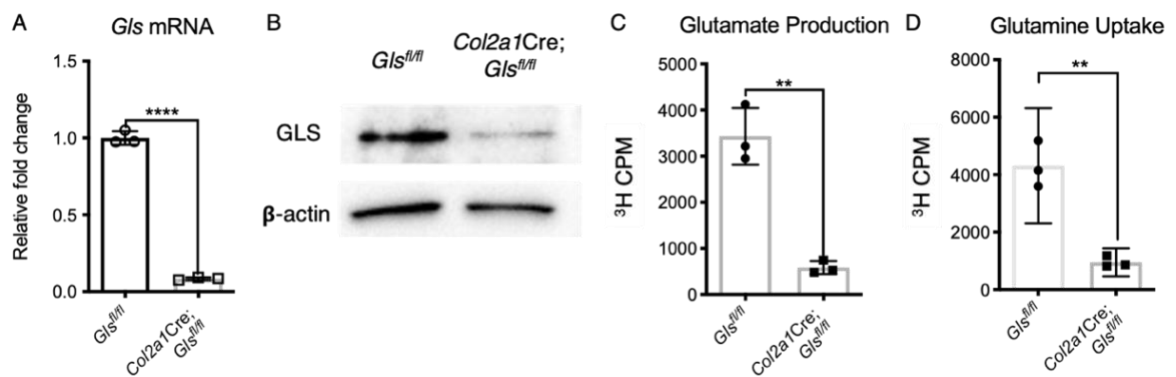


Figure 26 Deletion of *Gls* was efficient in *Col2a1Cre;Gls^{fl/fl}* chondrocytes.

(A) q-RT-PCR of *Gls*, (B) Representative western blot of GLS and β -actin, (C) ³H-Glutamate production, and (D) ³H-Glutamine uptake in *Gls^{fl/fl}* and *Col2a1Cre;Gls^{fl/fl}* chondrocytes. ** $p < 0.01$, **** $p < 0.0001$, unpaired, 2-tailed Student's *t* test. Mean \pm 95% confidence intervals are shown.

3.3.5 Deleting *Gls* in *Col2a1Cre;Idh1^{LSL/+}* chondrocytes affected chondrocyte differentiation

Dysregulated chondrocyte differentiation leads to development of enchondroma. We sought to determine whether *Gls* was needed for chondrocyte differentiation in animals expressing wildtype *Idh1/2* or mutant *Idh1* in their chondrocytes. To determine the role of *Gls* in chondrocyte differentiation, we conditionally deleted *Gls* in chondrocytes by crossing *Gls^{fl/fl}* mice to *Col2a1Cre* mice and *Idh1^{LSL/+}* mice, and then examined chondrocyte differentiation by conducting *in situ* hybridization and immunohistochemistry of chondrocyte markers at different differentiation stages on mouse tibias. *Col2a1* is a marker for early chondrocytes that have not undergone hypertrophic differentiation [14]. At embryonic day (E)14.5, early chondrocytes reside at the two ends of a tibia bone in a wildtype mouse. As shown by *in situ* hybridization, expression of *Col2a1* in the tibia was separated and restricted to the two ends in the Cre negative control animals (Fig 27 A). *Gls* deletion did not cause a significant alteration in its expression pattern (Fig 27 A). In *Col2a1Cre;Idh1^{LSL/+}* animals, the separation of *Col2a1* positive area was not complete. Some chondrocytes in the center of the tibia remained positive for *Col2a1* staining (Fig 27 A). In *Col2a1Cre;Gls^{fl/fl};Idh1^{LSL/+}* animals, no separation of *Col2a1* expression was observed in all the animals we examined (Fig 27 A). I quantified this phenotype by measuring the separation between *Col2a1* positive staining in the center of each tibia and used this measurement as the length of *Col2a1* negative zone. The length of *Col2a1* negative zone was significantly reduced in *Col2a1Cre;Idh1^{LSL/+}*

and *Col2a1Cre;Gls^{fl/fl};Idh1^{LSL/+}* animals (Fig 27 B). The average length of *Col2a1* negative area was slightly shorter in *Col2a1Cre;Gls^{fl/fl}* animals when compared to Cre negative control, but the difference was not statistically significant (Fig 27 B). Expression of parathyroid hormone 1 receptor (*Pth1r*) marks prehypertrophic chondrocytes [14]. At E14.5, expression of *Pth1r* was separated in Cre negative animals (Fig 27 C). *Gls* deletion alone in chondrocytes did not cause a noticeable alteration in *Pth1r* expression (Fig 27 C). In some *Col2a1Cre;Idh1^{LSL/+}* animals, we observed minimal separation of *Pth1r* expression, whereas in others its expression was not separated (Fig 27 C). In *Col2a1Cre;Gls^{fl/fl};Idh1^{LSL/+}* animals, expression of *Pth1r* was not separated in all animals we examined (Fig 27 C). We quantified this phenotype by measuring the separation between *Pth1r* positive staining in the center of each tibia and used this measurement as the length of *Pth1r* negative zone. The length of *Pth1r* negative zone was significantly reduced in *Col2a1Cre;Idh1^{LSL/+}* and *Col2a1Cre;Gls^{fl/fl};Idh1^{LSL/+}* animals (Fig 27 D). *Col10a1* is expressed by hypertrophic chondrocytes. In a wildtype mouse at E14.5, chondrocytes in the center of the tibia usually have gone through hypertrophic differentiation and express *Col10a1*. At this stage, expression pattern of *Col10a1* was comparable among Cre negative control, *Col2a1Cre;Gls^{fl/fl}* animals, and *Col2a1Cre;Idh1^{LSL/+}* animals (Fig 27 E). *Col10a1* expression was significantly reduced in *Col2a1Cre;Gls^{fl/fl};Idh1^{LSL/+}* animals (Fig 27 E). I quantified this phenotype by measuring the length of *Col10a1* positive staining in the center of each tibia and used this measurement as the length of *Col10a1* positive

zone. The average length of *Col10a1* positive zone was slightly shorter in *Col2a1Cre;Gls^{fl/fl}* animals and was slightly longer in *Col2a1Cre;Idh1^{LSL/+}* animals when compared to Cre negative control, but the differences were not statistically significant (Fig 27 F). The expression of *Col10a1* was significantly reduced in *Col2a1Cre;Gls^{fl/fl};Idh1^{LSL/+}* animals when compared to Cre negative control animals and *Col2a1Cre;Idh1^{LSL/+}* single mutant animals (Fig 27 F). We also examined the protein production of type X collagen (Col X) through immunohistochemistry. The staining pattern of Col X immunohistochemistry was similar to *in situ* hybridization of *Col10a1* (Fig 27 E, G), but the difference between *Col2a1Cre;Gls^{fl/fl};Idh1^{LSL/+}* animals and the other groups was more substantial at protein level. In some *Col2a1Cre;Gls^{fl/fl};Idh1^{LSL/+}* animals, the protein of Col X was not detected (Fig 27 H). Taken together, these data demonstrated that expression of mutant *Idh1* in chondrocytes affected proper hypertrophic differentiation. Although expression of the hypertrophic marker *Col10a1* was comparable between Cre negative control and *Col2a1Cre;Idh1^{LSL/+}* animals, expression of early and prehypertrophic chondrocyte markers *Col2a1* and *Pth1r* were not turned off properly in *Col2a1Cre;Idh1^{LSL/+}* animals, suggesting chondrocyte differentiation was dysregulated. Deleting *Gls* in *Idh1/2^{WT}* chondrocytes did not cause a significant phenotype but deleting *Gls* in *Col2a1Cre;Idh1^{LSL/+}* chondrocytes further affected hypertrophic differentiation, as expression of hypertrophic chondrocyte marker *Col10a1* was significantly reduced.

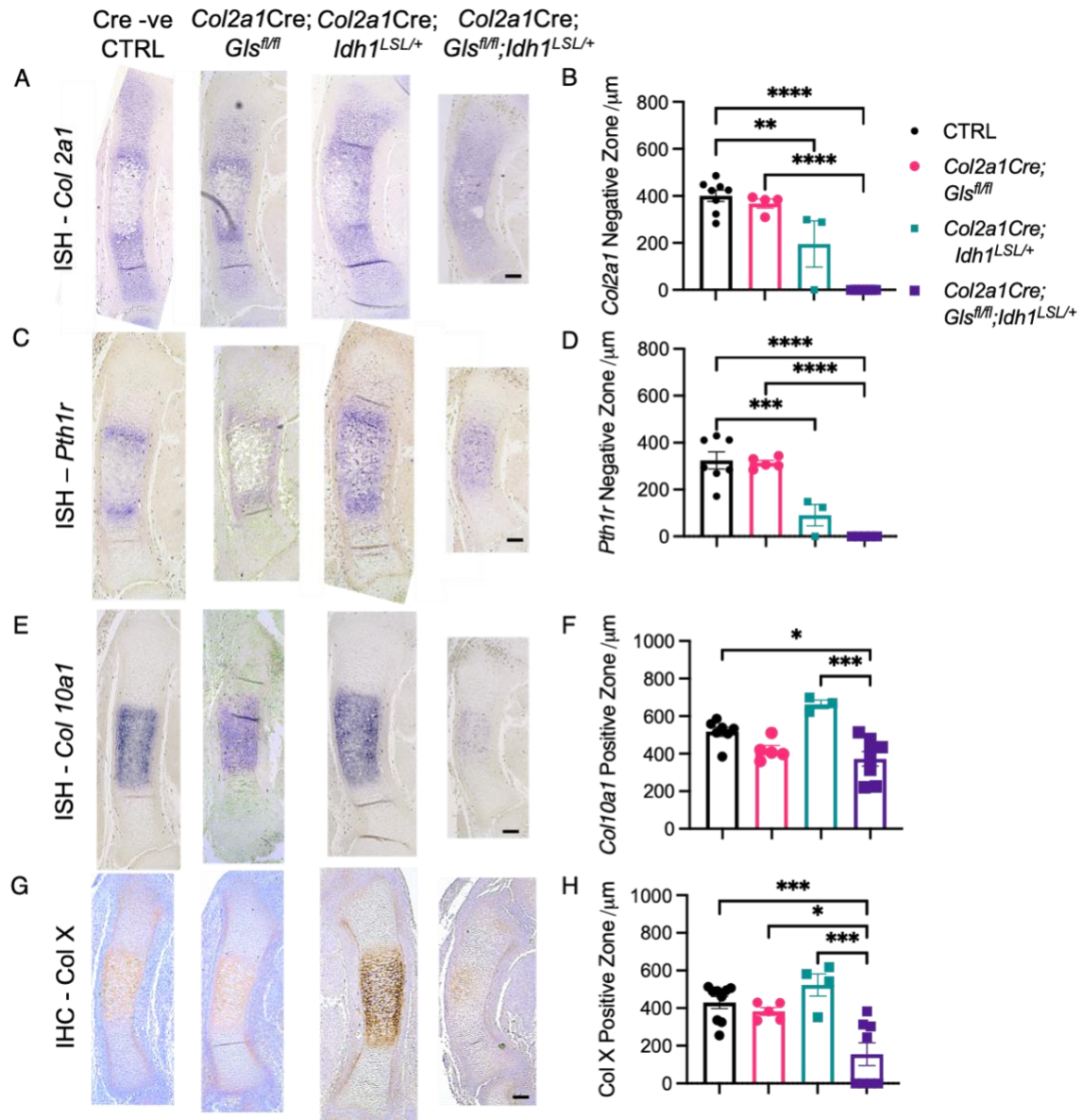


Figure 27 Expression of different chondrocyte markers.

(A) *In situ* hybridization of *Col2a1*. (B) Quantification of the length of *Col2a1* negative zone. (C) *In situ* hybridization of *Pth1r*. (D) Quantification of the length of *Pth1r* negative zone. (E) *In situ* hybridization of *Col10a1*. (F) Quantification of the length of *Col10a1* positive zone. (G) Immunohistochemistry of type X collagen. (H) Quantification of the length of Col X positive zone. mean±SEM are shown. one-way ANOVA was used to determine statistical significance. *p<0.05, **p<0.01, ***p<0.001, ****p<0.0001. Scale bar = 100 μm.

3.3.6 Deleting *Gls* in *Col2a1Cre;Idh1^{LSL/+}* chondrocytes increased cell proliferation and did not induce cell apoptosis

In the chondrocyte differentiation process during endochondral ossification, early resting chondrocytes would first become highly proliferative and then exit the cell cycle. After hypertrophic differentiation, some late hypertrophic chondrocytes would undergo apoptosis, whereas others would transdifferentiate into osteoblast. Next, we examined whether deleting *Gls* in chondrocytes would affect chondrocyte proliferation and apoptosis. To examine proliferation, we conducted BrdU staining. We found that the percentage of BrdU positive proliferating cells were significantly higher in *Col2a1Cre;Gls^{fl/fl};Idh1^{LSL/+}* animals when compared to *Col2a1Cre;Idh1^{LSL/+}* animals (Fig 28 A, B), suggesting deleting *Gls* increased proliferation in *Col2a1Cre;Idh1^{LSL/+}* animals. As chondrocytes are highly proliferative prior to hypertrophic differentiation, this finding echoed with our previous observation that deleting *Gls* in *Col2a1Cre;Idh1^{LSL/+}* chondrocytes affected their differentiation. To examine apoptosis, we conducted immunohistochemistry on the apoptotic marker cleaved caspase 3. At this stage, apoptosis was not detected in all the animals of four different genotypes, as shown by immunohistochemistry of cleaved caspase 3 (Fig 28 C, D). These data suggest that deleting *Gls* increased chondrocyte proliferation in *Col2a1Cre;Idh1^{LSL/+}* animals without affecting apoptosis.

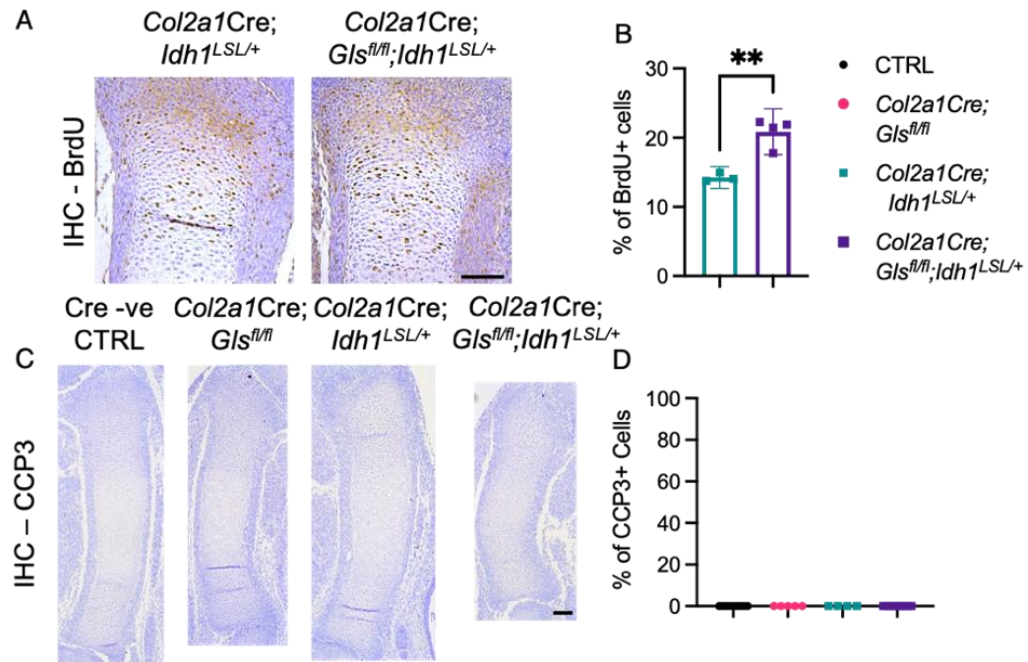


Figure 28 Proliferation and apoptosis in embryonic growth plate.

(A) Immunohistochemistry of BrdU. (B) Quantification of percentage of BrdU positive cells. (C) Immunohistochemistry of cleaved caspase 3. (D) Quantification of percentage of cleaved caspase 3 positive cells. For (B), mean \pm 95% confidence intervals are shown. ** $p < 0.01$, unpaired 2-tailed Student's *t* test was used to determine statistical significance. For (D), mean \pm SEM is shown. One-way ANOVA was used to determine statistical significance. Scale bar = 100 μ m.

3.3.7 Deleting *Gls* in *Col2a1Cre^{ERT2}; Idh1^{LSL/+}* chondrocytes increased the number and size of enchondroma-like lesions

We next examined how deleting *Gls* in chondrocyte postnatally affected chondrocyte homeostasis and enchondroma formation in adult animals. We induced deletion of *Gls* at four weeks of age by tamoxifen and examined the growth plate phenotype at 6 months of age. Histomorphometry analyses of the hind-limb growth plate of *Col2a1Cre^{ERT2}; Gls^{fl/fl}* animals did not reveal any noticeable phenotype (Fig 29 A),

suggesting that GLS may not be required for the homeostasis of growth plate chondrocytes postnatally. To examine the role of GLS in enchondroma, we induced *Gls* deletion together with mutant *Idh1* expression in chondrocytes by tamoxifen injection at four weeks of age, and then examined enchondroma-like lesions at 6 months of age. Enchondroma-like lesions were first identified by Safranin-O staining, which was performed on one slide in every ten consecutive slides. We then examined every consecutive slide under the light microscope to identify lesions that did not span to the Safranin O stained slide and recorded the number of lesions for each animal. For every Safranin O stained slide, we manually outlined each lesion and measured the area of each lesion. Lesion size of each animal was determined by adding up the areas of all the lesions in that animal. Relative lesion size was determined by normalizing the lesion size of each animal to the average lesion size of *Col2Cre^{ERT2};Idh1^{LSL/+}* animals. We also estimated the thickness of each enchondroma-like lesion. As each section was 5 μ m thick, we estimated the thickness of each enchondroma lesion by counting how many sections the lesion spanned. We observed that the number, size, and thickness of enchondroma-like lesions were significantly increased when *Gls* was deleted in *Col2a1Cre^{ERT2};Idh1^{LSL/+}* animals (Fig 29 B-D).

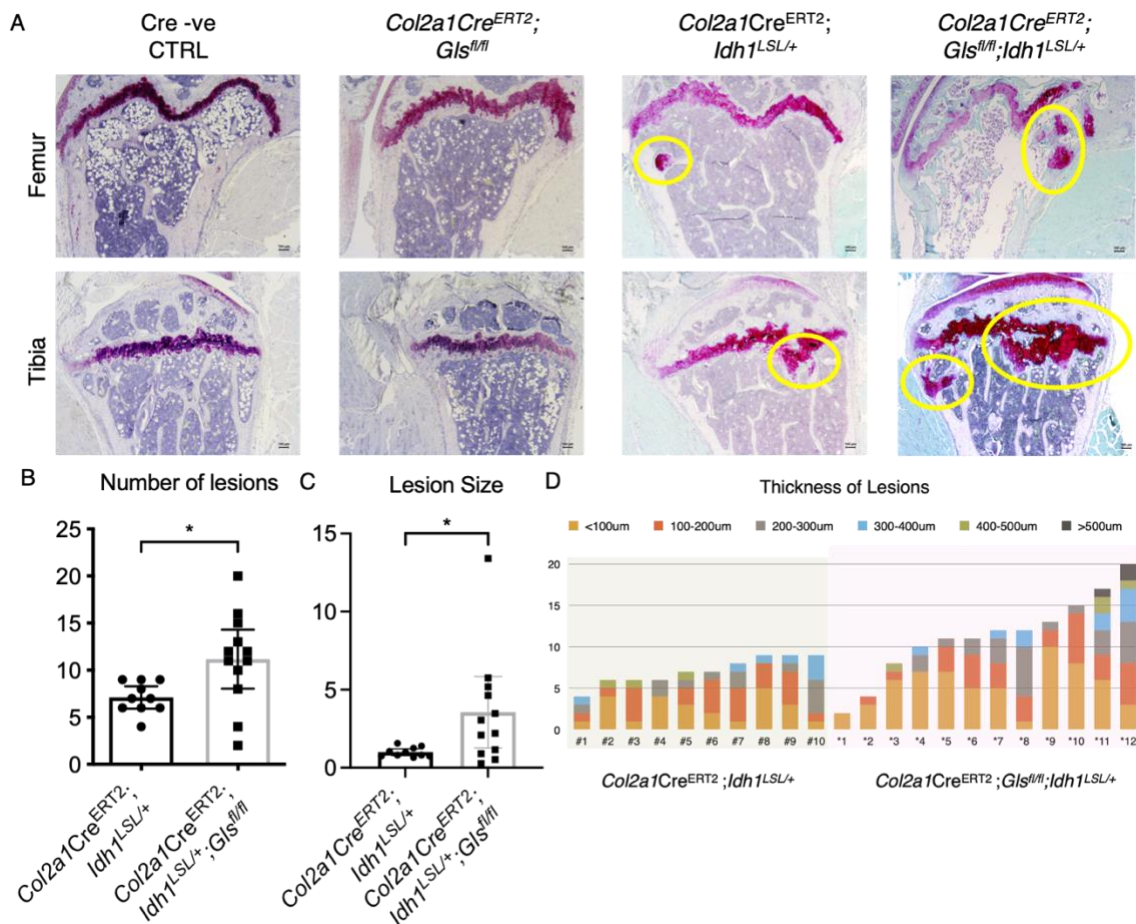


Figure 29 Safranin O staining of the growth plate cartilage and enchondroma-like lesions.

(A) Safranin O staining of the metaphysis of the femur and tibia bone of animals with indicated genotypes. (B) Quantification of number of lesions in animals with indicated genotypes. (C) Quantification of lesion size of animals with indicated genotypes. Each data point represents one animal. (D) The thickness of each enchondroma-like lesion in each animal. * $p < 0.05$, unpaired, 2-tailed Student's t test. Mean \pm 95% confidence intervals are shown.

3.3.8 Glutaminase regulated the differentiation of chondrocytes with *Idh1* mutation through downstream metabolite α -ketoglutarate

3.3.8.1 α -ketoglutarate level was lower in IDH1^{Mut} chondrocytes

Glutamine metabolism has been reported to regulate chondrocyte differentiation through its downstream metabolites α -KG and acetyl-CoA under IDH1/2^{WT} background [108]. We examined whether glutaminase could regulate the differentiation of chondrocytes with *Idh1* mutation through α -KG. ¹³C tracing experiment in IDH1^{WT} and IDH1^{Mut} chondrocytes revealed that more than 60% of α -KG in chondrocytes was derived from glutamine (Fig 22 B). The majority of ¹³C labeled α -KG had all five carbons labeled with ¹³C, confirming α -KG was a direct downstream metabolite of glutamine (Fig 22 B). Importantly, the percentage of ¹³C labeling in α -KG was significantly higher in IDH1^{Mut} chondrocytes, suggesting IDH1^{Mut} chondrocytes were more efficient in converting glutamine to α -KG (Fig 22B). Although IDH1^{Mut} chondrocytes were more efficient in converting glutamine to α -KG when compared to wildtype chondrocytes, the intracellular concentration of α -KG was lower in IDH1^{Mut} chondrocytes, likely because α -KG was used to synthesize D-2HG (Fig 30 A).

3.3.8.2 GLS inhibition reduced α -ketoglutarate levels in IDH1/2^{WT} and IDH1^{Mut} chondrocytes

We then sought to understand how α -KG was affected when GLS was blocked in IDH1^{WT} and IDH1^{Mut} chondrocytes. We used BPTES to mimic the effects of *Glis* deletion *in vitro* and *ex vivo*. First, we conducted metatarsal organ culture experiment to examine

the effects of BPTES treatment on chondrocyte differentiation *ex vivo*. Metatarsal bones were isolated from Cre negative control and *Col2a1Cre;Idh1^{LSL+}* embryos at E16.5 and cultured in the presence or absence of BPTES for five days. We examined hypertrophic chondrocyte differentiation through immunohistochemistry of type X collagen. The phenotype was quantified by measuring the length of Col X positive zone. The Col X positive zone was significantly shorter in metatarsals of *Col2a1Cre;Idh1^{LSL+}* animals, suggesting a delay in hypertrophic differentiation at this stage (Fig 30 B, C). BPTES treatment caused a slight but not significant reduction of Col X staining in the Cre negative control animals and it significantly reduced Col X staining in *Col2a1Cre;Idh1^{LSL+}* animals (Fig 30 B, C). The effect of BPTES treatment on chondrocyte hypertrophic differentiation was consistent with the effect of *Gls* deletion *in vivo* (Fig 27 G, H), confirming BPTES was a valid tool to examine the effects of GLS inhibition *in vitro*. When IDH1/2^{WT} and IDH1^{Mut} chondrocytes were treated with BPTES, the intracellular α -KG level was reduced (Fig 30 D). The relative α -KG level for each group was determined by normalizing its concentration to the average α -KG concentration of vehicle control group of each genotype.

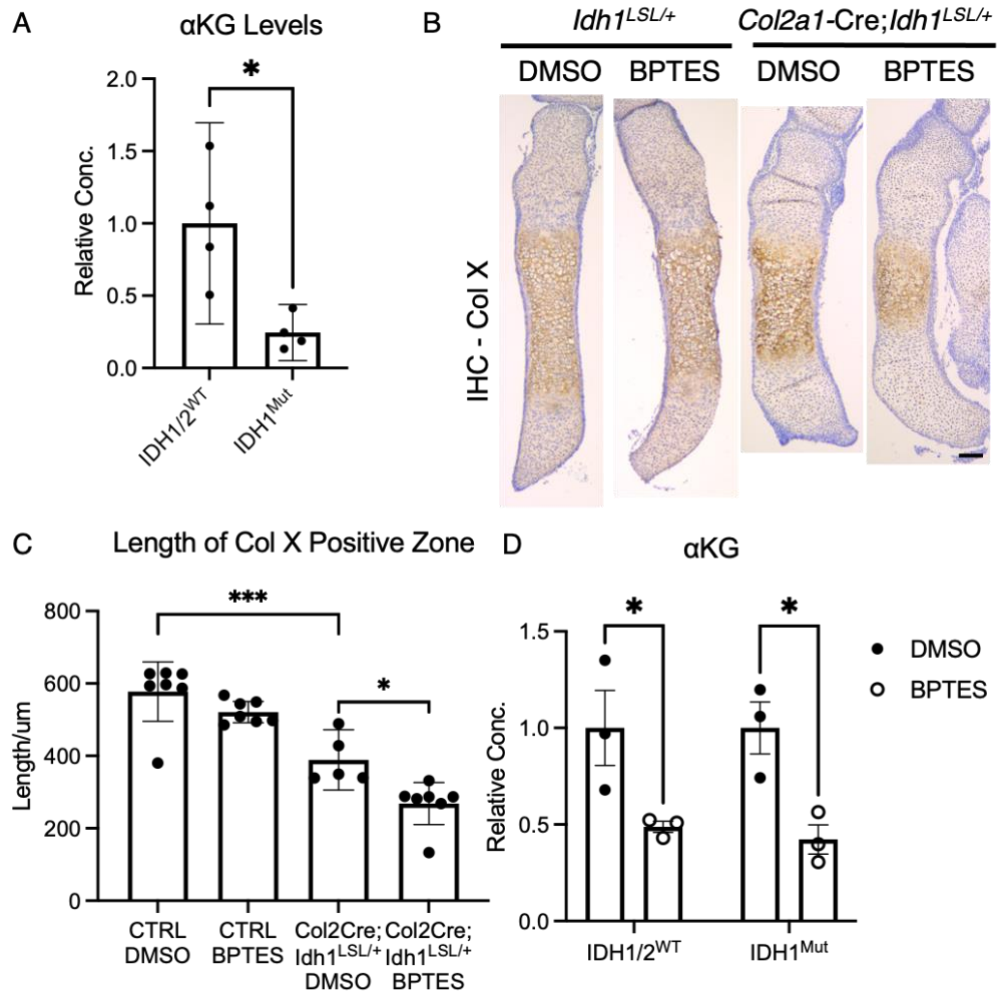


Figure 30 GLS inhibition led to suppressed hypertrophic differentiation and reduced α -KG levels.

(A) Relative intracellular α -KG concentrations in IDH1/2^{WT} and IDH1^{Mut} chondrocytes (B) Immunohistochemistry of Col X of metatarsal bones from organ culture. (C) Quantification of the length of Col X positive zone. (D) Relative intracellular α -KG concentration in IDH1/2^{WT} and IDH1^{Mut} chondrocytes in DMSO or BPTES treated group. For (A), mean \pm 95% CI are shown. * p <0.05 (unpaired student t-test). For (C), (D), mean \pm SEM are shown. * p <0.05, *** p <0.001 (ANOVA). Scale bar = 100 μ m.

3.3.8.3 Exogenous cell permeable dimethyl- α -KG restored chondrocyte differentiation in *Col2a1Cre;Gls^{fl/fl};Idh1^{LSL/+}* animals

Next, we investigated whether exogenous α -KG could rescue the defects of chondrocyte differentiation in *Col2a1Cre;Gls^{fl/fl};Idh1^{LSL/+}* animals. Chondrocyte differentiation in the mouse hindlimbs starts after mesenchymal condensation at E11.5. We injected cell permeable dimethyl- α -KG (DM- α -KG) to pregnant female every day from E11.5 to E13.5 and harvested the embryos for analysis at E14.5. We examined hypertrophic chondrocyte differentiation through *in situ* hybridization and immunohistochemistry staining of *Col10a1* and type X collagen (Fig 31 A, B). We quantified the length of type X collagen positive zone (Fig 31 C). In the vehicle control group, *Col2a1Cre;Gls^{fl/fl};Idh1^{LSL/+}* animals exhibited significantly less staining of *Col10a1* and type X collagen (Fig 31 A-C). DM- α -KG effectively restored expression of the hypertrophic chondrocyte marker *Col10a1* in *Col2a1Cre;Gls^{fl/fl};Idh1^{LSL/+}* animals both at mRNA and protein levels as shown by the *in situ* hybridization of *Col10a1* and the immunohistochemistry of Col X (Fig 31 A-C). DM- α -KG treatment also led to a reduction in chondrocyte proliferation in *Col2a1Cre;Gls^{fl/fl};Idh1^{LSL/+}* animals as shown by BrdU staining (Fig 31 D, E). DM- α -KG treatment did not induce apoptosis as no cleaved caspase 3 positive cells were detected (Fig 31 F). These data suggested that glutaminase regulated chondrocyte differentiation and proliferation through glutamine downstream metabolite α -KG.

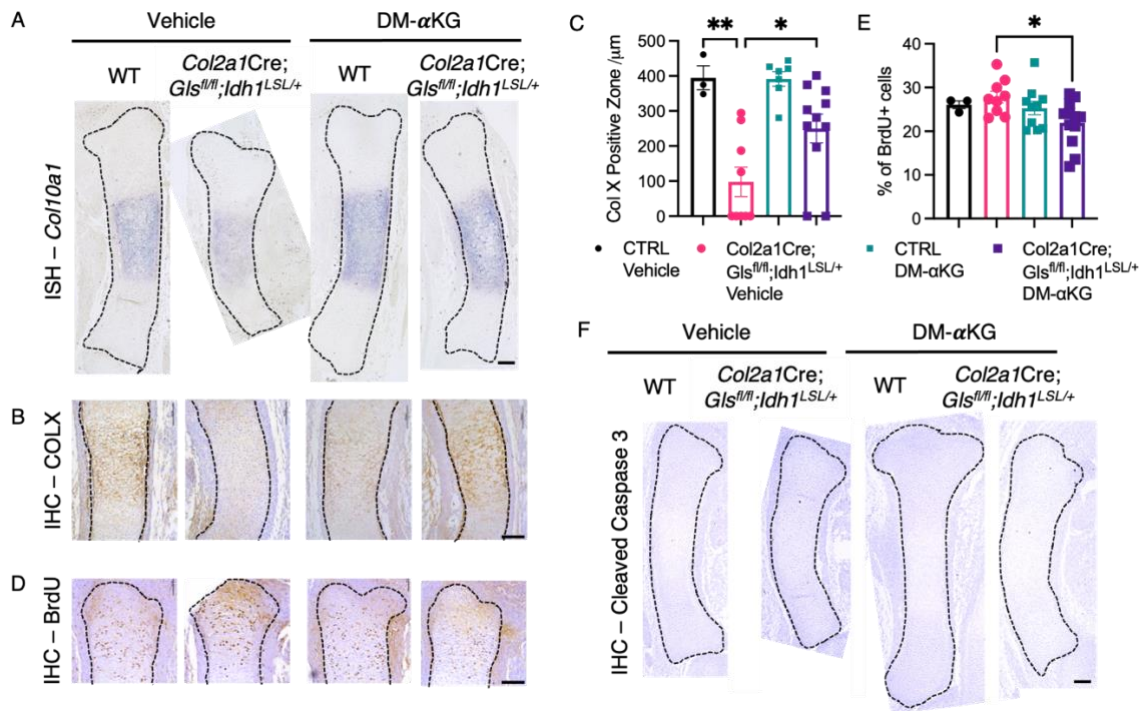


Figure 31 Exogenous cell permeable dimethyl- α -KG (DM- α -KG) restored chondrocyte differentiation and proliferation in *Col2a1Cre;Gls^{fl/fl};Idh1^{LSL/+}* animals.

(A) *In situ* hybridization of *Col10a1*. (B) Immunohistochemistry of Col X. (C) Quantification of the length of Col X positive zone. (D) Immunohistochemistry of BrdU. (E) Quantification of the percentage of BrdU positive cells. (F) Immunohistochemistry of cleaved caspase 3. mean \pm SEM are shown. * p <0.05, ** p <0.01, one-way ANOVA was used to determine statistical significance. Scale bar = 100 μ m.

3.3.9 Inhibiting GLS induced apoptosis in IDH1/2^{Mut} chondrosarcomas and led to reduced tumor weight

Previously it has been reported that inhibiting glutaminase reduced viability in chondrosarcoma cell lines, however, the effects of glutaminase inhibition on chondrosarcoma *in vivo* and the mechanism underlying such effects were not clear [166]. To investigate the effects of glutaminase inhibition on chondrosarcoma tumor *in vivo*, we

established patient-derived xenograft models as previously described [172].

Chondrosarcoma tumors were divided into pieces at 5 mm × 5 mm × 5 mm and implanted to immunodeficient Nod-scid-gamma mice subcutaneously. We waited for one week to allow the tumors to attach to the mice. Then we treated these animals with BPTES (0.2 g / kg body weight / day) or vehicle control via intraperitoneal injection every day for 14 days (Fig 32 A). We measured tumor weight at the time of harvest. For each patient sample, the tumor weight of each mouse was normalized to the average tumor weight in the vehicle control group of the same patient sample. This normalized value was used as the relative tumor weight of each tumor. We compared the relative tumor weight of tumors treated by BPTES or vehicle control and found that BPTES significantly reduced tumor weight of chondrosarcoma tumors with *IDH1* mutations (Fig 32 B, C). We examined proliferation and apoptosis in these tumors through immunohistochemistry of the proliferation marker Ki67 and apoptosis marker cleaved caspase 3 respectively. Relative proliferation rate and relative apoptosis rate of each tumor were determined by normalizing the percentage of Ki67 and cleaved caspase 3 positive cells of each tumor to the average percentage of Ki67 and cleaved caspase 3 positive cells in the vehicle control group of the same patient sample. In chondrosarcomas with *IDH1* mutations, BPTES treatment significantly increased apoptosis in the xenografts without altering proliferation (Fig 32 D-G). The primary chondrosarcoma patient cells with *IDH2* mutations failed to engraft to immunodeficient

Nod-scid-gamma mice, thus we could not determine the effects of BPTES treatment on these tumors *in vivo*. We also examined whether BPTES affected the tumor weight, proliferation, and apoptosis in chondrosarcomas with wildtype *IDH1* and *IDH2*. Interestingly, BPTES treatment of *IDH1/2^{WT}* chondrosarcoma did not cause significant difference in tumor weight, cell proliferation, or apoptosis (Fig 32 L-N), suggesting the reliance on glutamine metabolism might be specific for chondrosarcomas with *IDH* mutations. These data demonstrated that inhibiting glutaminase led to reduced tumor weight of *IDH1^{Mut}* chondrosarcoma *in vivo*, which might be through upregulation of programmed cell death.

To determine whether BPTES would exert similar effects on chondrosarcoma cells *in vitro*, we examined chondrosarcoma cell proliferation and apoptosis *in vitro* through EdU staining and TUNEL assay. Relative proliferation and apoptosis rate of each patient sample was determined by normalizing the average percentage of EdU and TUNEL positive cells in the BPTES treatment group of the patient sample to the average percentage of EdU and TUNEL positive cells in the vehicle group of the same patient sample. Thus, the relative proliferation and apoptosis rate of the vehicle group was "1", and each dot represented the relative proliferation and apoptosis rate of one patient sample that was treated with BPTES. We observed that BPTES treatment increased cell apoptosis in *IDH1/2^{Mut}* chondrosarcoma but did not alter cell proliferation (Fig 32 H-K), which was consistent with our findings *in vivo*.

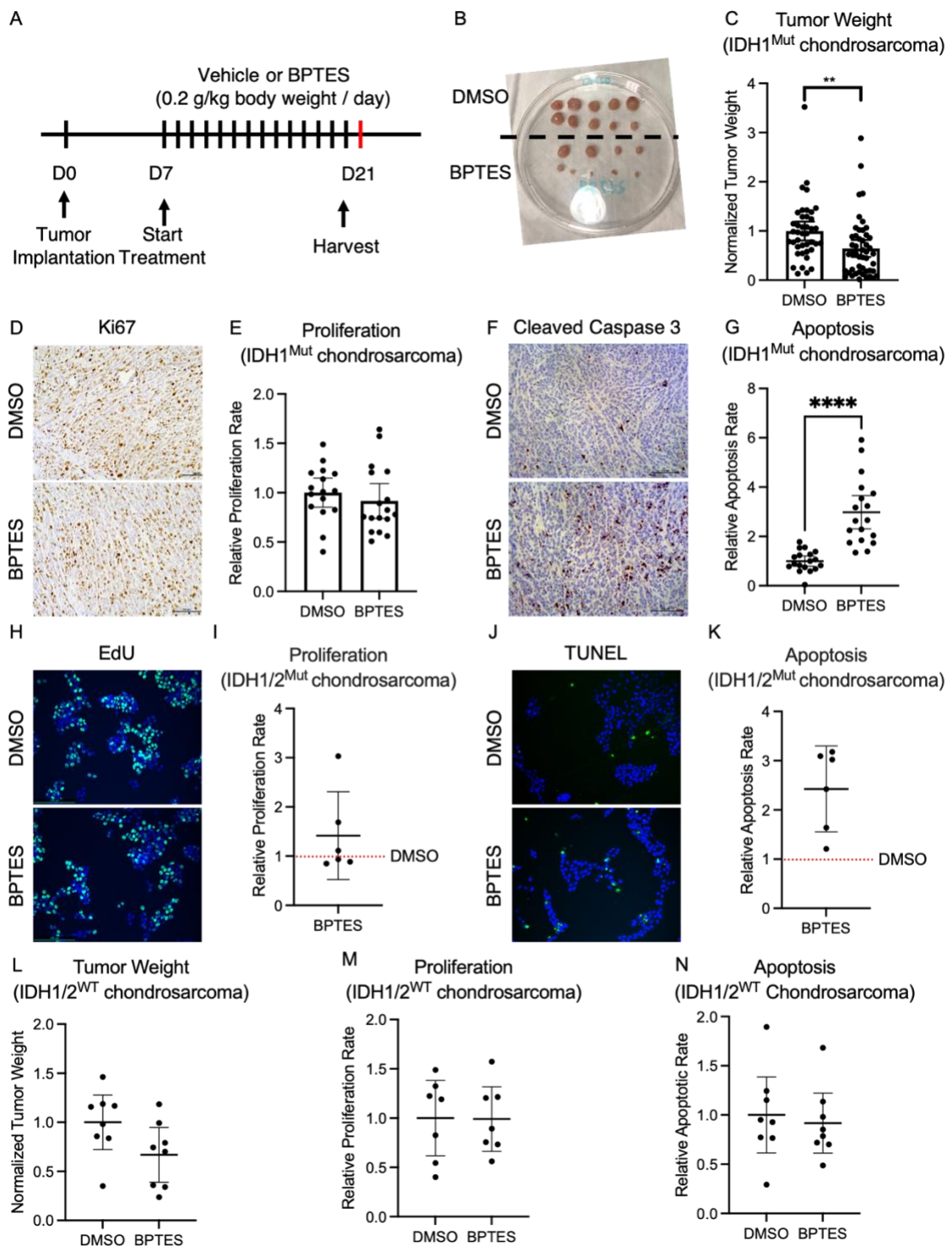


Figure 32 Inhibiting glutaminase reduced tumor weight and induced apoptosis in chondrosarcomas with *IDH1/2* mutations.

(A) Experimental design for the xenograft experiment. (B) Representative pictures of xenografted tumor at the time of harvest. (C) Relative tumor weight of xenografted *IDH1^{Mut}* chondrosarcoma tumors at the time of harvest. (D) Representative picture of immunohistochemistry of Ki67 of xenografted tumors. (E) Quantification of relative proliferation rate of each tumor determined by percentage of Ki67 positive cells. (F) Representative picture of immunohistochemistry of cleaved caspase 3 of xenografted tumors. (G) Relative apoptotic rate of each tumor determined by percentage of cleaved caspase 3 positive cells. (H) Representative EdU staining of chondrosarcoma cells treated with DMSO or BPTES. (I) Relative proliferation rate of *IDH1/2^{Mut}* chondrosarcoma cells *in vitro* determined by EdU staining. Each dot represents one patient sample. (J) Representative TUNEL staining of chondrosarcoma cells treated with DMSO or BPTES. (K) Relative apoptotic rate of *IDH1/2^{Mut}* chondrosarcoma cells *in vitro* determined by TUNEL staining. Each dot represents one patient sample. (L) Relative tumor weight of xenografted *IDH1/2^{WT}* chondrosarcoma tumors at the time of harvest. (M) Relative proliferation rate of each *IDH1/2^{WT}* tumor determined by percentage of Ki67 positive cells. (N) Relative apoptotic rate of each *IDH1/2^{WT}* tumor determined by percentage of cleaved caspase 3 positive cells. mean±95% CI are shown. **p<0.01. ***p<0.0001, unpaired Student t-test was used to determine statistical significance.

3.3.10 Glutaminase regulated apoptosis in *IDH1/2^{Mut}* chondrosarcoma cells through production of non-essential amino acids

We next sought to understand how glutamine metabolism regulates cell survival of *IDH1/2^{Mut}* chondrosarcomas. After GLS deaminates glutamine to glutamate, glutamate could be converted to α -KG through two different pathways. Transaminases transfer the amino group from glutamate to other keto acids to produce non-essential amino acids (NEAA) and α -KG. Glutamate could also be deaminated to α -KG by glutamate dehydrogenase (Fig 33 A). To determine how glutamine metabolism affects cell viability of chondrosarcomas, we treated *IDH1/2^{Mut}* chondrosarcomas with GLS inhibitor BPTES or CB839 [197], transaminase inhibitor aminooxyacetate (AOA), or glutamate dehydrogenase inhibitor epigallocatechin gallate (EGCG) and measured cell

viability using Cell-Titer Glo viability assay (Fig 33 A). For each patient sample, the relative cell viability was determined by normalizing the cell viability in each treatment group to the average cell viability in the vehicle control group of the same patient sample. Thus, the relative cell viability of the vehicle group was always “1”, and each dot represented one patient sample. BPTES, CB839 and AOA treatment significantly reduced cell viability of IDH1/2^{Mut} chondrosarcomas, whereas EGCG treatment did not cause significant reduction in cell viability (Fig 33 B). These data suggested transaminases, rather than glutamate dehydrogenase, controlled IDH1/2^{Mut} chondrosarcoma cell viability downstream of glutaminase.

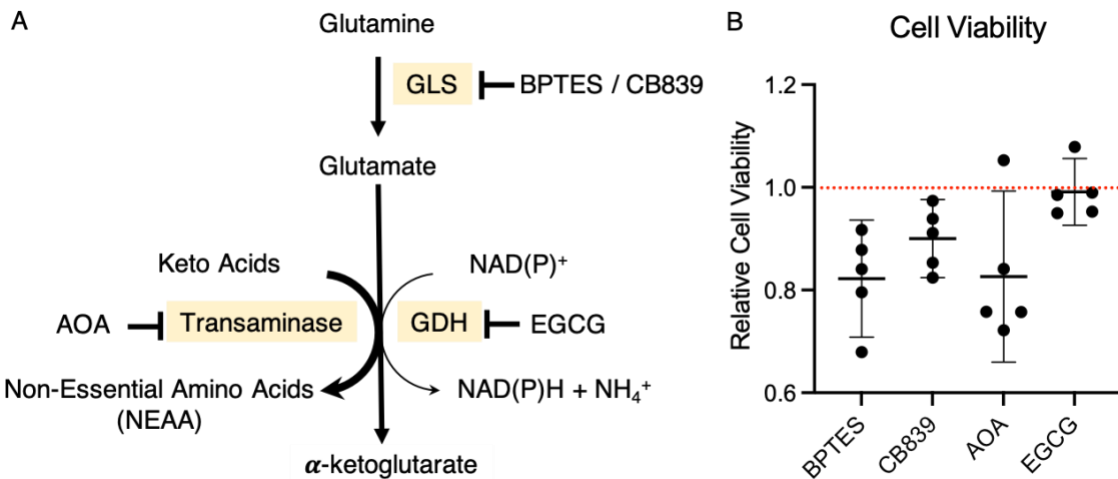


Figure 33 Glutaminase and transaminases regulated cell viability of chondrosarcomas with IDH1/2 mutations.

(A) Graphical illustration of glutamine metabolism pathway and specific inhibitors targeting different enzymes. (B) Cell viability of IDH1/2^{Mut} chondrosarcoma cells treated with 10 μ M BPTES, 1 μ M CB839, 100 μ M AOA, and 500 μ M EGCG. Each dot represents one patient sample. Mean \pm 95% CI are shown.

Transaminases generate non-essential amino acids and α -KG. α -KG could subsequently enter the TCA cycle. We measured the concentration of TCA cycle intermediates and some non-essential amino acids. Relative concentration of each metabolite was determined by normalizing the absolute concentration of each metabolite in the BPTES treatment group to the average concentration of the same metabolite in the vehicle control group of the same patient sample. We found that BPTES treatment reduced the concentrations of all these metabolites in *IDH1/2^{Mut}* chondrosarcomas (Fig 34 A).

BPTES induced apoptosis in *IDH1/2^{Mut}* chondrosarcoma cells. We next sought to determine which category of downstream metabolites were key regulators of cell apoptosis of *IDH1/2^{Mut}* chondrosarcoma. We examined cell apoptosis through Annexin V staining. For each patient sample, relative apoptosis was determined by normalizing the percentage of Annexin V positive cells of each treatment group to the average percentage of Annexin V positive cells of the vehicle control group of the same patient sample. BPTES significantly induced apoptosis in *IDH1/2^{Mut}* chondrosarcoma (Fig 34 B, C). Supplementation of NEAA, but not DM- α -ketoglutarate, led to a consistent partial rescue of BPTES-induced apoptosis (Fig 34 B, C). Taken together, these data suggested that glutaminase regulated apoptosis in *IDH1/2^{Mut}* chondrosarcoma cells through production of non-essential amino acids.

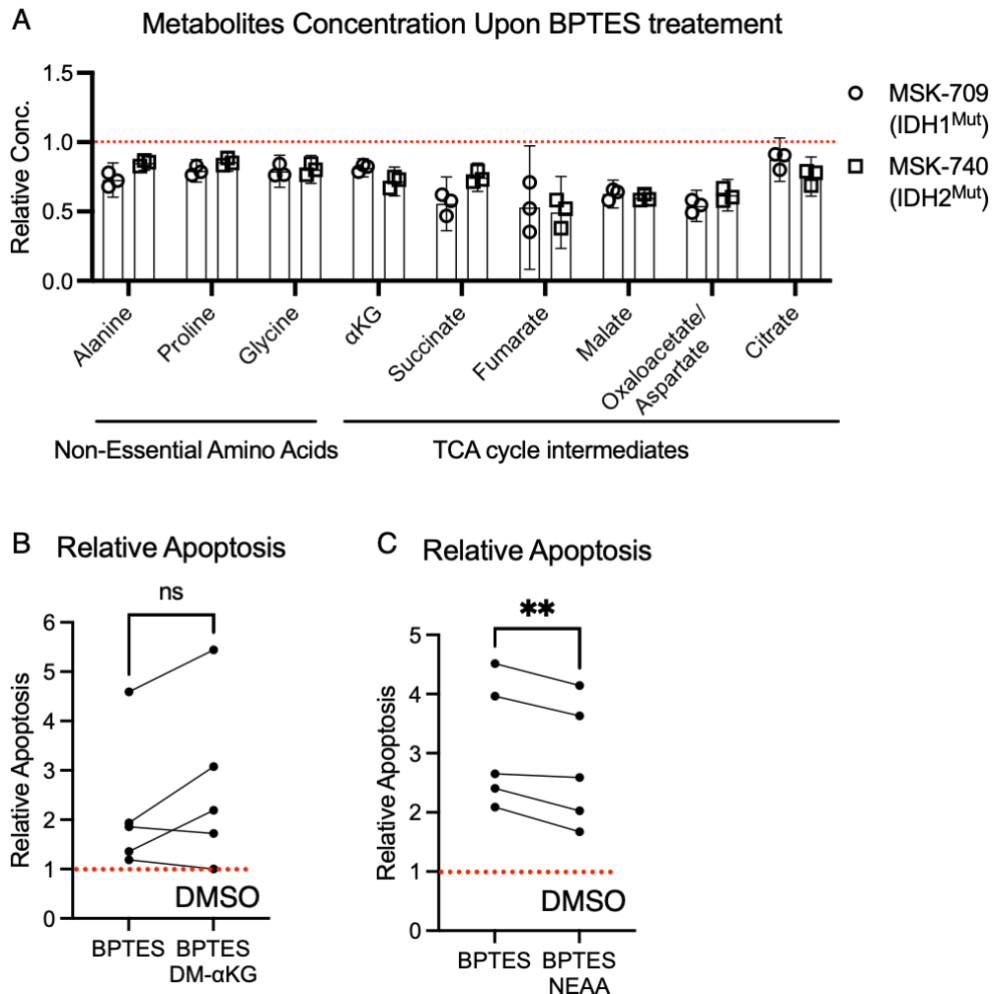


Figure 34 Glutaminase regulated chondrosarcoma apoptosis through non-essential amino acids.

(A) Relative concentration of different metabolites in $IDH1^{Mut}$ and $IDH2^{Mut}$ chondrosarcomas. Mean \pm 95% CI are shown. (B) Relative apoptosis of $IDH1/2^{Mut}$ chondrosarcoma cells treated 10 μ M BPTES, or 10 μ M BPTES+1mM DM- α -ketoglutarate. (C) Relative apoptosis of $IDH1/2^{Mut}$ chondrosarcoma cells treated 10 μ M BPTES, or 10 μ M BPTES+2X NEAA. For (B) and (C), each dot represents one patient sample. ** $p < 0.01$, paired student t-test was used to determine statistical significance.

3.4 Discussion

In this study, we found that glutaminase-mediated glutamine metabolism was upregulated in *IDH1/2^{Mut}* cartilage tumors enchondroma and chondrosarcoma.

Glutamine metabolism played distinct roles in the benign tumor enchondroma and the malignant cancer chondrosarcoma. Deleting glutaminase in murine chondrocytes with *Idh1* mutation interrupted hypertrophic differentiation during embryonic development and led to increased number and size of enchondroma-like lesions in the adult animals. In malignant *IDH1/2^{Mut}* chondrosarcomas of human patients, pharmacological inhibition of GLS led to reduced tumor weight.

The distinct roles of glutamine metabolism enchondroma and chondrosarcoma are likely due to different metabolic needs at different stages of tumor development. Enchondroma arises from dysregulated chondrocyte differentiation. Glutamine metabolism is known to regulate chondrocyte differentiation through α -KG [108]. In our mouse model, we observed that *IDH1^{Mut}* chondrocytes had significantly lower α -KG levels and blocking GLS further decreased α -KG concentration. Supplementing exogenous cell permeable DM- α -KG rescued chondrocyte differentiation defects in *Col2a1Cre;Gls^{fl/fl};Idh1^{LSL/+}* animals, thus it is possible that glutamine metabolism regulates chondrocyte differentiation and enchondroma-like phenotype of *IDH1^{Mut}* animals through its downstream metabolites α -KG. In malignant chondrosarcomas, tumor weight was mainly determined by cancer cell survival. Inhibiting GLS induced

apoptosis in IDH1/2^{Mut} chondrosarcomas and led to reduced tumor weight. Mechanistic investigation suggested that IDH1/2^{Mut} chondrosarcomas relied on glutamine metabolism for the production of non-essential amino acids to prevent apoptosis.

Glutamine is known to regulate cell differentiation through its downstream metabolites in the skeletal system. In chondrocytes, Stegen et al. reported that deleting glutaminase impaired chondrocyte differentiation from postnatal P3 to P14. Supplementation of cell permeable dimethyl- α -KG could rescue such defects [108]. They proposed that glutamine metabolism controlled chondrogenic gene expression, chondrocyte biosynthesis, and redox homeostasis through acetyl-CoA synthesis, aspartate production, and glutathione synthesis respectively [108]. In their study, they did not observe any difference in the chondrocytes and long bones between *Col2a1Cre;Gls^{fl/fl}* and wild-type littermates at birth [108], which is consistent with our observations that during embryonic development, deleting *Gls* in chondrocytes did not cause a significant change in chondrocyte differentiation. Glutamine metabolism was also reported to regulate the proliferation and differentiation of skeletal stem cells (SSCs) [186]. Deleting *Gls* in SSCs led to increased adipogenic differentiation and compromised osteogenic differentiation as well as reduced cell proliferation [186]. Exogenous dimethyl- α -KG rescued the defects in proliferation caused by lack of glutamine metabolism [186]. In osteoprogenitors, glutamine metabolism was reported to regulate osteogenic differentiation through non-essential amino acids [198]. Deleting *Gls* in

osteoprogenitors impaired osteogenic differentiation capacity. Supplementation of non-essential amino acids completely restored such defects [198].

Glutamine metabolism is an attractive target in various cancers, especially the ones with *IDH1/2* mutations. In glioma cells, inhibiting glutaminase preferentially slowed down growth of cancer cells with *IDH1* mutation without affecting D-2HG levels [191], suggesting these *IDH1*^{Mut} cancer cells were metabolically reprogrammed and became sensitive to glutaminase inhibition independent of D-2HG. The authors proposed that the reduction in growth was due to inhibition of α -KG production because supplementation of dimethyl- α -KG rescued the phenotype, and transaminase or glutamate dehydrogenase inhibition caused a similar phenotype [191]. Similar observations were made in AML as BPTES preferentially reduced growth of *IDH1*^{Mut} cancer cells without affecting D-2HG levels [193]. However, in another study in AML, the authors reported inhibiting GLS in *IDH1/2*^{Mut} cancer cells did reduce D-2HG concentration, suppressed cancer growth, and induced cell differentiation, suggesting glutamine metabolism might also regulate cancer behavior through D-2HG in certain contexts [192].

Glutamine metabolism has also been exploited as a therapeutic target in cancers that do not harbor mutations of *IDH1/2*. It supports cancer cell survival and proliferation through different mechanisms. In breast cancer, pancreatic cancer, and Ehrlich ascites-tumor cells, glutamine metabolism supported cancer cell survival through producing

adenosine triphosphate (ATP) [199, 200]. In multiple different cancer cell lines, glutamine supported cancer cell proliferation and suppressed apoptosis and autophagy through producing other non-essential amino acids [103, 104, 201-203]. Glutamine could also regulate cancer cells through maintaining cellular redox levels. Glutamine contributes to the production of antioxidant glutathione through providing amino acid precursors glutamate, glycine, and cystine as well as the NADPH directly or indirectly [85]. In pancreatic cancer cells, glutamine deprivation led to increased oxidative stress, reduced glutathione levels, and growth arrest [105]. Supplementation of glutathione rescued cancer cell growth [105].

In conclusion, our study showed that glutaminase-mediated glutamine metabolism played distinct roles in IDH1/2^{Mut} enchondromas and chondrosarcomas although it was upregulated in both conditions. In the context of enchondroma, deleting glutaminase in IDH1^{Mut} chondrocytes increased the number and size of enchondroma-like lesions. In chondrosarcoma, inhibiting glutaminase led to decreased tumor weight. Glutamine regulated the proliferation and apoptosis in these tumors differently through different downstream metabolites. Glutamine-derived α -ketoglutarate is a key regulator of chondrocyte differentiation. Deleting glutaminase in IDH1^{Mut} chondrocytes impaired hypertrophic differentiation and increased cell proliferation, which may lead to increased number and size of enchondroma-like lesions. In chondrosarcoma, glutaminase regulated cell apoptosis partially through producing non-essential amino

acids. Inhibiting glutaminase reduced cell viability and increased cell apoptosis.

Supplementation of non-essential amino acids partially rescued such effects.

4. Methods and Materials:

Animals:

Mice used in this study include *Scap^{fl/fl}* mice [204], *Gls^{fl/fl}* (JAX: #017894) [186], *Idh1^{LSL/+}* mice [169], *Col2a1Cre* mice [170], *Col2a1Cre^{ERT2}* mice [205], and NOD *scid* gamma (NSG) mice [206]. All the mice other than NSG were on BL6 background. *Idh1^{LSL/+}* mice bear an R132Q mutation rather than an R132H as previously clarified [4]. Adult growth plate and enchondroma-like phenotypes were analyzed on 6-month-old mice. Tamoxifen was administered daily via intraperitoneal injection for 10 days at 100 mg / kg body weight / day at 4 weeks of age. Hind limbs were harvested for histological analysis.

Cell Culture:

Chondrocytes were cultured in high-glucose DMEM with 10% FBS and 1% penicillin / streptomycin. Primary chondrosarcoma cells were cultured in α -MEM with 10% FBS and 1% penicillin / streptomycin. In some experiments, chondrocytes and chondrosarcoma cells were treated with Bis-2-(5-phenylacetamido-1,2,4-thiadiazol-2-yl)ethyl sulfide (BPTES), epigallocatechin gallate (EGCG), aminooxyacetate (AOA), non-essential amino acids (NEAA), or DMSO at indicated concentration and for indicated time period.

Metatarsal Organ Culture:

The 2nd, 3rd, and 4th metatarsal bones were dissected from the hindlimbs of embryos at E16.5. They were transferred to 24-well non-adherent plate with 1mL α -MEM supplemented with 50 μ g/ml ascorbic acid, 1mM β -glycerophosphate, and 0.2% bovine serum albumin. The media was changed every other day. In specified experiments, BrdU (Invitrogen™ Catlog#000103, 1/100) was added to the cell culture 16 hours prior to fixation. Explants were cultured at 37°C humidified 5% CO₂ incubator for five days and then fixed with 10% neutral buffered formalin (NBF).

Transfection:

In indicated experiment, chondrocytes were transfected with adenovirus-GFP and adenovirus-Cre at 400 MOI.

EdU assay:

EdU assay (ThermoFisher C10337) was performed according to manufacturer's instructions. In brief, cells were cultured with 10 mM EdU for 12 hours prior to fixation with 4% PFA / PBS for 15 min and permeabilization with 0.5% Triton™ X-100 for 20 min at room temperature. Cells were then incubated with Click-iT® reaction cocktail for 30 min in dark at room temperature and stained with DAPI.

TUNEL assay:

TUNEL assay was performed according to manufacturer's instructions (Roche, 11684795910). In brief, cells were fixed with 4% PFA / PBS at room temperature for 1 hr and permeabilized with 0.1% Triton™ X-100 in 0.1% sodium citrate for 2 min on ice.

After rinse with PBS, cells were incubated with TUNEL reaction mixture at 37°C for 1 hr and stained with DAPI.

Cell Viability Assay:

Cell viability was determined by CellTiter-Glo® Assay according to manufacturer's instructions (Promega G7570). In brief, CellTiter-Glo® Buffer was thawed at room temperature and transferred to CellTiter-Glo® Substrate. Cell culture plate was equilibrated to room temperature for 30min. 100 µL of CellTiter-Glo® Reagent was added to the cell culture media in each well. The plate was mixed for 2 min on an orbital shaker and incubated for 10 minutes at room temperature. Luminescence was then recorded. Cell viability of each primary chondrosarcoma patient sample was normalized to the average cell viability in the vehicle group of the same sample.

Annexin V / PI staining:

Annexin V and Propidium Iodide staining was performed according to manufacturer's instructions (Invitrogen™ R37176, Invitrogen™P1304MP). In brief, 1 drop of Annexin V APC Ready Flow Conjugate was added to 0.5 mL of annexin-binding buffer with 2.5 mM calcium. 1mg/mL PI was added to the APC binding buffer with 1/1000 dilution. The cells were incubated for 15 minutes at room temperature. Fluorescence was detected by flow cytometry.

Glutaminase activity assay:

Primary chondrocytes were cultured to prior to experiment. After washing cells with Hanks Buffered Saline Solution (HBSS) for three times, cells were cultured in α -MEM containing media containing 2 μ M Glutamine and 4 mCi/mL L-[3,4-³H(N)]-Glutamine (PerkinElmer, NET551250UC). Glutaminase activity was terminated by washing cells with ice cold HBSS for three times followed by scraping cells with 1 mL ice cold milliQ water. Cells were lysed by sonication for 1 min with 1 sec pulse at 20% amplitude. Cell lysates were bound onto AG 1-X8 polyprep anion exchange column. Uncharged glutamine was eluted with 2 mL of milliQ water for three times. Negatively charged glutamate and downstream metabolites were eluted with 2 mL of 0.1M HCl for three times. After adding 4 mL of scintillation cocktail to the eluent, DPM of the solution was measured by a Beckman LS6500 Scintillation counter.

Skeletal Preparations:

Embryos and neonates were incubated in 95% ethanol, acetone, Alcian Blue solution (30% Alcian Blue in 20% glacial acetic acid / H₂O), 95% ethanol, and Alizarin Red solution (5% alizarin red in 1% KOH / H₂O) for 1 day each serially at room temper, followed by incubation in 1% KOH / H₂O for three days prior to transfer to 80% glycerol.

Xenograft:

Xenograft for cholesterol study

Primary chondrosarcoma cells derived from five different patients were used in the study. Chondrosarcoma cells derived from each patient were xenografted onto 10

animals, 5 animals for lovastatin treatment and 5 animals for vehicle treatment. One million chondrosarcoma cells were subcutaneously injected to each NSG mouse. Lovastatin and vehicle control treatment started 3 to 4 weeks following injection, a time when the tumor became palpable. For each individual human xenograft, the controls and treatments were started at the same time following implantation. The mice were treated with lovastatin (4.5 mg/kg/day) or vehicle (100% ethanol) for four weeks. 5 mg/kg bodyweight of BrdU was administered via intravenous infusion 4 hours before sacrificing the mice. Tumors were harvested, weighted, and processed for immunohistochemistry.

Xenograft for glutamine study

Prior to the experiment, chondrosarcoma cells from each patient's tumor were maintained subcutaneously in vivo in NSG mice. For the xenograft experiment, tumors were surgically removed from each mouse and divided into explants of 5 x 5 x 5 mm each, and implanted into the subcutaneous tissue on the back of NSG mice. BPTES and vehicle control treatment started 10 days after implantation. Mice were treated with BPTES at 0.2 g / kg or vehicle control via intraperitoneal injection daily for 14 days. Tumor weights were recorded upon harvest. For each patient-derived xenograft experiment, relative tumor weight was determined by normalizing the tumor weight of each tumor to the average tumor weight of the vehicle control group.

D-2HG measurement:

D-2HG is analyzed by liquid chromatography – tandem mass spectrometry (LC/MS/MS). Cell culture media was collected from each sample. After adding 2-HG-²H₄ (internal standard), the sample was dried under nitrogen and derivatized by (+)-O,O'-diacetyl-L-tartaric anhydride (DATAN) for measurement.

Carbon Isotope Labeling:

Chondrocytes were cultured in DMEM with 4500mg/L Glucose and 4mM ¹⁵C₅-Glutamine in 6cm cell culture plates for specified time. 500μL methanol was used to extract metabolites from each plate. After centrifuge at 12000rpm for 15min, supernatant was dried at 37°C. The dried residues were resuspended in 25 μL of methoxylamine hydrochloride (2% (w/v) in pyridine) and incubated at 40°C for 1.5 hours in a heating block. After brief centrifugation, 35 μL of MTBSTFA + 1% TBDMS was added, and the samples were incubated at 60°C for 30 minutes. The derivatized samples were centrifuged for 5 minutes at 20,000 x g, and the supernatants were transferred to GC vials for GC-MS analysis. A modified GC-MS method was employed ²³. The injection volume was 1 μL, and samples were injected in splitless mode. GC oven temperature was held at 80°C for two minutes, increased to 280°C at 7°C/min, and held at 280°C for a total run time of forty minutes. GC-MS analysis was performed on an Agilent 7890B GC system equipped with a HP-5MS capillary column (30 m, 0.25 mm i.d., 0.25 μm-phase thickness; Agilent J&W Scientific, Santa Clara, CA), connected to an Agilent 5977A Mass Spectrometer operating under ionization by electron impact (EI) at 70 eV. Helium flow

was maintained at 1 mL/min. The source temperature was maintained at 230°C, the MS quad temperature at 150°C, the interface temperature at 280°C, and the inlet temperature at 250°C. Mass spectra were recorded in mass scan mode with m/z from 50 to 700.

¹³C-based Stable Isotope Analysis:

M₀, M₁, ..., M_n refers to the isotopologues containing n heavy atoms in a molecule. The stable isotope distribution of individual metabolites was measured by GC-MS as described above. The isotopologue enrichment or labeling in this work refers to the corrected isotope distribution ^{24,25}.

Histological Analysis:

Tissue processing: Hind limbs were fixed in 10% neutral buffered formalin for 3 days, decalcified with 14% EDTA for 2 weeks at room temperature, and embedded in paraffin. Xenografted tumors were fixed in 4% PFA overnight. Tissues were sectioned at 5µm and used for Safranin O staining, von Kossa Staining, and immunohistochemistry.

Safranin O staining

Deparaffinized slides were incubated with Weigert's Iron Hematoxylin for 5 minutes, washed with distilled water until excess dyes stopped leaching out, and then differentiated in 1% Acid-Alcohol for 2 seconds. After that, slides were rinsed with distilled water, stained with 0.02% Fast Green for 1 minutes, incubated in 1% Acetic Acid for 30 seconds, stained with 1% Safranin O for 2 hours, and dehydrated.

Von Kossa Staining

Deparaffinized slides were incubated with 1% Silver Nitrate and exposed to bright light until color appeared. The slides were washed with MilliQ water, counter-stained with Nuclear Fast Red for 5 minutes, and dehydrated.

Immunohistochemistry:

Immunohistochemistry was performed on 5 μm paraffin-sectioned limbs. For type X collagen, antigen retrieval was performed by citrate buffer incubation at 85°C for 15min and hyaluronidase digestion at 10 mg/ml at 37°C for 30 min. For BrdU staining, BrdU labeling reagent (Invitrogen, 000103) was injected to pregnant female mice at 1 mL / 100 g body weight 2 hours prior to euthanasia. Antigen retrieval was performed by proteinase K digestion at 10 $\mu\text{g}/\text{ml}$ at room temperature for 10 min. For MMP13, antigen retrieval was performed by hyaluronidase digestion at 5 mg/ml at 37°C for 30 min. For all immunohistochemistry, endogenous peroxidase activity was blocked by incubation with 3% H_2O_2 / Methanol for 10 minutes followed by incubation with Dako Dual Endogenous Enzyme Block reagent (Agilent Dako, S2003) for 30 min at room temperature. The specimen was blocked with 2% horse serum at room temperature for 30 min followed by incubation with antibodies for Col X (1:500, ThermoFisher, 14-9771-82), BrdU (1:1000, ThermoFisher, MA3-071), MMP13 (1:100, MilliporeSigma MAB13424) overnight at 4°C. TUNEL assay was performed according to manufacturer's instructions (Roche, 11684795910). In brief, the tissue was incubated with proteinase K at 10 $\mu\text{g}/\text{ml}$ at

room temperature for 20 min, and then in TUNEL labeling reagent 37°C for 1 hour.

Quantification of the length of hypertrophic zone and bone elements was done using the image processing software Fiji Image J.

In situ hybridization:

In situ hybridization was performed on 5 µm paraffin-sectioned limbs. Paraffin sections were deparaffinized and rehydrated, followed by fixation with 4% PFA at room temperature for 15 minutes. Sections were then treated with 20 µg/ml proteinase K for 15 minutes at room temperature, fixed with 4% PFA at room temperature for 10 minutes, and acetylated with for 10 minutes. Sections were then incubated with hybridization buffer at 58°C for 3 hours, and then incubated with Digoxigenin-labeled RNA probe (*Col2a1*, *Pth1r*, *Co10a1*) at 58°C overnight. Sections were then washed with 5x SSC for one time at 65°C, followed by RNase A treatment at 37°C for 30 minutes. Sections were then washed 2x SSC for one times, 0.2x SSC for two times at 65°C, and then blocked with 2% Boehringer Blocking Reagent / 20% Heat Inactivated Sheep Serum for one hour. Sections were then blocked with Anti-Digoxigenin antibody (1:4000 in blocking solution) at 4°C overnight. Sections were developed with BM Purple at room temperature until color developed. The probe sequences were described before [207].

Quantification of enchondroma-like lesions:

Enchondroma-like lesions were firstly detected by Safranin O staining. We stained 1 slide (2 sections, 10 µm) in every 10 slides (100µm) to identify enchondroma-

like lesions. We then examined every section of each bone under the microscope to determine the exact number of sections each enchondroma-like lesion spans and identify any lesions that were missed by Safranin O staining. In this way, we examined these lesions continuously. Each section is 5 μ m thick. The width of each lesion was determined by the number of sections the lesion spanned. For every Safranin O stained section, we manually outlined each lesion and measured lesion area using the image processing software Fiji Image J. We estimated tumor volume of each animal by adding up the lesion areas of every Safranin O stained section. Relative tumor volume was determined by normalizing the tumor volume of each animal to the average tumor volume of *Col2a1Cre^{ERT2};Idh1^{LSL/+}* animals.

Isolation and culturing of primary costal chondrocytes:

Costal chondrocytes were isolated from E18.5 embryos and P4 pups. Mouse sterna and ribs were digested by Pronase (Roche) (2 mg/ml) for 30min with constant agitation at 37°C, washed by PBS, then digested by Collagenase IV (Worthington) (3 mg/ml) for 1 hr in 37°C humidified chamber, washed by PBS, digested by Collagenase IV (0.5 mg/ml) for 16 hr in 37°C humidified chamber, and filtered using 45 μ m cell strainer. Costal chondrocytes from *Idh1^{LSL/+}* mice were cultured in DMEM with 10% FBS and 1% Penicillin / Streptomycin.

Filipin staining and quantification:

Filipin staining (Abcam ab133116) was performed on sternal chondrocytes according to manufacturer's instructions. Primary sternal chondrocytes were isolated from E18.5 mouse embryos from the same litter. We quantified the fluorescent intensity of the filipin staining using the image processing software Fiji Image J. Outlines of cells were drawn manually. Mean fluorescence intensities of chondrocytes isolated from control and *Col2a1Cre;Idh1^{LSL/+}* animals were measured. 10 fields of each sample were used for measurement, and the average of the 10 measurements was used as the intensity of that sample. The relative intensity was given as a ratio of the intensity of each animal normalized to the average intensity of control animals.

RNA sequencing and analysis:

RNA-seq analysis was performed on sternal chondrocytes from *Col2a1Cre*, *Idh1^{LSL/+}*, *Col2a1Cre;Idh1^{LSL/+}* animals at E18.5. RNA was extracted using RNeasy Mini Kit (QIAGEN). Extracted total RNA quality and concentration was assessed on a 2100 Bioanalyzer (Agilent Technologies) and Qubit 2.0 (ThermoFisher Scientific), respectively. Only extracts with RNA Integrity Number (RIN) greater than 7 were processed for sequencing. RNA-seq libraries were prepared using the commercially available KAPA Stranded mRNA-Seq Kit. In brief, mRNA transcripts were first captured using magnetic oligo-dT beads, fragmented using heat and magnesium, and reverse transcribed using random priming. During the 2nd strand synthesis, the cDNA:RNA hybrid was converted into to double-stranded cDNA (dscDNA) and dUTP

incorporated into the 2nd cDNA strand, effectively marking the second strand. Illumina sequencing adapters were then ligated to the dscDNA fragments and amplified to produce the final RNA-seq library. The strand marked with dUTP was not amplified, allowing strand-specificity sequencing. Libraries were indexed using a six base pairs index allowing for multiple libraries to be pooled and sequenced on the same sequencing lane on a HiSeq 4000 Illumina sequencing platform. Before pooling and sequencing, fragment length distribution and library quality were first assessed on a 2100 Bioanalyzer using the High Sensitivity DNA Kit (Agilent Technologies). All libraries were then pooled in equimolar ratio and sequenced. Multiplexing 8 libraries on one lane of an Illumina HiSeq 4000 flow cell yielded about 40 million 50bp single end sequences per sample. Once generated, sequence data was demultiplexed and Fastq files generated using Bcl2Fastq conversion software provided by Illumina.

RNA-seq data was processed using the TrimGalore toolkit which employs Cutadapt [208] to trim low quality bases and Illumina sequencing adapters from the 3' end of the reads. Only reads that were 20nt or longer after trimming were kept for further analysis. Reads were mapped to the GRCm38v75 version of the mouse genome and transcriptome [209] using the STAR RNA-seq alignment tool [210]. Reads were kept for subsequent analysis if they mapped to a single genomic location. Gene counts were compiled using the HTSeq tool. Only genes that had at least 10 reads in any given library were used in subsequent analysis. Normalization and differential expression

was carried out using the DESeq2 [211] Bioconductor [212] package with the R statistical programming environment. The false discovery rate was calculated to control for multiple hypothesis testing. Gene set enrichment analysis was performed to identify differentially regulated pathways and gene ontology terms for each of the comparisons performed [213].

Gene expression of *Gls* from chondrosarcoma patient samples:

We used retrospective data from RESOS INCA network of bone, collected from 102 cartilage tumors in different French hospitals. Multiple samples may be taken from each tumor and sequenced. More details about the experiment, such as RNA isolation method and profiling, can be found the original paper [194]. For our purposes, we utilized IDH mutation information to categorize samples into two groups: IDH1/2 mutation (n=46) and IDH1/2 wild type (n=98). We examined several gene expression levels across these two groups and reported adjusted p-value for *Gls* result (with Benjamini–Hochberg correction). All the data processing and calculation was performed using Bioconductor docker (devel), with R version 4.0.3 and Bioconductor version 3.13.

Chondrosarcoma cell and explant culture:

Chondrosarcoma cells and/or xenograft explants were cultured in MEM- α with 10% FBS and 1% Penicillin / Streptomycin. Cells / explants were treated with 20 μ M lovastatin and vehicle (100% ethanol) for 48 hours. Cell viability was measured by SRB cell cytotoxicity assay.

Measurement of cholesterol levels:

We measured cholesterol levels from cryopreserved chondrosarcoma tissues using the cholesterol / cholesteryl ester assay kit (Abcam ab65359) according to manufacturer's instruction. 10 mg tissue from each chondrosarcoma was used for the measurement.

RNA isolation and qPCR

Total RNA isolation was isolated using Trizol and chloroform. 1ml Trizol was added to cell pellet. After resuspension, the tubes were incubated at room temperature for 10 minutes. 200 μ L of chloroform was added to the tube and mixed well. After centrifuge at maximum speed for 10 minutes, the solution was separated to three layers. The top layer of aqueous phase solution was transferred to a clean tube and mixed with 200 μ L of isopropanol to precipitate RNA. After incubation at room temperature for 10 minutes, the tube was centrifuged at maximum speed for 10 minutes, and supernatant was discarded. RNA pellet was washed with 70% ethanol for two times. After that, RNA was dissolved in molecular grade water.

1 μ g of RNA was used to synthesize cDNA through reverse transcription using iScript cDNA synthesis kit. Quantitative real-time PCR (qPCR) was then performed with using the Powerup SYBR green reagent (Invitrogen, A25777) on a QuantStudio 3 real-time PCR system (Thermo Fisher Scientific). Relative gene expression was calculated

and normalized to a housekeeping gene (beta-actin) using the $2^{\Delta\Delta Ct}$ method. Primer sequences were listed in Appendix B.

Western blotting:

Cultured chondrocytes were lysed in RIPA Buffer containing protease and phosphatase inhibitor tablet (Roche, 11836170001 & SIGMA – 4906845001, respectively). E18.5 growth plate cartilages were harvested from E18.5 embryos, snap frozen and lysed in the same way. Protein concentration was quantified using the BCA method (Pierce). Proteins were resolved on 8% polyacrylamide gels and transferred onto Immuno-Blot PVDF membrane (Bio- Rad). After the wet transfer, the membranes were blocked for 1 h at room temperature in 5% milk powder in TBS with 0.1% Tween (TBST) and then incubated at 4°C with the primary antibody overnight. Membranes were washed three times with TBST and further incubated with anti-rabbit IgG, HRP-linked antibody (RRID: AB_2099233) in 5% milk (in TBST) for 1 h at room temperature. All blots were developed using either enhanced or normal chemiluminescence (Clarity Substrate Kit, Bio-Rad). Each experiment was repeated with a minimum of three independently prepared protein samples. Antibodies were listed in Appendix B.

Quantification and Statistical Analysis:

Statistical analyses were performed using Graphpad Prism 9 software. Data were presented as mean±SEM, mean±SD, or mean±95% as specified in each figure. Statistical

significance was determined by two tailed student-t test or one-way or two-way ANOVA with multiple comparisons test as specified in each figure.

5. Conclusion and Future Directions:

Mutations of *IDH1* and *IDH2* are identified in a wide variety of tumors.

However, how such mutations differentially regulate the tumors at different stages are not clearly understood. Furthermore, pharmacological intervention of the mutant *IDH1/2* enzymatic functions have not led to clinical success in solid tumors, suggesting the regulation by mutant *IDH1/2* genes might be beyond production of D-2HG. Answers to these questions would shed light on our understanding of tumor development and potentially lead to therapeutic solutions to cancers with these mutations.

The majority of cartilage tumors enchondromas and chondrosarcomas harbor mutations of *IDH1* or *IDH2*. The benign tumor enchondroma could progress to the malignant cancer chondrosarcoma. As these tumors are at different stages of tumor progression, they provide a good model for us to understand how *IDH1/2* mutations regulate tumor biology from the initiation step to cancer maintenance. In addition, currently there is no universally effective therapeutic options for these tumors and high-grade chondrosarcomas had a poor prognosis even after surgical removal, thus it is necessary and urgent to understand how *IDH1/2* mutations regulate these tumors and develop therapies based on such knowledge. For this dissertation, I examined the transcriptomic and metabolic regulation in these *IDH1/2* mutant cartilage tumors and focused on the role of cholesterol biosynthesis and glutamine metabolism in enchondroma and chondrosarcoma.

In terms of transcriptional regulation, I identified that cholesterol biosynthesis pathway was upregulated in chondrocytes with *Idh1* mutation. I confirmed that the change in gene expression did lead to increased cholesterol levels in these chondrocytes. *IDH1*-mutant human chondrosarcomas had higher cholesterol concentrations. Furthermore, inhibiting cholesterol biosynthesis using genetic approach and pharmacological inhibitors led to reduced tumor development in enchondroma and reduced weight of chondrosarcoma xenograft respectively, suggesting cholesterol biosynthesis is important for the tumor development of the benign cartilage tumor enchondroma as well as the cancer maintenance of the malignant cartilage cancer chondrosarcoma.

Regarding metabolic regulation, I found that both enchondromas and chondrosarcomas with *IDH1/2* mutations have upregulated glutamine metabolism. However, the role of glutamine metabolism in these two tumors are different. In the benign tumor enchondroma, deleting glutaminase (*Gls*) increased tumor number and tumor size, likely through interruption of chondrocyte differentiation. Whereas in the malignant cancer chondrosarcoma, inhibiting GLS reduced tumor weight *in vivo* potentially through increased programmed cell death. Specifically, I identified that glutamine-derived α -KG served as a key regulator for the differentiation of *Idh1*-mutant chondrocytes, and potentially regulate the enchondroma-like phenotype. Whereas in *IDH1/2*-mutant chondrosarcoma, glutamine-derived non-essential amino acids were

important for cancer cell survival. Inhibiting *GLS* reduced the concentration of some of these amino acids, and eventually led to increased apoptosis. These data suggested the metabolic adaptation and regulation may vary during tumor progression; thus, it is critical to understand the specific metabolic needs at different stages of tumor development when designing targeted therapy and differentiate tumors at different stages when prescribing these therapies.

My work provided insights on how *IDH1/2* mutations regulate tumor behaviors through transcriptional and metabolic alterations in enchondroma and chondrosarcoma. Such insights provide novel knowledge of the mechanisms of action of these commonly present oncogenic mutations, deepen our understanding of the process of tumor development, and provide direction for identifying therapeutic targets. However, many questions regarding the molecular mechanisms of how these changes regulate chondrocyte and cartilage tumors remain unclear. In addition, it is also unknown whether these mutations could regulate chondrocytes and cartilage tumors through other signaling pathways. In the following part of this chapter, I will discuss the potential future directions to address these questions.

5.2 Cholesterol in Cancer.

In chapter 2, I found that cholesterol biosynthesis and cholesterol levels were increased in chondrocytes and chondrosarcomas with mutant *IDH1* enzyme. Cholesterol biosynthesis pathway was significantly upregulated in chondrocytes with *Idh1* mutation

and intracellular cholesterol levels were higher in these *Idh1*-mutant chondrocytes. Suppressing cholesterol biosynthesis by genetically knocking out *Scap* (a positive regulator of cholesterol biosynthesis) led to reduced enchondroma formation. Intracellular cholesterol biosynthesis also plays critical role in human chondrosarcomas. Cholesterol levels were significantly higher in these *IDH1*-mutant chondrosarcomas compared to the ones with wildtype *IDH1/2* genes. Pharmacological inhibition of cholesterol biosynthesis with lovastatin led to impaired cancer cell viability *in vitro* and smaller xenograft tumors *in vivo*. In the patient-derived xenograft tumors, lovastatin suppressed cell proliferation consistently and upregulated apoptosis in some chondrosarcoma patient samples. Together these data suggest intracellular cholesterol synthesis has an important role in regulating cartilage tumors, but the mechanisms are not clear.

Aberrant overexpression or overactivation of enzymes in the cholesterol biosynthesis pathway (e.g. *HMGCR*) or the regulators of the pathway has been reported in a variety of human cancers such as glioma, melanoma, breast, colorectal, prostate, and ovarian cancer, etc. [214]. However, the relationship between upregulated *HMGCR* gene expression and cancer prognosis is not clear as different studies have reported controversial results. Take breast cancer as an example, in one study of 511 breast cancers, the protein level of *HMGCR* was reported to be associated with better prognostic parameters including tumor size, histological grade, and proliferation rate

[215]. Whereas in another meta-analysis of 865 patients, high *HMGCR* mRNA expression was associated with poor prognosis and reduced survival [216]. *SQLE* encodes for another key enzyme in cholesterol biosynthesis pathway squalene epoxidase. Overexpression of *SQLE* was associated with more aggressive breast cancer outcome [217]. The transcription factor regulating cholesterol biosynthesis pathway, SREBPs, are also disrupted in some human cancers. In breast cancer, SREBP1 level was positively correlated with poor prognosis and it could promote invasion and migration [218]. In the human liver cancer cell line HepG2 cells, SREBP2 regulates the oncogene *SND1*, which could promote cancer growth and metastasis [219, 220]. In glioblastoma, genes upregulated by SREBPs were reported to be associated with poor prognosis, and nuclear SREBP1 levels were higher in glioblastoma than in neighboring normal tissues [221, 222].

Cholesterol biosynthesis could be activated through different mechanisms in different cancer types. In glioblastoma, activation of SREBPs is by part mediated by EGFR signaling [221, 223]. Mechanistically, active EGFR signaling promotes glucose uptake and N-glycosylation of SCAP, which consequently enhanced SREBP translocation and activation [223]. In prostate cancer, activation of SREBP was mediated through androgen receptor signaling [214]. SREBPs could also be activated by mTOR signaling, Wnt/ β -catenin signaling, and mutant p53, etc. [214]. In addition, *HMGCR* is also a direct transcriptional target of HIF-1 α [224].

Cholesterol could also impact tumorigenesis and carcinogenesis through a wide variety of mechanisms. Cholesterol is a regulator of hedgehog signaling, a pathway that is dysregulated in multiple cancers including chondrosarcoma. Extracellular cholesterol causes conformational changes in Smoothed after binding with it, which is sufficient to activate Smoothed and Hedgehog signaling [63]. Lysosomal cholesterol could regulate mTORC1 signaling through a putative amino acid transporter SLC38A9 and the major lysosomal cholesterol transporter Niemann-Pick C1 protein [225]. Cholesterol could also promote cancer formation through interaction with the immune system. In a mouse model of colorectal cancer, high-cholesterol diet promoted inflammatory response in macrophages and consequently caused greater tumor burden [226].

Statins are competitive inhibitors for HMGCR, the rate limiting enzyme in mevalonate pathway. They are used to treat hypercholesterolemia and cardiovascular diseases. In certain cancers, statins have also showed anti-cancer effects. In a recent study in patients with head and neck cancer, statin use was reported to be associated with improved outcome [227]. The antitumor effects of statins could be exerted by regulation of cell cycle and apoptosis. In the regulation of cell cycle, statins affect expression of cell-cycle regulatory proteins [228]. In breast cancer cells, lovastatin treatment led to accumulation of cyclin-dependent kinase inhibitors p21 and p27 by inhibiting proteasome function, and consequently caused cell cycle arrest in G1 phase [229]. In breast cancer cells transfected with *BRCA1* genes, statin treatment caused

downregulation of cyclin D1, cyclin-dependent kinase 4 (CDK4) and retinoblastoma protein (pRb), and upregulation of cyclin-dependent kinase inhibitor p21WAF1/CIP1 [230]. Statins induce apoptosis in cancers through interaction with different signaling pathways. In prostate cancer, simvastatin induced apoptosis by inhibiting the phosphorylation and activity of Akt [231]. In lymphoma, Fluvastatin induced apoptosis through enhanced oxidative stress [232]. In osteosarcoma, statins (atorvastatin, simvastatin, cerivastatin) treatment led to defected protein geranylgeranylation, which resulted in inhibited p42/p44-MAPKs-Bcl-2 signaling and apoptosis [233].

More work needs to be done to determine whether cholesterol biosynthesis could be a therapeutic target in cartilage tumors. It will be ideal if we could investigate clinical data and find whether the occurrence and prognosis of these cartilage tumors are associated with statin usage. As statin is widely prescribed for other conditions, such data may be available. In addition, we could also conduct in-depth analysis of published -omics datasets of these cartilage tumors to identify dysregulated signaling pathways that are known to be affected by cholesterol. Such information will provide insights about potential mechanisms by which cholesterol biosynthesis regulates cartilage tumors. Hedgehog signaling is known to be regulated by cholesterol in different cancer cells and chondrocytes. It is also frequently upregulated in enchondromas and chondrosarcomas. It is interesting to examine whether *Scap* and lovastatin regulated enchondroma and chondrosarcoma by altering Hedgehog signaling.

5.2 α -KG and Chondrocyte Differentiation

In my study, I identified that deleting *Gls* in *Idh1*-mutant chondrocytes disrupted their differentiation *in vivo* and *ex vivo*. Glutamine-derived α -KG served as a key regulator of chondrocyte differentiation in *Col2a1Cre;Gls^{fl/fl};Idh1^{LSL/+}* animals. As enchondromas arise from dysregulated chondrocyte differentiation, I propose that glutamine metabolism regulates enchondroma through its downstream metabolites α -KG. I observed that mutant IDH enzymes diverted α -KG to the production of D-2HG and consequently depleted this key metabolite. Inhibiting GLS further reduced intracellular α -KG concentration, which caused an additional block in chondrocyte differentiation in *Idh1*-mutant chondrocytes and potentially led to aggravated enchondroma-like phenotype. Supplementing exogenous cell permeable DM- α -KG to pregnant female partially rescued the defects in chondrocyte differentiation in *Col2a1Cre;Gls^{fl/fl};Idh1^{fl/+}* animals, indicating *Gls* regulated chondrocyte differentiation in *Col2a1Cre;Gls^{fl/fl};Idh1^{fl/+}* animals through the downstream metabolite α -KG. It remains unknown how α -KG exerts its function in regulating chondrocyte differentiation in *Col2a1Cre;Gls^{fl/fl};Idh1^{LSL/+}* animals.

α -KG is known to be able to regulate cell differentiation through epigenetic modifications in different cell types including the ones in the skeletal system. During endochondral ossification, glutaminase was reported to control expression of

chondrogenic markers through regulating histone acetylation by producing the metabolites α -KG and consequently acetyl-CoA [108]. It was reported that genetically deleting or pharmacological inhibiting GLS suppressed chondrogenic gene expression in growth plate chondrocytes through compromised H3K9 acetylation and H3K27 acetylation [108]. Treating *Col2a1Cre;Gls^{fl/fl}* mice with DM- α -KG or acetate *in vivo* restored chondrogenic gene expression in growth plate chondrocytes [108]. α -KG was reported to control osteogenic potential in aged mesenchymal stromal cells (MSCs) through regulating H3K9 trimethylation (H3K9me3) and H3K27 trimethylation (H3K27me3) [234]. In that study, the authors observed that supplementing α -KG to the drinking water for aged rodents increased their bone mass, reduced aged-related bone loss, and promoted bone regeneration [234]. α -KG-treated aged MSCs had reduced H3K9me3 and H3K27me3, displayed increased number of MSCs, and decreased percentage of H3K9me3 positive and H3K27me3 positive MSCs [234]. The authors proposed that α -KG could rejuvenate MSCs through modifying histone methylations [234].

In addition to cells in the skeletal system, α -KG also regulates the lineage allocation of other cell types through epigenic modification, mostly promoting histone demethylation and DNA demethylation by serving as a co-factor for 2-oxoglutarate-dependent oxygenases. In mouse embryonic stem cells, α -KG suppressed cell differentiation by promoting demethylation of DNA, demethylation of repressive

histone marks H3K9me3, H3K27me3, H3K4me3, and demethylation of active histone mark H3K36me3 through TET-family of DNA demethylase and Jumonji C-domain containing histone demethylases [235, 236]. In committed human pluripotent stem cells, α -KG promoted differentiation through altering DNA and histone methylation [237]. In hematopoietic stem cells, α -KG promoted myeloid differentiation through altering DNA methylation [238]. In old hematopoietic stem cells, α -KG production was restricted at low concentration through autophagy to maintain the stemness of the cells [238]. In the context of T cells, α -KG promoted T helper 1 cell (T_H1) differentiation over regulatory T cell (T_{reg}) differentiation [239] and it enhanced expression of effector T cell gene expression through regulating H3K27me3 and DNA methylation [240]. α -KG also promoted differentiation of epidermal stem cells by facilitating H3K27me3 demethylation and suppressed malignant progression of squamous cell carcinoma [241]. In colorectal cancer, α -KG promoted DNA demethylation and H3K4me3 demethylation to promote expression of differentiation-associated genes and to downregulate Wnt target genes to suppress cancer cell stemness [242].

For the next step, it is important to understand how α -KG controls chondrocyte differentiation in *Col2a1Cre;Gls^{fl/fl};Idh1^{LSL/+}* animals. I hypothesize that α -KG could affect chondrocyte differentiation through epigenetic modifications such as DNA methylation, histone methylation, and/or histone acetylation. DNA methylation could be examined by 5-hydroxymethylcytosine (5hmC) dot blot. First, it is important to determine whether

DNA methylation pattern is different in chondrocytes in *Col2a1Cre;Gls^{fl/fl};Idh1^{LSL/+}*, *Col2a1Cre;Idh1^{LSL/+}*, *Col2a1Cre;Gls^{fl/fl}*, and wildtype animals. Next, it is important to understand whether DM- α -KG treatment affects DNA methylation. If a difference is observed, we could examine whether the rescue effects of exogenous DM- α -KG would be blunted when TET-enzymes are inhibited by inhibitors Bobcat339 or C35 [243, 244]. In this way, we would determine if α -KG regulates chondrocyte differentiation through DNA methylation in these animals. To examine alterations in histone modification, we can examine different histone marks (e.g., H2AK5 acetylation, H3K9 acetylation, H3K27 acetylation, H3K14 acetylation, H3K9 methylation, H3K27 methylation, H3K36 methylation, H3K4 methylation, H4K4 acetylation, H4K8 acetylation, etc.) by western blot. First, we would determine if any of these histone marks are different in chondrocytes from *Col2a1Cre;Gls^{fl/fl};Idh1^{LSL/+}*, *Col2a1Cre;Idh1^{LSL/+}*, *Col2a1Cre;Gls^{fl/fl}*, and wildtype animals and if any of them are altered by DM- α -KG treatment. Next, we could determine whether the rescue effects of exogenous DM- α -KG would be blunted when the histone modifying enzymes for the histone marks are inhibited. To investigate whether there is a mechanistic link between histone modifications and chondrocyte differentiation, we could conduct ChIP-seq analysis of these histone marks to examine whether these histone modifications regulate expression of chondrogenic genes. ChIP-seq may also reveal the mechanisms that orchestrate chondrocyte differentiation.

5.3 Non-Essential Amino Acids in Cancer.

In chondrosarcomas with *IDH1/2* mutation, inhibiting glutaminase by small molecule inhibitor BPTES led to reduced tumor weight and cell viability through upregulated apoptosis. This suggests that glutaminase plays a role in regulating cell apoptosis in these *IDH1/2*-mutant malignant chondrosarcoma. Treatment with the pan-transaminases inhibitor AOA led to a similar reduction of cell viability in these cancer cells, but treatment with glutamate dehydrogenase inhibitor EGCG did not affect cell viability, suggesting transaminases may play a more important role in regulating chondrosarcoma cell viability downstream of glutamines. BPTES reduced glutamine contribution and intracellular concentration of glutamine-derived metabolites, including α -KG, other TCA cycle intermediates, and NEAA. Supplementation of NEAA, but not cell permeable DM- α -KG, to chondrosarcoma cell culture led to a partial rescue of BPTES-induced apoptosis. These data suggest GLS regulates cell apoptosis in *IDH1/2*-mutant chondrosarcomas partially through generating NEAA. For next steps, it is important to understand how NEAA regulate the viability of chondrosarcoma cells, and which non-essential amino acid(s) becomes essential when glutaminase is inhibited.

5.3.1 Glutathione and Reactive Oxygen Species

NEAA play important roles in regulating cancer cell proliferation and apoptosis in various types of cancer. A key mechanism by which NEAA regulate cancer cell apoptosis is through maintaining cellular redox balance. Reactive oxygen species (ROS)

such as superoxide anion (O_2^-), hydrogen peroxide (H_2O_2), and hydroxyl radical ($OH\cdot$) are usually higher in highly proliferative cancer cells. Low levels of ROS are reported to be essential for regulating normal physiological functions, whereas excessive ROS could induce cell death by oxidizing and damaging macromolecules (protein, DNA, lipid, etc.) [245]. Reduced glutathione (GSH) is a key mediator of ROS levels. They serve as an hydride donor to neutralize ROS and become oxidized to oxidized glutathione (GSSG) [246]. GSH is a tripeptide made of glutamate, cysteine, and glycine. Glutamine could contribute to the production or uptake of all three amino acids either directly or indirectly. Glutaminase deaminates glutamine to glutamate. Glutamate could also be used in exchange for cystine (the dimer of cysteine) through the antiporter xCT. Cysteine is the key amino acid for redox regulation due to its thiol group. Glutamate could also contribute to glycine synthesis. Through transamination reaction mediated by phosphoserine aminotransferase 1, glutamate transfers its amino group to 3-phosphohydroxypyruvate to synthesize phosphoserine, which could be converted to serine and then glycine [85]. Oxidative stress, such as H_2O_2 treatment, could induce cell death in multiple cancer types through p53-mediated apoptosis [245]. Inhibiting xCT induced apoptosis in gliomas, pancreatic cancers, and prostate cancers due to increased ROS [247-249]. Specifically, glioma cells with *IDH1* mutations displayed increased demand for GSH metabolism through nuclear factor erythroid 2-related factor 2 (Nrf2) signaling [250]. Inhibiting Nrf2 pathway in these cancer cells showed anti-cancer effects,

supporting the notion that GSH plays key roles in regulating cell survival in *IDH1/2*-mutant cancers [250].

For the next step, I would like to examine whether GLS inhibition induced apoptosis through increased oxidative stress and whether NEAA rescued apoptosis through enhanced GSH synthesis. In *IDH1/2*-mutant chondrosarcomas, the intracellular concentrations of glutamate and glycine were reduced upon GLS inhibition, which could potentially lead to compromised GSH synthesis. To test whether this is true, I would measure the intracellular ROS and GSH levels with and without BPTES treatment using commercial kits. We could also trace glutamine contribution to GSH synthesis through isotope labeling and examine whether it is affected by BPTES. Furthermore, we could also add exogenous cell permeable GSH-ethyl ester to BPTES treated chondrosarcomas and examine whether apoptosis could be rescued. If BPTES induced apoptosis through increased ROS by compromised GSH synthesis, I would expect to observe increased ROS, decreased GSH levels, and decreased glutamine contribution to GSH upon BPTES treatment. In addition, I would also expect to observe a rescue in BPTES-induced apoptosis by GSH-ethyl ester.

Exogenous glutamate and glycine were provided by the NEAA supplementation solution. I would like to examine whether ROS and GSH levels can be restored in BPTES treated chondrosarcoma cells upon NEAA supplementation. In addition, I would like to examine whether the rescue effects by NEAA would be abolished upon buthionine

sulfoximine (BSO, an inhibitor for gamma-glutamylcysteine synthetase, the rate limiting enzyme for GSH synthesis) treatment. If NEAA rescued apoptosis through enhanced GSH synthesis, I would expect to see increased GSH levels and decreased ROS levels with NEAA supplementation in BPTES-treated chondrosarcoma cells; and the BPTES-induced apoptosis would not be rescued when NEAA is added together with BSO.

5.3.2 “Essential” Non-Essential Amino Acids upon GLS Inhibition

NEAA mixture provides seven non-essential amino acids alanine, asparagine, aspartate, glycine, serine, proline, and glutamate. Many of them have been shown to be critical for cancer cell viability, especially under metabolic stress. In glioblastoma and neuroblastoma, glutamine deprivation induced apoptosis, which could be restored by exogenous asparagine [203]. In addition, knocking down citrate synthesis had similar rescue effects as it diverts oxaloacetate for aspartate and asparagine synthesis [203]. Asparagine also rescued apoptosis and translation when glutamine was deprived, but it did not serve as a precursor for glutamine synthesis due to the lack of asparaginase [251]. Under glutamine-deprivation condition, forced expression of zebrafish asparaginase in cancer cells restored anaplerosis, but hindered cell proliferation and survival [251]. Asparagine was reported to support cancer cell survival by serving as an amino acid exchange factor [252]. In some cancers, aspartate becomes “essential” when glutamine availability or metabolism is limited. Alkan et al. reported that glutamine was used for aspartate synthesis through anaplerosis [253]. When cancer cells could not

sustain cytosolic aspartate, their survival were compromised upon glutamine starvation [253]. In this study, aspartate could rescue cell survival in the presence of the transaminase inhibitor AOA, whereas NEAA could only rescue cell survival without AOA, suggesting aspartate might be the end product of transamination in support of cell survival [253]. Loss of aspartate glutamate carrier 1 (*AGC1*, the transporter that exports aspartate from mitochondrial to the cytosol) sensitized cancer cells to glutaminase inhibition *in vitro* and *in vivo* [253]. In another study, Tajan et al. showed that p53 induced expression of the glutamate / aspartate transporter *SLC1A3* to increase aspartate uptake upon glutamine deprivation [254]. Aspartate supported cell viability through maintaining electron transport chain, TCA cycle activity, and biosynthesis of glutamine / glutamate and nucleotides [254]. Furthermore, deleting *SLC1A3* impaired cancer growth *in vitro* and *in vivo* when glutamine was limited [254]. Serine is another non-essential amino acid that could regulate cancer cell survival. During serine deprivation, p53 rewired cellular metabolism for serine and GSH synthesis, and thus maintained cell survival [255]. In mouse models of breast cancer and melanoma, dietary serine or increased expression of phosphoglycerate dehydrogenase (*PHGDH*, the first enzyme in serine synthesis pathway) accelerated cancer growth [256]. Dietary restriction of serine and glycine restrained tumor growth in multiple cancer cells [255-257].

These studies demonstrated that several non-essential amino acids could become “essential” under glutamine starvation or glutamine restriction. Combinational

inhibition of glutamine utilization and other amino acids' utilization could lead to more prominent effects in restricting cancer growth. My study demonstrated that NEAA could rescue BPTES-induced apoptosis in *IDH1/2*-mutant chondrosarcomas. In the future, it will be interesting to identify the “essential non-essential amino acid(s)” in these cancers to elucidate the cellular mechanisms underlying these observations. To do so, we could add exogenous non-essential amino acids separately or in combination to the BPTES treated *IDH1/2*-mutant chondrosarcomas and examine whether any of them could rescue the apoptosis induced by BPTES. One potential limitation of this proposed study is that exogenous amino acids might not be taken up efficiently as amino acid uptake is restricted by expression level of their transporters. To solve this problem, cell permeable amino acids or overexpression of certain amino acid transporters might be necessary. Supplementation of NEAA only caused a partial rescue in these cancer cells, which might be a result of inefficient amino acid uptake. In addition, although DM- α -KG could not rescue BPTES-induced apoptosis in these cancer cells, it will be important and interesting to examine whether addition of DM- α -KG and NEAA simultaneously could cause a synergistic effect in rescuing BPTES-induced cell death.

5.4 Divergent Roles of D-2HG in Tumor Initiation and Cancer Maintenance in Cartilage Tumors.

The concept that D-2HG functions as an “oncometabolite” is prevalent in many cancers with *IDH1/2* mutations. However, its role in cartilage tumors is not clearly

understood. It is also not known whether inhibiting D-2HG could be an effective therapeutic option for these *IDH1/2*-mutant cartilage tumors.

In *IDH1/2*-mutant chondrosarcomas, the effects of blocking D-2HG production on cancer maintenance are variable. In one study, it was reported inhibition of D-2HG production led to compromised chondrosarcoma viability in chondrosarcomas with *IDH1* mutation [12], but a second study reported that chondrosarcoma cell viability was not affected upon treatment by mutant IDH1 inhibitor despite effective reduction of D-2HG production [7]. Importantly, several clinical trials of mutant IDH inhibitors have been conducted in patients with chondrosarcoma [258]. The results to date have been variable, showing at best stabilization of the disease [141].

In the early stage of enchondroma development, production of D-2HG might be of greater importance in regulating tumorigenesis. In chapter 3, I showed that α -KG played an important role in governing chondrocyte differentiation and potentially enchondroma development. Though the mechanism through which α -KG exerted its regulation remains to be investigated, it is likely that α -KG might regulate chondrocyte differentiation by serving as a co-factor for 2-oxoglutarate dependent oxygenases. D-2HG is structurally similar to α -KG and could compete with α -KG for binding with 2-oxoglutarate dependent oxygenases. Production of D-2HG consumes α -KG so that α -KG levels is lower in chondrocytes with *Idh1* mutation. Thus, D-2HG could impair the activities of these enzymes by competitively inhibiting the enzymes and / or depleting α -

KG. Furthermore, preliminary data from our lab has shown that addition of exogenous 2-HG to metatarsal organ culture suppressed chondrocyte mineralization (Fig 35, Appendix A). These data suggested that D-2HG might be able to promote tumorigenesis in enchondroma and there is a possibility blocking mutant IDH1 function might be able to rescue chondrocyte differentiation in *Col2a1Cre;Idh1^{LSL/+}* animals.

A main approach through which D-2HG promotes tumorigenesis / carcinogenesis in different cancers is through regulating cell differentiation via epigenetic modifications. In many cancers, D-2HG keeps cancer cells in a less mature progenitor stage through these epigenetic modification. These immature cells with *IDH1/2* mutations then become neoplastic and form a cancer. However, whether blocking D-2HG would restrain tumorigenesis and whether the epigenetic changes and differentiation defects are reversible seem to be context dependent. The gene expression profile of *IDH1/2*-mutant glioma patient tumors showed enrichment in genes expressed by neural progenitor cells [134]. Importantly, the genomic and epigenetic alterations caused by prolonged exposure of mutant IDH1 were not reversible in human astrocytes and glioma tumorsphere, raising the question whether inhibiting mutant IDH1/2 enzymes could suppress the malignant behavior of a tumor once it is formed [259]. In the context of AML, the story is different. Pharmacologic 2-HG blockade showed anti-cancer activity in AML and is now approved for patient use [260]. Expression of mutant *IDH1/2* or addition of cell permeable D-2HG effectively blocked adipocyte differentiation and

astrocyte differentiation by suppressing histone demethylation [134]. In the context of acute myeloid leukemia (AML), D-2HG produced by mutant IDH1/2 inhibited TET2 enzyme and caused DNA hypermethylation, which was associated with impaired myeloid differentiation [136]. Expression of mutant *Idh2* or knocking down *Tet2* in myeloid cells or primary bone marrow cells suppressed myeloid differentiation and increased the proportion of hematopoietic progenitor cells [136]. When a mutant *Idh1* gene was knocked in in murine myeloid lineage, the cells also exhibited DNA hypermethylation and the mice had increased hematopoietic progenitor cells [169]. Acute myeloid leukemia cells can derive from progenitor cells in myelodysplastic syndromes [261]. It is possible that 2-HG blockade could inhibit the initiation of new leukemic cells from progenitors, thus having an anticancer effect by blocking tumor initiation. These studies suggest that D-2HG may play a critical role in tumor initiation through impairing cell differentiation, but it may not be as important in tumor cell maintenance or tumor progression. This could also explain the seemingly contradictory data in preclinical studies as they had different experimental design and were conducted in tumors of different stages.

The fact that D-2HG may be playing divergent roles in tumor initiation versus cancer maintenance could also explain the phenotype we observed in chondrocytes and cartilage tumors. In cartilage tumors, it is possible that D-2HG production leads to epigenetic changes and facilitates tumor initiation. However, further neoplastic cell

maintenance might be regulated by other mechanisms, such as metabolic alterations, than D-2HG production itself. It will be interesting to examine whether D-2HG is sufficient and necessary to initiate enchondroma formation. To test whether D-2HG is sufficient to initiate enchondroma formation, we could administer cell permeable D-2HG to mice starting from 4 weeks of age and examine whether these animals will develop enchondroma-like lesions after three months. If so, we could conclude that D-2HG is sufficient for tumor initiation of enchondroma. To test whether D-2HG is necessary for the tumor initiation process, we could treat *Col2a1Cre^{ERT2};Idh1^{LSL/+}* mice with mutant IDH1 inhibitor since the start of tamoxifen injection until harvest. If the mice in the IDH1 inhibitor group developed fewer or no enchondroma-like lesions, it suggests D-2HG is necessary for the tumor initiation of enchondroma. Effectiveness of the drug treatment could be monitored by measuring D-2HG levels in cartilage tissues. If D-2HG is sufficient and / or necessary for enchondroma initiation, I would like to examine whether the tumor initiation process is associated epigenic changes. We could isolate primary chondrocytes from wildtype BL6 mice, treat them with D-2HG, and then examine whether histone and DNA methylation patterns are altered upon D-2HG treatment.

The effects of mutant IDH1 inhibition on chondrosarcoma growth and survival have been variable in different studies. It will also be important to examine the effects of

inhibiting mutant IDH1/2 on chondrosarcoma viability and growth in more tumor samples, especially *in vivo*.

5.5 HIF Signaling in Cartilage Tumors

In addition to the findings in the above chapters, I also observed activation of HIF-1 α -signaling in chondrocytes with *Idh1* mutation. Expression of several HIF-1 α target genes was upregulated in chondrocytes expressing mutant *Idh1* when compared with control (Fig 36 A-C, Appendix A). In addition, protein level of HIF-1 α was significantly increased in chondrocytes with *Idh1* mutation when they were cultured with deferoxamine (DFX, an iron chelator that stabilizes HIF-1 α) (Fig 36 D). The protein of HIF-1 α was not detected in the absence of DFX, likely because it was degraded during the process of protein preparation. Furthermore, when metatarsals were cultured under hypoxic condition (1% O₂), chondrocyte mineralization was significantly compromised in wildtype control animals (Fig 36 E, F). No changes were observed in *Col2a1Cre;Idh1^{LSL+}* metatarsals between normoxic and hypoxic conditions as mineralization was not detected in either condition. These data demonstrated that 1) *Idh1* mutation caused activation of HIF-1 α -signaling in chondrocytes; and 2) hypoxia could suppress chondrocyte differentiation and mineralization, a phenotype resembling *Idh1*-mutant animals. However, whether *Idh1* mutation causes the chondrocyte differentiation defects and enchondroma-like phenotypes through overactivation of

HIF-1 α -signaling is not known. Thus, it is interesting to examine whether *Idh1* mutation could regulate chondrocyte differentiation and tumorigenesis through HIF-1 α signaling.

HIF-1 α signaling plays a critical role in regulating chondrocyte survival and differentiation [42]. In 2001, Schipani et al. reported that chondrocytes of *Hif1a*^{-/-} animals exhibited massive cell death in the center of growth plates, suggesting HIF-1 α is necessary in maintaining cell viability of growth plate chondrocytes [42]. Yao et al. showed that the cell death phenotype in *Hif1a*-deficient chondrocytes was partially caused by enhanced mitochondrial respiration [47]. Conditionally inhibiting mitochondrial respiration in mesenchymal progenitors by deleting mitochondrial transcription factor A (*Tfam*) rescued the massive cell death phenotype caused by *Hif1a*-deletion [47]. Deleting *Vegfa*, a HIF-1 α target gene, in chondrocytes resulted in apoptosis phenotype that resembled *Hif1a* deletion. Overexpressing a VEGF isoform in *Hif1a*-deficient chondrocytes prevented cell death. These data suggested HIF-1 α signaling could potentially regulate chondrocyte apoptosis partially through its downstream target gene *Vegfa* [44-46]. Conditionally deleting *Phd2* using *Col2a1*Cre led to upregulated HIF signaling, higher bone mass, and decreased bone length [52-54]. Conditional deleting *Vhlh* in mesenchymal progenitors or chondrocytes led to reduced chondrocyte proliferation, severe dwarfism, and delayed chondrocyte terminal differentiation [55, 56]. Moreover, deleting *Vhlh* in mesenchymal progenitors led to the formation of a cartilage remnant in the bone marrow postnatally [56]. This phenotype

resembles the enchondroma-like phenotype in *Col2a1Cre^{ERT2};Idh1^{LSL/+}* animals, which further supports the hypothesis that *Idh1*-mutation might cause enchondroma formation partially through upregulating HIF-1 α signaling.

To examine whether *Idh1*-mutation regulates chondrocyte differentiation and enchondroma formation through upregulating HIF-1 α signaling, we could attenuate HIF-1 α signaling in these *Idh1*-mutant chondrocytes or mice and examine whether chondrocyte differentiation defects and enchondroma formation would be rescued. This could be achieved by administering pharmacological inhibitor of HIF-1 α signaling to these *Col2a1Cre;Idh1^{LSL/+}* and *Col2a1Cre^{ERT2};Idh1^{LSL/+}* animals or their organ culture. Because HIF-1 α signaling is critical for maintaining the normal function of many cells and tissues in our body including chondrocytes, it is critical to ensure precise administration to the growth plate chondrocytes and dose the inhibitor to a level that is not affecting normal function of HIF-1 α signaling.

Appendix A

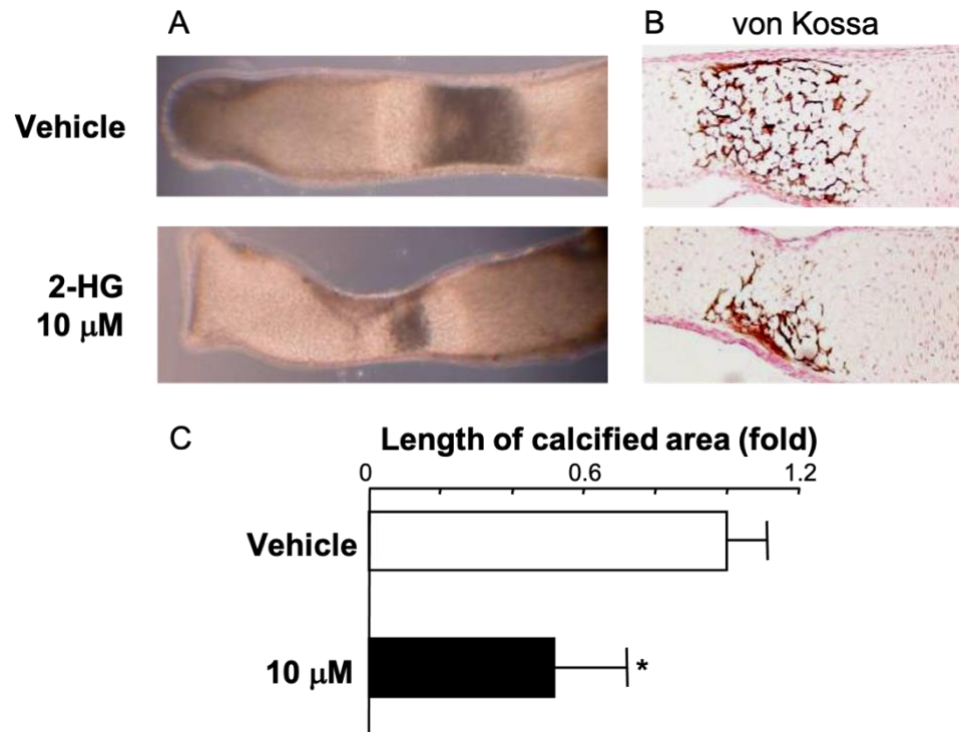


Figure 35 Mineralization in metatarsal organ culture.

(A) Whole-mount picture of metatarsal organ culture under the light microscope. (B) Von Kossa staining of metatarsal organ culture. (C) Quantification of length of calcified area in metatarsal organ culture.

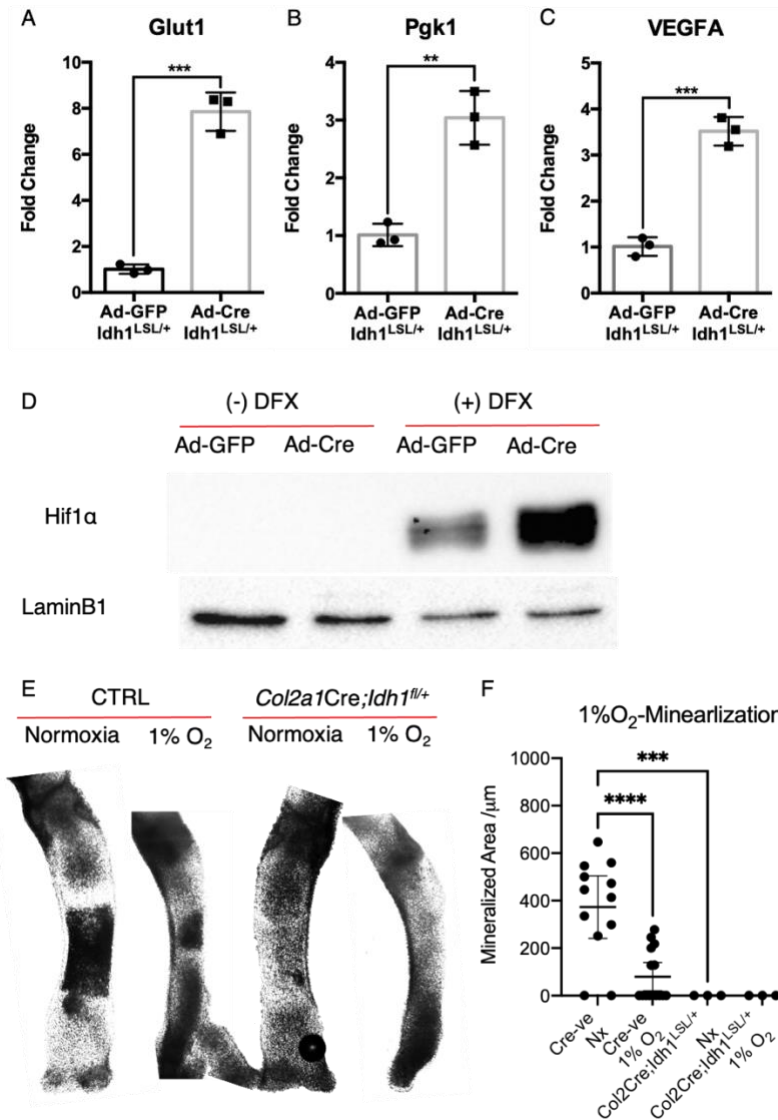


Figure 36 HIF-1 α signaling is activated in *Idh1*-mutant chondrocytes.

(A-C) qPCR of HIF-1 α target genes in AdGFP;*Idh1*^{fl/+} and AdCre;*Idh1*^{fl/+} chondrocytes (D) Western blot of HIF-1 α in AdGFP;*Idh1*^{fl/+} and AdCre;*Idh1*^{fl/+} chondrocytes. (E) Metatarsals from Cre-ve control and *Col2a1Cre;Idh1*^{fl/+} cultured under normoxic or hypoxic (1% O₂) conditions. (F) Quantification of the mineralized area of metatarsal organ culture in (E).

Appendix B

Table 1 Antibodies

Antibodies	Company	Catalog #
Anti-Col X	Invitrogen	14-9771-82
Anti-Sox9	Sigma-Aldrich	AB5535
Anti-Ki67	Novus Biologicals	NB110-89717
Anti-Cleaved Caspase 3	Cell Signaling Technology	9661
Anti-BrdU	Invitrogen	MA3-071
Anti-GLS	Abcam	AB93434
Anti- β -actin	Invitrogen	MA5-15739
Anti-Hif-1 α	Novus Biologicals	NB100-449
Anti Lamin B1	Abcam	AB16048

Table 2 qPCR Primers

Genes	Forward	Reverse
<i>Hmgcr</i>	CTTGTGGAATGCCTTGTGATTG	AGCCGAAGCAGCACATGAT
<i>Gls</i>	AGGGTGAAGTCGGTGATAAAC	GGGCTGTTCTGGAGTCATAAT
<i>Glut1</i>	AGAGGTGTCACCTACAGCTC	AACAGGATACACTGTAGCAG
<i>Pgk1</i>	CAAGGCTTTGGAGAGTCCAG	TGTGCCAATCTCCATGTTGT
<i>Vegfa</i>	TTACTGCTGTACCTCCAC	ACAGGACGGCTTGAAGATG
β -actin	AGATGTGGATCAGCAAGCAG	GCGCAAGTTAGGTTTTGTCA

Table 3 Mouse Strains

Mouse Strain	MGI ID
Tg(Col2a1-cre)3Amc	MGI: 2176263
Tg(Col2a1-cre/ERT2)1Dic	MGI: 3698311
Scap ^{tm1Mbfg}	MGI: 2148743
Gls ^{tm2.1Sray}	MGI: 5430235
Idh1 ^{tm3Mak}	MGI: 5635887

References

1. Kronenberg, H.M., *Developmental regulation of the growth plate*. Nature, 2003. **423**(6937): p. 332-336.
2. Yang, L., et al., *Hypertrophic chondrocytes can become osteoblasts and osteocytes in endochondral bone formation*. Proceedings of the National Academy of Sciences, 2014. **111**(33): p. 12097-12102.
3. Hopyan, S., et al., *A mutant PTH/PTHrP type I receptor in enchondromatosis*. Nat Genet, 2002. **30**(3): p. 306-10.
4. Hirata, M., et al., *Mutant IDH is sufficient to initiate enchondromatosis in mice*. Proceedings of the National Academy of Sciences, 2015. **112**(9): p. 2829-2834.
5. Fletcher, C.D.M., et al., *Pathology and Genetics of Tumours of Soft Tissue and Bone*. 2002: IARC Press.
6. Bovée, J.V.M.G., et al., *Cartilage tumours and bone development: molecular pathology and possible therapeutic targets*. Nat Rev Cancer, 2010. **10**(7): p. 481-488.
7. Suijker, J., et al., *Inhibition of mutant IDH1 decreases D-2-HG levels without affecting tumorigenic properties of chondrosarcoma cell lines*. Oncotarget, 2015. **6**(14): p. 12505-19.
8. *WHO Classification of Tumours of Soft Tissue and Bone*. 4 ed. WHO Classification of Tumours, , ed. C.D.M. Fletcher, et al. Vol. 5. 2013: IARC.
9. Amary, M.F., et al., *Ollier disease and Maffucci syndrome are caused by somatic mosaic mutations of IDH1 and IDH2*. Nature genetics, 2011. **43**(12): p. 1262-1265.
10. Pansuriya, T.C., et al., *Somatic mosaic IDH1 and IDH2 mutations are associated with enchondroma and spindle cell hemangioma in Ollier disease and Maffucci syndrome*. Nat Genet, 2011. **43**(12): p. 1256-61.

11. Amary, M.F., et al., *IDH1 and IDH2 mutations are frequent events in central chondrosarcoma and central and periosteal chondromas but not in other mesenchymal tumours*. *J Pathol*, 2011. **224**(3): p. 334-43.
12. Li, L., et al., *Treatment with a Small Molecule Mutant IDH1 Inhibitor Suppresses Tumorigenic Activity and Decreases Production of the Oncometabolite 2-Hydroxyglutarate in Human Chondrosarcoma Cells*. *PLoS One*, 2015. **10**(9): p. e0133813.
13. Parker, S.J. and C.M. Metallo, *Metabolic consequences of oncogenic IDH mutations*. *Pharmacology & Therapeutics*, 2015. **152**: p. 54-62.
14. Kozhemyakina, E., A.B. Lassar, and E. Zelzer, *A pathway to bone: signaling molecules and transcription factors involved in chondrocyte development and maturation*. *Development*, 2015. **142**(5): p. 817-831.
15. Zhou, X., et al., *Chondrocytes transdifferentiate into osteoblasts in endochondral bone during development, postnatal growth and fracture healing in mice*. *PLoS Genet*, 2014. **10**(12): p. e1004820.
16. Bi, W., et al., *Sox9 is required for cartilage formation*. *Nature Genetics*, 1999. **22**(1): p. 85-89.
17. Akiyama, H., et al., *The transcription factor Sox9 has essential roles in successive steps of the chondrocyte differentiation pathway and is required for expression of Sox5 and Sox6*. *Genes & Development*, 2002. **16**(21): p. 2813-2828.
18. Smits, P., et al., *The Transcription Factors L-Sox5 and Sox6 Are Essential for Cartilage Formation*. *Developmental Cell*, 2001. **1**(2): p. 277-290.
19. Lefebvre, V., P. Li, and B. de Crombrughe, *A new long form of Sox5 (L-Sox5), Sox6 and Sox9 are coexpressed in chondrogenesis and cooperatively activate the type II collagen gene*. *The EMBO Journal*, 1998. **17**(19): p. 5718-5733.

20. Lefebvre, V., et al., *SOX9 is a potent activator of the chondrocyte-specific enhancer of the pro alpha1(II) collagen gene*. *Molecular and Cellular Biology*, 1997. **17**(4): p. 2336.
21. Bell, D.M., et al., *SOX9 directly regulates the type-II collagen gene*. *Nature Genetics*, 1997. **16**(2): p. 174-178.
22. Long, F. and D.M. Ornitz, *Development of the endochondral skeleton*. *Cold Spring Harb Perspect Biol*, 2013. **5**(1): p. a008334.
23. Roach, H.I., *Trans-differentiation of hypertrophic chondrocytes into cells capable of producing a mineralized bone matrix*. *Bone and Mineral*, 1992. **19**(1): p. 1-20.
24. Descalzi Cancedda, F., et al., *Hypertrophic chondrocytes undergo further differentiation in culture*. *J Cell Biol*, 1992. **117**(2): p. 427-35.
25. Galotto, M., et al., *Hypertrophic chondrocytes undergo further differentiation to osteoblast-like cells and participate in the initial bone formation in developing chick embryo*. *Journal of Bone and Mineral Research*, 1994. **9**(8): p. 1239-1249.
26. Gibson, G., *Active role of chondrocyte apoptosis in endochondral ossification*. *Microsc Res Tech*, 1998. **43**(2): p. 191-204.
27. Park, J., et al., *Dual pathways to endochondral osteoblasts: a novel chondrocyte-derived osteoprogenitor cell identified in hypertrophic cartilage*. *Biology open*, 2015. **4**(5): p. 608-621.
28. Alman, B.A., *Skeletal dysplasias and the growth plate*. *Clin Genet*, 2008. **73**(1): p. 24-30.
29. Lee, K., J.D. Deeds, and G.V. Segre, *Expression of parathyroid hormone-related peptide and its receptor messenger ribonucleic acids during fetal development of rats*. *Endocrinology*, 1995. **136**(2): p. 453-63.

30. Vortkamp, A., et al., *Regulation of rate of cartilage differentiation by Indian hedgehog and PTH-related protein*. *Science*, 1996. **273**(5275): p. 613-22.
31. St-Jacques, B., M. Hammerschmidt, and A.P. McMahon, *Indian hedgehog signaling regulates proliferation and differentiation of chondrocytes and is essential for bone formation*. *Genes & development*, 1999. **13**(16): p. 2072-2086.
32. Lanske, B., et al., *PTH/PTHrP receptor in early development and Indian hedgehog--regulated bone growth*. *Science*, 1996. **273**(5275): p. 663-666.
33. Karaplis, A.C., et al., *Lethal skeletal dysplasia from targeted disruption of the parathyroid hormone-related peptide gene*. *Genes Dev*, 1994. **8**(3): p. 277-89.
34. Karaplis, A.C., et al., *Inactivating mutation in the human parathyroid hormone receptor type 1 gene in Blomstrand chondrodysplasia*. *Endocrinology*, 1998. **139**(12): p. 5255-8.
35. Schipani, E., K. Kruse, and H. Juppner, *A constitutively active mutant PTH-PTHrP receptor in Jansen-type metaphyseal chondrodysplasia*. *Science*, 1995. **268**(5207): p. 98-100.
36. Schipani, E., et al., *Constitutively activated receptors for parathyroid hormone and parathyroid hormone-related peptide in Jansen's metaphyseal chondrodysplasia*. *N Engl J Med*, 1996. **335**(10): p. 708-14.
37. Schipani, E., et al., *Targeted expression of constitutively active receptors for parathyroid hormone and parathyroid hormone-related peptide delays endochondral bone formation and rescues mice that lack parathyroid hormone-related peptide*. *Proc Natl Acad Sci U S A*, 1997. **94**(25): p. 13689-94.
38. Kobayashi, T., et al., *Indian hedgehog stimulates periarticular chondrocyte differentiation to regulate growth plate length independently of PTHrP*. *J Clin Invest*, 2005. **115**(7): p. 1734-42.

39. Koziel, L., et al., *Gli3 acts as a repressor downstream of Ihh in regulating two distinct steps of chondrocyte differentiation*. *Development*, 2005. **132**(23): p. 5249-5260.
40. Mau, E., et al., *PTHrP regulates growth plate chondrocyte differentiation and proliferation in a Gli3 dependent manner utilizing hedgehog ligand dependent and independent mechanisms*. *Developmental Biology*, 2007. **305**(1): p. 28-39.
41. Maes, C., G. Carmeliet, and E. Schipani, *Hypoxia-driven pathways in bone development, regeneration and disease*. *Nature Reviews Rheumatology*, 2012. **8**(6): p. 358.
42. Schipani, E., et al., *Hypoxia in cartilage: HIF-1 α is essential for chondrocyte growth arrest and survival*. *Genes & development*, 2001. **15**(21): p. 2865-2876.
43. Pfander, D., et al., *HIF-1 α controls extracellular matrix synthesis by epiphyseal chondrocytes*. *Journal of Cell Science*, 2003. **116**(9): p. 1819-1826.
44. Maes, C., et al., *Soluble VEGF isoforms are essential for establishing epiphyseal vascularization and regulating chondrocyte development and survival*. *J Clin Invest*, 2004. **113**(2): p. 188-99.
45. Maes, C., et al., *VEGF-independent cell-autonomous functions of HIF-1 α regulating oxygen consumption in fetal cartilage are critical for chondrocyte survival*. *Journal of Bone and Mineral Research*, 2012. **27**(3): p. 596-609.
46. Zelzer, E., et al., *VEGFA is necessary for chondrocyte survival during bone development*. *Development*, 2004. **131**(9): p. 2161-71.
47. Yao, Q., et al., *Suppressing Mitochondrial Respiration Is Critical for Hypoxia Tolerance in the Fetal Growth Plate*. *Developmental Cell*, 2019. **49**(5): p. 748-763.e7.
48. Amarilio, R., et al., *HIF1 α regulation of Sox9 is necessary to maintain differentiation of hypoxic prechondrogenic cells during early skeletogenesis*. *Development*, 2007. **134**(21): p. 3917-28.

49. Provot, S., et al., *Hif-1 α regulates differentiation of limb bud mesenchyme and joint development*. *Journal of Cell Biology*, 2007. **177**(3): p. 451-464.
50. Saito, T., et al., *Transcriptional regulation of endochondral ossification by HIF-2 α during skeletal growth and osteoarthritis development*. *Nature Medicine*, 2010. **16**(6): p. 678-686.
51. Araldi, E., et al., *Lack of HIF-2 α in limb bud mesenchyme causes a modest and transient delay of endochondral bone development*. *Nature Medicine*, 2011. **17**(1): p. 25-26.
52. Cheng, S., et al., *Prolyl Hydroxylase Domain-Containing Protein 2 (Phd2) Regulates Chondrocyte Differentiation and Secondary Ossification in Mice*. *Scientific Reports*, 2016. **6**(1): p. 35748.
53. Cheng, S., et al., *Conditional Deletion of Prolyl Hydroxylase Domain-Containing Protein 2 (Phd2) Gene Reveals Its Essential Role in Chondrocyte Function and Endochondral Bone Formation*. *Endocrinology*, 2016. **157**(1): p. 127-140.
54. Stegen, S., et al., *HIF-1 α metabolically controls collagen synthesis and modification in chondrocytes*. *Nature*, 2019. **565**(7740): p. 511-515.
55. Pfander, D., et al., *Deletion of Vhlh in chondrocytes reduces cell proliferation and increases matrix deposition during growth plate development*. *Development*, 2004. **131**(10): p. 2497-2508.
56. Mangiavini, L., et al., *Loss of VHL in mesenchymal progenitors of the limb bud alters multiple steps of endochondral bone development*. *Developmental Biology*, 2014. **393**(1): p. 124-136.
57. Brown, A.J. and L.J. Sharpe, *Chapter 11 - Cholesterol Synthesis*, in *Biochemistry of Lipids, Lipoproteins and Membranes (Sixth Edition)*, N.D. Ridgway and R.S. McLeod, Editors. 2016, Elsevier: Boston. p. 327-358.
58. Suzuki, A., et al., *Role of Metabolism in Bone Development and Homeostasis*. *Int J Mol Sci*, 2020. **21**(23).

59. Mullen, P.J., et al., *The interplay between cell signalling and the mevalonate pathway in cancer*. *Nat Rev Cancer*, 2016. **16**(11): p. 718-731.
60. Porter, J.A., K.E. Young, and P.A. Beachy, *Cholesterol modification of hedgehog signaling proteins in animal development*. *Science*, 1996. **274**(5285): p. 255-9.
61. Cooper, M.K., et al., *A defective response to Hedgehog signaling in disorders of cholesterol biosynthesis*. *Nature Genetics*, 2003. **33**(4): p. 508-513.
62. Lewis, P.M., et al., *Cholesterol Modification of Sonic Hedgehog Is Required for Long-Range Signaling Activity and Effective Modulation of Signaling by Ptc1*. *Cell*, 2001. **105**(5): p. 599-612.
63. Huang, P., et al., *Cellular Cholesterol Directly Activates Smoothed in Hedgehog Signaling*. *Cell*, 2016. **166**(5): p. 1176-1187.e14.
64. Xiao, X., et al., *Cholesterol Modification of Smoothed Is Required for Hedgehog Signaling*. *Molecular Cell*, 2017. **66**(1): p. 154-162.e10.
65. Signore, I.A., et al., *Inhibition of the 3-hydroxy-3-methyl-glutaryl-CoA reductase induces orofacial defects in zebrafish*. *Birth Defects Research Part A: Clinical and Molecular Teratology*, 2016. **106**(10): p. 814-830.
66. Yamashita, A., et al., *Statin treatment rescues FGFR3 skeletal dysplasia phenotypes*. *Nature*, 2014. **513**(7519): p. 507.
67. Keber, R., et al., *Mouse knockout of the cholesterologenic cytochrome P450 lanosterol 14 α -demethylase (Cyp51) resembles Antley-Bixler syndrome*. *The Journal of biological chemistry*, 2011. **286**(33): p. 29086-29097.
68. Waterham, H.R., et al., *Autosomal Recessive HEM/Greenberg Skeletal Dysplasia Is Caused by 3 β -Hydroxysterol \rightarrow 14 \rightarrow -Reductase Deficiency Due to Mutations in the Lamin B Receptor Gene*. *The American Journal of Human Genetics*, 2003. **72**(4): p. 1013-1017.

69. Wassif, C.A., et al., *HEM dysplasia and ichthyosis are likely laminopathies and not due to 3beta-hydroxysterol Delta14-reductase deficiency*. Hum Mol Genet, 2007. **16**(10): p. 1176-87.
70. Bornholdt, D., et al., *Mutational spectrum of NSDHL in CHILD syndrome*. Journal of Medical Genetics, 2005. **42**(2): p. e17.
71. Porter, F.D. and G.E. Herman, *Malformation syndromes caused by disorders of cholesterol synthesis*. Journal of lipid research, 2011. **52**(1): p. 6-34.
72. Liu, X.Y., et al., *The gene mutated in bare patches and striated mice encodes a novel 3β-hydroxysteroid dehydrogenase*. Nature Genetics, 1999. **22**(2): p. 182-187.
73. Krakowiak, P.A., et al., *Lathosterolosis: an inborn error of human and murine cholesterol synthesis due to lathosterol 5-desaturase deficiency*. Human Molecular Genetics, 2003. **12**(13): p. 1631-1641.
74. Yaplito-Lee, J., et al., *Successful treatment of lathosterolosis: A rare defect in cholesterol biosynthesis—A case report and review of literature*. JIMD Reports, 2020. **56**(1): p. 14-19.
75. Ho, A.C.C., et al., *Lathosterolosis: a disorder of cholesterol biosynthesis resembling smith-lemli-opitz syndrome*. JIMD reports, 2014. **12**: p. 129-134.
76. Porter, F.D., *Smith–Lemli–Opitz syndrome: pathogenesis, diagnosis and management*. European Journal of Human Genetics, 2008. **16**(5): p. 535-541.
77. Fitzky, B.U., et al., *7-Dehydrocholesterol-dependent proteolysis of HMG-CoA reductase suppresses sterol biosynthesis in a mouse model of Smith-Lemli-Opitz/RSH syndrome*. The Journal of clinical investigation, 2001. **108**(6): p. 905-915.
78. Wu, S. and F. De Luca, *Role of cholesterol in the regulation of growth plate chondrogenesis and longitudinal bone growth*. J Biol Chem, 2004. **279**(6): p. 4642-7.

79. Horton, J.D., et al., *Combined analysis of oligonucleotide microarray data from transgenic and knockout mice identifies direct SREBP target genes*. Proceedings of the National Academy of Sciences, 2003. **100**(21): p. 12027.
80. Horton, J.D., J.L. Goldstein, and M.S. Brown, *SREBPs: activators of the complete program of cholesterol and fatty acid synthesis in the liver*. J Clin Invest, 2002. **109**.
81. Reed, B.D., et al., *Genome-wide occupancy of SREBP1 and its partners NFY and SP1 reveals novel functional roles and combinatorial regulation of distinct classes of genes*. PLoS Genet, 2008. **4**(7): p. e1000133.
82. Tsushima, H., et al., *Intracellular biosynthesis of lipids and cholesterol by Scap and Insig in mesenchymal cells regulates long bone growth and chondrocyte homeostasis*. Development, 2018.
83. Stein, W.H. and S. Moore, *THE FREE AMINO ACIDS OF HUMAN BLOOD PLASMA*. Journal of Biological Chemistry, 1954. **211**(2): p. 915-926.
84. Shen, L., et al., *Biphasic regulation of glutamine consumption by WNT during osteoblast differentiation*. J Cell Sci, 2021. **134**(1).
85. Altman, B.J., Z.E. Stine, and C.V. Dang, *From Krebs to clinic: glutamine metabolism to cancer therapy*. Nat Rev Cancer, 2016. **16**(10): p. 619-34.
86. Bhutia, Y.D., et al., *Amino Acid transporters in cancer and their relevance to "glutamine addiction": novel targets for the design of a new class of anticancer drugs*. Cancer Res, 2015. **75**(9): p. 1782-8.
87. Bröer, A., F. Rahimi, and S. Bröer, *Deletion of Amino Acid Transporter ASCT2 (SLC1A5) Reveals an Essential Role for Transporters SNAT1 (SLC38A1) and SNAT2 (SLC38A2) to Sustain Glutaminolysis in Cancer Cells*. J Biol Chem, 2016. **291**(25): p. 13194-205.
88. Yoo, H.C., et al., *Glutamine reliance in cell metabolism*. Experimental & Molecular Medicine, 2020. **52**(9): p. 1496-1516.

89. Aledo, J.C., et al., *Identification of two human glutaminase loci and tissue-specific expression of the two related genes*. *Mammalian Genome*, 2000. **11**(12): p. 1107-1110.
90. Elgadi, K.M., et al., *Cloning and analysis of unique human glutaminase isoforms generated by tissue-specific alternative splicing*. *Physiological Genomics*, 1999. **1**(2): p. 51-62.
91. Gao, P., et al., *c-Myc suppression of miR-23a/b enhances mitochondrial glutaminase expression and glutamine metabolism*. *Nature*, 2009. **458**(7239): p. 762-765.
92. Zhao, L., et al., *Interferon- α regulates glutaminase 1 promoter through STAT1 phosphorylation: Relevance to HIV-1 associated neurocognitive disorders*. *PLoS one*, 2012. **7**(3): p. e32995.
93. Colombo, S.L., et al., *Molecular basis for the differential use of glucose and glutamine in cell proliferation as revealed by synchronized HeLa cells*. *Proceedings of the National Academy of Sciences*, 2011. **108**(52): p. 21069-21074.
94. Kita, K., T. Suzuki, and T. Ochi, *Diphenylarsinic Acid Promotes Degradation of Glutaminase C by Mitochondrial Lon Protease**. *Journal of Biological Chemistry*, 2012. **287**(22): p. 18163-18172.
95. Thangavelu, K., et al., *Structural basis for the allosteric inhibitory mechanism of human kidney-type glutaminase (KGA) and its regulation by Raf-Mek-Erk signaling in cancer cell metabolism*. *Proceedings of the National Academy of Sciences*, 2012. **109**(20): p. 7705-7710.
96. Wang, J.-B., et al., *Targeting Mitochondrial Glutaminase Activity Inhibits Oncogenic Transformation*. *Cancer Cell*, 2010. **18**(3): p. 207-219.
97. Han, T., et al., *Phosphorylation of glutaminase by PKC ϵ is essential for its enzymatic activity and critically contributes to tumorigenesis*. *Cell Research*, 2018. **28**(6): p. 655-669.

98. Katt, W.P. and R.A. Cerione, *Glutaminase regulation in cancer cells: a druggable chain of events*. *Drug Discovery Today*, 2014. **19**(4): p. 450-457.
99. Timmerman, L.A., et al., *Glutamine sensitivity analysis identifies the xCT antiporter as a common triple-negative breast tumor therapeutic target*. *Cancer Cell*, 2013. **24**(4): p. 450-65.
100. DeBerardinis, R.J., et al., *Beyond aerobic glycolysis: Transformed cells can engage in glutamine metabolism that exceeds the requirement for protein and nucleotide synthesis*. *Proceedings of the National Academy of Sciences*, 2007. **104**(49): p. 19345.
101. Islam, M.S., et al., *2-Oxoglutarate-dependent oxygenases*. *Annual review of biochemistry*, 2018. **87**: p. 585-620.
102. Nowicki, S. and E. Gottlieb, *Oncometabolites: tailoring our genes*. *The FEBS journal*, 2015. **282**(15): p. 2796-2805.
103. Sullivan, L.B., et al., *Supporting Aspartate Biosynthesis Is an Essential Function of Respiration in Proliferating Cells*. *Cell*, 2015. **162**(3): p. 552-63.
104. Birsoy, K., et al., *An Essential Role of the Mitochondrial Electron Transport Chain in Cell Proliferation Is to Enable Aspartate Synthesis*. *Cell*, 2015. **162**(3): p. 540-51.
105. Son, J., et al., *Glutamine supports pancreatic cancer growth through a KRAS-regulated metabolic pathway*. *Nature*, 2013. **496**(7443): p. 101-105.
106. Speight, G., C.J. Handley, and D.A. Lowther, *Extracellular matrix metabolism by chondrocytes 4. Role of glutamine in glycosaminoglycan synthesis in vitro by chondrocytes*. *Biochimica et Biophysica Acta (BBA) - General Subjects*, 1978. **540**(2): p. 238-245.
107. Handley, C.J., et al., *Extracellular matrix metabolism by chondrocytes 7. Evidence that L-glutamine is an essential amino acid for chondrocytes and other connective tissue cells*. *Biochimica et Biophysica Acta (BBA) - General Subjects*, 1980. **627**(3): p. 324-331.

108. Stegen, S., et al., *Glutamine Metabolism Controls Chondrocyte Identity and Function*. *Dev Cell*, 2020. **53**(5): p. 530-544.e8.
109. Polat, O., S.S. Kilicoglu, and E. Erdemli, *A controlled trial of glutamine effects on bone healing*. *Advances in therapy*, 2007. **24**(1): p. 154-160.
110. Marsell, R. and T.A. Einhorn, *The biology of fracture healing*. *Injury*, 2011. **42**(6): p. 551-555.
111. Hinoi, E., et al., *Glutamate signaling in peripheral tissues*. *Eur J Biochem*, 2004. **271**(1): p. 1-13.
112. Cowan, R.W., E.P. Seidlitz, and G. Singh, *Glutamate signaling in healthy and diseased bone*. *Frontiers in endocrinology*, 2012. **3**: p. 89.
113. Hinoi, E., et al., *Functional expression of particular isoforms of excitatory amino acid transporters by rodent cartilage*. *Biochemical pharmacology*, 2005. **70**(1): p. 70-81.
114. Wang, L., et al., *Glutamate inhibits chondral mineralization through apoptotic cell death mediated by retrograde operation of the cystine/glutamate antiporter*. *J Biol Chem*, 2006. **281**(34): p. 24553-65.
115. Wang, L., et al., *Abolition of chondral mineralization by group III metabotropic glutamate receptors expressed in rodent cartilage*. *Br J Pharmacol*, 2005. **146**(5): p. 732-43.
116. Wang, L., et al., *Release of endogenous glutamate by AMPA receptors expressed in cultured rat costal chondrocytes*. *Biol Pharm Bull*, 2005. **28**(6): p. 990-3.
117. Piepoli, T., et al., *Glutamate signaling in chondrocytes and the potential involvement of NMDA receptors in cell proliferation and inflammatory gene expression*. *Osteoarthritis and Cartilage*, 2009. **17**(8): p. 1076-1083.

118. Qasem, S.A. and B.R. DeYoung, *Cartilage-forming tumors*. *Semin Diagn Pathol*, 2014. **31**(1): p. 10-20.
119. Walden, M.J., M.D. Murphey, and J.A. Vidal, *Incidental enchondromas of the knee*. *American Journal of Roentgenology*, 2008. **190**(6): p. 1611-1615.
120. Hong, E.D., et al., *Prevalence of shoulder enchondromas on routine MR imaging*. *Clinical imaging*, 2011. **35**(5): p. 378-384.
121. Leddy, L.R. and R.E. Holmes, *Chondrosarcoma of bone*, in *Orthopaedic Oncology*. 2014, Springer. p. 117-130.
122. Cairns, R.A., I.S. Harris, and T.W. Mak, *Regulation of cancer cell metabolism*. *Nat Rev Cancer*, 2011. **11**(2): p. 85-95.
123. Cairns, R.A. and T.W. Mak, *Oncogenic isocitrate dehydrogenase mutations: mechanisms, models, and clinical opportunities*. *Cancer Discov*, 2013. **3**(7): p. 730-41.
124. Losman, J.A. and W.G. Kaelin, Jr., *What a difference a hydroxyl makes: mutant IDH, (R)-2-hydroxyglutarate, and cancer*. *Genes Dev*, 2013. **27**(8): p. 836-52.
125. Parsons, D.W., et al., *An integrated genomic analysis of human glioblastoma multiforme*. *Science*, 2008. **321**(5897): p. 1807-12.
126. Yan, H., et al., *IDH1 and IDH2 mutations in gliomas*. *N Engl J Med*, 2009. **360**(8): p. 765-73.
127. Mardis, E.R., et al., *Recurring mutations found by sequencing an acute myeloid leukemia genome*. *N Engl J Med*, 2009. **361**(11): p. 1058-66.
128. Zhao, S., et al., *Glioma-derived mutations in IDH1 dominantly inhibit IDH1 catalytic activity and induce HIF-1alpha*. *Science*, 2009. **324**(5924): p. 261-5.

129. Dang, L., et al., *Cancer-associated IDH1 mutations produce 2-hydroxyglutarate*. Nature, 2009. **462**(7274): p. 739-744.
130. Leonardi, R., et al., *Cancer-associated isocitrate dehydrogenase mutations inactivate NADPH-dependent reductive carboxylation*. J Biol Chem, 2012. **287**(18): p. 14615-20.
131. Wanders, R.J. and P. Mooyer, *D-2-hydroxyglutaric acidaemia: identification of a new enzyme, D-2-hydroxyglutarate dehydrogenase, localized in mitochondria*. J Inherit Metab Dis, 1995. **18**(2): p. 194-6.
132. Chowdhury, R., et al., *The oncometabolite 2-hydroxyglutarate inhibits histone lysine demethylases*. EMBO Rep, 2011. **12**(5): p. 463-9.
133. Xu, W., et al., *Oncometabolite 2-Hydroxyglutarate Is a Competitive Inhibitor of α -Ketoglutarate-Dependent Dioxygenases*. Cancer cell, 2011. **19**(1): p. 17-30.
134. Lu, C., et al., *IDH mutation impairs histone demethylation and results in a block to cell differentiation*. Nature, 2012. **483**(7390): p. 474-8.
135. Turcan, S., et al., *IDH1 mutation is sufficient to establish the glioma hypermethylator phenotype*. Nature, 2012. **483**(7390): p. 479-83.
136. Figueroa, M.E., et al., *Leukemic IDH1 and IDH2 mutations result in a hypermethylation phenotype, disrupt TET2 function, and impair hematopoietic differentiation*. Cancer cell, 2010. **18**(6): p. 553-567.
137. Jin, Y., et al., *Mutant IDH1 Dysregulates the Differentiation of Mesenchymal Stem Cells in Association with Gene-Specific Histone Modifications to Cartilage- and Bone-Related Genes*. PLoS One, 2015. **10**(7): p. e0131998.
138. Gross, S., et al., *Cancer-associated metabolite 2-hydroxyglutarate accumulates in acute myelogenous leukemia with isocitrate dehydrogenase 1 and 2 mutations*. J Exp Med, 2010. **207**(2): p. 339-44.

139. Ward, P.S., et al., *The common feature of leukemia-associated IDH1 and IDH2 mutations is a neomorphic enzyme activity converting alpha-ketoglutarate to 2-hydroxyglutarate*. *Cancer Cell*, 2010. **17**(3): p. 225-34.
140. Suijker, J., et al., *The oncometabolite D-2-hydroxyglutarate induced by mutant IDH1 or-2 blocks osteoblast differentiation in vitro and in vivo*. *Oncotarget*, 2015. **6**(17): p. 14832.
141. Cojocaru, E., et al., *Is the IDH Mutation a Good Target for Chondrosarcoma Treatment?* *Current Molecular Biology Reports*, 2020.
142. Tiet, T.D., et al., *Constitutive Hedgehog Signaling in Chondrosarcoma Up-Regulates Tumor Cell Proliferation*. *The American Journal of Pathology*, 2006. **168**(1): p. 321-330.
143. Couvineau, A., et al., *PTHR1 mutations associated with Ollier disease result in receptor loss of function*. *Hum Mol Genet*, 2008. **17**(18): p. 2766-75.
144. Deng, Q., et al., *Activation of hedgehog signaling in mesenchymal stem cells induces cartilage and bone tumor formation via Wnt/ β -Catenin*. *eLife*, 2019. **8**: p. e50208.
145. Chen, Z., et al., *ERK1 and ERK2 regulate chondrocyte terminal differentiation during endochondral bone formation*. *J Bone Miner Res*, 2015. **30**(5): p. 765-74.
146. Chan, G., D. Kalaitzidis, and B.G. Neel, *The tyrosine phosphatase Shp2 (PTPN11) in cancer*. *Cancer and metastasis reviews*, 2008. **27**(2): p. 179-192.
147. Yang, W., et al., *Ptpn11 deletion in a novel progenitor causes metachondromatosis by inducing hedgehog signalling*. *Nature*, 2013. **499**(7459): p. 491-5.
148. Bowen, M.E., et al., *SHP2 regulates chondrocyte terminal differentiation, growth plate architecture and skeletal cell fates*. *PLoS Genet*, 2014. **10**(5): p. e1004364.

149. Wang, L., et al., *SHP2 Regulates the Osteogenic Fate of Growth Plate Hypertrophic Chondrocytes*. *Scientific Reports*, 2017. **7**(1): p. 12699.
150. Giacinti, C. and A. Giordano, *RB and cell cycle progression*. *Oncogene*, 2006. **25**(38): p. 5220-5227.
151. Landman, A.S., P.S. Danielian, and J.A. Lees, *Loss of pRB and p107 disrupts cartilage development and promotes enchondroma formation*. *Oncogene*, 2013. **32**(40): p. 4798-4805.
152. Cobrinik, D., et al., *Shared role of the pRB-related p130 and p107 proteins in limb development*. *Genes Dev*, 1996. **10**(13): p. 1633-44.
153. Rossi, F., et al., *p107 and p130 Coordinately regulate proliferation, Cbfa1 expression, and hypertrophic differentiation during endochondral bone development*. *Developmental biology*, 2002. **247**(2): p. 271-285.
154. Zhou, S., et al., *FGFR3 Deficiency Causes Multiple Chondroma-like Lesions by Upregulating Hedgehog Signaling*. *PLoS Genet*, 2015. **11**(6): p. e1005214.
155. Yang, G., et al., *PTEN deficiency causes dyschondroplasia in mice by enhanced hypoxia-inducible factor 1 α signaling and endoplasmic reticulum stress*. *Development*, 2008. **135**(21): p. 3587-3597.
156. Totoki, Y., et al., *Unique mutation portraits and frequent COL2A1 gene alteration in chondrosarcoma*. *Genome research*, 2014. **24**(9): p. 1411-1420.
157. Saiji, E., et al., *IDH1 immunohistochemistry reactivity and mosaic IDH1 or IDH2 somatic mutations in pediatric sporadic enchondroma and enchondromatosis*. *Virchows Archiv*, 2019. **475**(5): p. 625-636.
158. Lai, L.P., et al., *Lkb1/Stk11 regulation of mTOR signaling controls the transition of chondrocyte fates and suppresses skeletal tumor formation*. *Proceedings of the National Academy of Sciences*, 2013. **110**(48): p. 19450-19455.

159. Zhou, S., et al., *Inactivation of Lkb1 in postnatal chondrocytes leads to epiphyseal growth-plate abnormalities and promotes enchondroma-like formation*. *Faseb j*, 2019. **33**(8): p. 9476-9488.
160. Tarpey, P.S., et al., *Frequent mutation of the major cartilage collagen gene COL2A1 in chondrosarcoma*. *Nature genetics*, 2013. **45**(8): p. 923.
161. Ho, L., et al., *Gli2 and p53 cooperate to regulate IGFBP-3-mediated chondrocyte apoptosis in the progression from benign to malignant cartilage tumors*. *Cancer cell*, 2009. **16**(2): p. 126-136.
162. Wagner, A., et al. *Results from a phase 2 randomized, placebo-controlled, double blind study of the hedgehog (HH) pathway antagonist IPI-926 in patients (PTS) with advanced chondrosarcoma (CS)*. in *Connective Tissue Oncology Society 18th Annual Meeting*. New York, NY. 2013.
163. Italiano, A., et al., *GDC-0449 in patients with advanced chondrosarcomas: a French Sarcoma Group/US and French National Cancer Institute Single-Arm Phase II Collaborative Study*. *Ann Oncol*, 2013. **24**(11): p. 2922-6.
164. Li, L., et al., *Mutant IDH1 Depletion Downregulates Integrins and Impairs Chondrosarcoma Growth*. *Cancers*, 2020. **12**(1): p. 141.
165. Loeser, R.F., *Integrins and cell signaling in chondrocytes*. *Biorheology*, 2002. **39**(1, 2): p. 119-124.
166. Peterse, E.F.P., et al., *Targeting glutaminolysis in chondrosarcoma in context of the IDH1/2 mutation*. *British Journal of Cancer*, 2018. **118**(8): p. 1074-1083.
167. Salamanca-Cardona, L., et al., *In vivo imaging of glutamine metabolism to the oncometabolite 2-hydroxyglutarate in IDH1/2 mutant tumors*. *Cell metabolism*, 2017. **26**(6): p. 830-841. e3.
168. Kuzu, O.F., M.A. Noory, and G.P. Robertson, *The Role of Cholesterol in Cancer*. *Cancer Research*, 2016. **76**(8): p. 2063.

169. Sasaki, M., et al., *IDH1 (R132H) mutation increases murine haematopoietic progenitors and alters epigenetics*. *Nature*, 2012. **488**(7413): p. 656-659.
170. Long, F., et al., *Genetic manipulation of hedgehog signaling in the endochondral skeleton reveals a direct role in the regulation of chondrocyte proliferation*. *Development*, 2001. **128**(24): p. 5099-108.
171. Osmak, M., *Statins and cancer: Current and future prospects*. *Cancer Letters*, 2012. **324**(1): p. 1-12.
172. Campbell, V.T., et al., *Hedgehog Pathway Inhibition in Chondrosarcoma Using the Smoothed Inhibitor IPI-926 Directly Inhibits Sarcoma Cell Growth*. *Molecular Cancer Therapeutics*, 2014. **13**(5): p. 1259-1269.
173. Farnaghi, S., et al., *Cholesterol metabolism in pathogenesis of osteoarthritis disease*. *Int J Rheum Dis*, 2017. **20**(2): p. 131-140.
174. Porstmann, T., et al., *SREBP activity is regulated by mTORC1 and contributes to Akt-dependent cell growth*. *Cell metabolism*, 2008. **8**(3): p. 224-236.
175. Montero, J., et al., *Mitochondrial cholesterol contributes to chemotherapy resistance in hepatocellular carcinoma*. *Cancer Res*, 2008. **68**(13): p. 5246-56.
176. Warita, K., et al., *Statin-induced mevalonate pathway inhibition attenuates the growth of mesenchymal-like cancer cells that lack functional E-cadherin mediated cell cohesion*. *Sci Rep*, 2014. **4**: p. 7593.
177. Shechter, I., et al., *IDH1 gene transcription is sterol regulated and activated by SREBP-1a and SREBP-2 in human hepatoma HepG2 cells: evidence that IDH1 may regulate lipogenesis in hepatic cells*. *J Lipid Res*, 2003. **44**(11): p. 2169-80.
178. Ricoult, S.J., et al., *Sterol Regulatory Element Binding Protein Regulates the Expression and Metabolic Functions of Wild-Type and Oncogenic IDH1*. *Mol Cell Biol*, 2016. **36**(18): p. 2384-95.

179. Cohen, A.L., S.L. Holmen, and H. Colman, *IDH1 and IDH2 Mutations in Gliomas*. Current Neurology and Neuroscience Reports, 2013. **13**(5): p. 345.
180. Angelini, A., et al., *Clinical outcome of central conventional chondrosarcoma*. Journal of Surgical Oncology, 2012. **106**(8): p. 929-937.
181. Meijer, D., et al., *Genetic characterization of mesenchymal, clear cell, and dedifferentiated chondrosarcoma*. Genes Chromosomes Cancer, 2012. **51**(10): p. 899-909.
182. Zhang, H. and B.A. Alman, *Enchondromatosis and Growth Plate Development*. Current Osteoporosis Reports, 2021. **19**(1): p. 40-49.
183. Yang, M., T. Soga, and P.J. Pollard, *Oncometabolites: linking altered metabolism with cancer*. J Clin Invest, 2013. **123**(9): p. 3652-8.
184. Pathmanapan, S., et al., *Mutant IDH and non-mutant chondrosarcomas display distinct cellular metabolomes*. Cancer Metab, 2021. **9**(1): p. 13.
185. Wise, D.R. and C.B. Thompson, *Glutamine addiction: a new therapeutic target in cancer*. Trends in biochemical sciences, 2010. **35**(8): p. 427-433.
186. Yu, Y., et al., *Glutamine Metabolism Regulates Proliferation and Lineage Allocation in Skeletal Stem Cells*. Cell Metabolism, 2019. **29**(4): p. 966-978.e4.
187. Crawford, J. and H.J. Cohen, *The essential role of L-glutamine in lymphocyte differentiation in vitro*. Journal of cellular physiology, 1985. **124**(2): p. 275-282.
188. Johnson, M.O., et al., *Distinct regulation of Th17 and Th1 cell differentiation by glutaminase-dependent metabolism*. Cell, 2018. **175**(7): p. 1780-1795. e19.
189. Wang, Y., et al., *Glutaminase 1 is essential for the differentiation, proliferation, and survival of human neural progenitor cells*. Stem cells and development, 2014. **23**(22): p. 2782-2790.

190. Izquierdo-Garcia, J.L., et al., *IDH1 mutation induces reprogramming of pyruvate metabolism*. *Cancer research*, 2015. **75**(15): p. 2999-3009.
191. Seltzer, M.J., et al., *Inhibition of glutaminase preferentially slows growth of glioma cells with mutant IDH1*. *Cancer Res*, 2010. **70**(22): p. 8981-7.
192. Matre, P., et al., *Inhibiting glutaminase in acute myeloid leukemia: metabolic dependency of selected AML subtypes*. *Oncotarget*, 2016. **7**(48): p. 79722-79735.
193. Emadi, A., et al., *Inhibition of glutaminase selectively suppresses the growth of primary acute myeloid leukemia cells with IDH mutations*. *Experimental Hematology*, 2014. **42**(4): p. 247-251.
194. Nicolle, R., et al., *Integrated molecular characterization of chondrosarcoma reveals critical determinants of disease progression*. *Nat Commun*, 2019. **10**(1): p. 4622.
195. Robinson, Mary M., et al., *Novel mechanism of inhibition of rat kidney-type glutaminase by bis-2-(5-phenylacetamido-1,2,4-thiadiazol-2-yl)ethyl sulfide (BPTES)*. *Biochemical Journal*, 2007. **406**(3): p. 407-414.
196. Mingote, S., et al., *Genetic Pharmacotherapy as an Early CNS Drug Development Strategy: Testing Glutaminase Inhibition for Schizophrenia Treatment in Adult Mice*. *Front Syst Neurosci*, 2015. **9**: p. 165.
197. Gross, M.I., et al., *Antitumor activity of the glutaminase inhibitor CB-839 in triple-negative breast cancer*. *Mol Cancer Ther*, 2014. **13**(4): p. 890-901.
198. Stegen, S., et al., *Glutamine Metabolism in Osteoprogenitors Is Required for Bone Mass Accrual and PTH-Induced Bone Anabolism in Male Mice*. *Journal of Bone and Mineral Research*, 2021. **36**(3): p. 604-616.
199. Fan, J., et al., *Glutamine-driven oxidative phosphorylation is a major ATP source in transformed mammalian cells in both normoxia and hypoxia*. *Molecular Systems Biology*, 2013. **9**(1): p. 712.

200. Kovacević, Z., *The pathway of glutamine and glutamate oxidation in isolated mitochondria from mammalian cells*. *Biochem J*, 1971. **125**(3): p. 757-63.
201. Qing, G., et al., *ATF4 Regulates MYC-Mediated Neuroblastoma Cell Death upon Glutamine Deprivation*. *Cancer Cell*, 2012. **22**(5): p. 631-644.
202. Ye, J., et al., *The GCN2-ATF4 pathway is critical for tumour cell survival and proliferation in response to nutrient deprivation*. *The EMBO Journal*, 2010. **29**(12): p. 2082-2096.
203. Zhang, J., et al., *Asparagine Plays a Critical Role in Regulating Cellular Adaptation to Glutamine Depletion*. *Molecular Cell*, 2014. **56**(2): p. 205-218.
204. Matsuda, M., et al., *SREBP cleavage-activating protein (SCAP) is required for increased lipid synthesis in liver induced by cholesterol deprivation and insulin elevation*. *Genes Dev*, 2001. **15**(10): p. 1206-16.
205. Chen, M., et al., *Generation of a transgenic mouse model with chondrocyte-specific and tamoxifen-inducible expression of Cre recombinase*. *Genesis*, 2007. **45**(1): p. 44-50.
206. Shultz, L.D., et al., *Human lymphoid and myeloid cell development in NOD/LtSz-scid IL2R gamma null mice engrafted with mobilized human hemopoietic stem cells*. *J Immunol*, 2005. **174**(10): p. 6477-89.
207. Hilton, M.J., et al., *Ihh controls cartilage development by antagonizing Gli3, but requires additional effectors to regulate osteoblast and vascular development*. *Development*, 2005. **132**(19): p. 4339-4351.
208. Martin, M., *Cutadapt removes adapter sequences from high-throughput sequencing reads*. *EMBnet. journal*, 2011. **17**(1): p. pp. 10-12.
209. Kersey, P.J., et al., *Ensembl Genomes: an integrative resource for genome-scale data from non-vertebrate species*. *Nucleic acids research*, 2011. **40**(D1): p. D91-D97.

210. Dobin, A., et al., *STAR: ultrafast universal RNA-seq aligner*. *Bioinformatics*, 2013. **29**(1): p. 15-21.
211. Love, M.I., W. Huber, and S. Anders, *Moderated estimation of fold change and dispersion for RNA-seq data with DESeq2*. *Genome biology*, 2014. **15**(12): p. 550.
212. Huber, W., et al., *Orchestrating high-throughput genomic analysis with Bioconductor*. *Nature methods*, 2015. **12**(2): p. 115.
213. Mootha, V.K., et al., *PGC-1 α -responsive genes involved in oxidative phosphorylation are coordinately downregulated in human diabetes*. *Nature genetics*, 2003. **34**(3): p. 267.
214. Göbel, A., et al., *Cholesterol and beyond - The role of the mevalonate pathway in cancer biology*. *Biochimica et Biophysica Acta (BBA) - Reviews on Cancer*, 2020. **1873**(2): p. 188351.
215. Borgquist, S., et al., *HMG-CoA reductase expression in breast cancer is associated with a less aggressive phenotype and influenced by anthropometric factors*. *International Journal of Cancer*, 2008. **123**(5): p. 1146-1153.
216. Clendening, J.W., et al., *Dysregulation of the mevalonate pathway promotes transformation*. *Proceedings of the National Academy of Sciences*, 2010. **107**(34): p. 15051.
217. Brown, D.N., et al., *Squalene epoxidase is a bona fide oncogene by amplification with clinical relevance in breast cancer*. *Scientific reports*, 2016. **6**: p. 19435-19435.
218. Bao, J., et al., *SREBP-1 is an independent prognostic marker and promotes invasion and migration in breast cancer*. *Oncol Lett*, 2016. **12**(4): p. 2409-2416.
219. Armengol, S., et al., *SREBP-2-driven transcriptional activation of human *SND1* oncogene*. *Oncotarget*, 2017. **8**(64).

220. Jariwala, N., et al., *Oncogenic Role of SND1 in Development and Progression of Hepatocellular Carcinoma*. *Cancer Research*, 2017. **77**(12): p. 3306.
221. Guo, D., et al., *EGFR Signaling Through an Akt-SREBP-1–Dependent, Rapamycin-Resistant Pathway Sensitizes Glioblastomas to Antilipogenic Therapy*. *Science Signaling*, 2009. **2**(101): p. ra82.
222. Lewis, C.A., et al., *SREBP maintains lipid biosynthesis and viability of cancer cells under lipid- and oxygen-deprived conditions and defines a gene signature associated with poor survival in glioblastoma multiforme*. *Oncogene*, 2015. **34**(40): p. 5128-5140.
223. Cheng, C., et al., *Glucose-Mediated N-glycosylation of SCAP Is Essential for SREBP-1 Activation and Tumor Growth*. *Cancer Cell*, 2015. **28**(5): p. 569-581.
224. Pallottini, V., et al., *Regulation of HMG-CoA reductase expression by hypoxia*. *Journal of Cellular Biochemistry*, 2008. **104**(3): p. 701-709.
225. Castellano, B.M., et al., *Lysosomal cholesterol activates mTORC1 via an SLC38A9–Niemann-Pick C1 signaling complex*. *Science*, 2017. **355**(6331): p. 1306.
226. Du, Q., et al., *Dietary cholesterol promotes AOM-induced colorectal cancer through activating the NLRP3 inflammasome*. *Biochemical Pharmacology*, 2016. **105**: p. 42-54.
227. Gupta, A., et al., *Statin use associated with improved overall and cancer specific survival in patients with head and neck cancer*. *Oral Oncology*, 2019. **90**: p. 54-66.
228. Matuszewicz, L., et al., *The effect of statins on cancer cells – review*. *Tumor Biology*, 2015. **36**(7): p. 4889-4904.
229. Rao, S., et al., *Lovastatin-mediated G₁ arrest is through inhibition of the proteasome, independent of hydroxymethyl glutaryl-CoA reductase*. *Proceedings of the National Academy of Sciences*, 1999. **96**(14): p. 7797.

230. Yu, X., et al., *BRCA1 overexpression sensitizes cancer cells to lovastatin via regulation of cyclin D1-CDK4-p21WAF1/CIP1 pathway: analyses using a breast cancer cell line and tumoral xenograft model*. *Int J Oncol*, 2008. **33**(3): p. 555-63.
231. Kochuparambil, S.T., et al., *Anticancer Efficacy of Simvastatin on Prostate Cancer Cells and Tumor Xenografts Is Associated with Inhibition of Akt and Reduced Prostate-Specific Antigen Expression*. *Journal of Pharmacology and Experimental Therapeutics*, 2011. **336**(2): p. 496.
232. Qi, X.F., et al., *HMG-CoA reductase inhibitors induce apoptosis of lymphoma cells by promoting ROS generation and regulating Akt, Erk and p38 signals via suppression of mevalonate pathway*. *Cell Death & Disease*, 2013. **4**(2): p. e518-e518.
233. Fromigué, O., et al., *RhoA GTPase inactivation by statins induces osteosarcoma cell apoptosis by inhibiting p42/p44-MAPKs-Bcl-2 signaling independently of BMP-2 and cell differentiation*. *Cell Death & Differentiation*, 2006. **13**(11): p. 1845-1856.
234. Wang, Y., et al., *Alpha-ketoglutarate ameliorates age-related osteoporosis via regulating histone methylations*. *Nature Communications*, 2020. **11**(1): p. 5596.
235. Carey, B.W., et al., *Intracellular α -ketoglutarate maintains the pluripotency of embryonic stem cells*. *Nature*, 2015. **518**(7539): p. 413-416.
236. Hwang, I.-Y., et al., *Psat1-Dependent Fluctuations in α -Ketoglutarate Affect the Timing of ESC Differentiation*. *Cell Metabolism*, 2016. **24**(3): p. 494-501.
237. TeSlaa, T., et al., *α -Ketoglutarate Accelerates the Initial Differentiation of Primed Human Pluripotent Stem Cells*. *Cell Metabolism*, 2016. **24**(3): p. 485-493.
238. Ho, T.T., et al., *Autophagy maintains the metabolism and function of young and old stem cells*. *Nature*, 2017. **543**(7644): p. 205-210.
239. Klysz, D., et al., *Glutamine-dependent α -ketoglutarate production regulates the balance between T helper 1 cell and regulatory T cell generation*. *Science Signaling*, 2015. **8**(396): p. ra97.

240. Chisolm, D.A., et al., *CCCTC-Binding Factor Translates Interleukin 2- and α -Ketoglutarate-Sensitive Metabolic Changes in T_H17 Cells into Context-Dependent Gene Programs*. *Immunity*, 2017. **47**(2): p. 251-267.e7.
241. Baksh, S.C., et al., *Extracellular serine controls epidermal stem cell fate and tumour initiation*. *Nature Cell Biology*, 2020. **22**(7): p. 779-790.
242. Tran, T.Q., et al., *α -Ketoglutarate attenuates Wnt signaling and drives differentiation in colorectal cancer*. *Nature Cancer*, 2020. **1**(3): p. 345-358.
243. Singh, A.K., et al., *Selective targeting of TET catalytic domain promotes somatic cell reprogramming*. *Proceedings of the National Academy of Sciences*, 2020. **117**(7): p. 3621.
244. Chua, G.N.L., et al., *Cytosine-Based TET Enzyme Inhibitors*. *ACS Medicinal Chemistry Letters*, 2019. **10**(2): p. 180-185.
245. Redza-Dutordoir, M. and D.A. Averill-Bates, *Activation of apoptosis signalling pathways by reactive oxygen species*. *Biochimica et Biophysica Acta (BBA) - Molecular Cell Research*, 2016. **1863**(12): p. 2977-2992.
246. Lieu, E.L., et al., *Amino acids in cancer*. *Experimental & Molecular Medicine*, 2020. **52**(1): p. 15-30.
247. Doxsee, D.W., et al., *Sulfasalazine-induced cystine starvation: Potential use for prostate cancer therapy*. *The Prostate*, 2007. **67**(2): p. 162-171.
248. Lo, M., et al., *The xc⁻ cystine/glutamate antiporter: a mediator of pancreatic cancer growth with a role in drug resistance*. *British Journal of Cancer*, 2008. **99**(3): p. 464-472.
249. Chung, W.J., et al., *Inhibition of Cystine Uptake Disrupts the Growth of Primary Brain Tumors*. *The Journal of Neuroscience*, 2005. **25**(31): p. 7101.

250. Tang, X., et al., *Blockade of Glutathione Metabolism in IDH1-Mutated Glioma*. *Molecular Cancer Therapeutics*, 2020. **19**(1): p. 221.
251. Pavlova, N.N., et al., *As Extracellular Glutamine Levels Decline, Asparagine Becomes an Essential Amino Acid*. *Cell Metabolism*, 2018. **27**(2): p. 428-438.e5.
252. Krall, A.S., et al., *Asparagine promotes cancer cell proliferation through use as an amino acid exchange factor*. *Nature Communications*, 2016. **7**(1): p. 11457.
253. Alkan, H.F., et al., *Cytosolic Aspartate Availability Determines Cell Survival When Glutamine Is Limiting*. *Cell Metabolism*, 2018. **28**(5): p. 706-720.e6.
254. Tajan, M., et al., *A Role for p53 in the Adaptation to Glutamine Starvation through the Expression of SLC1A3*. *Cell Metabolism*, 2018. **28**(5): p. 721-736.e6.
255. Maddocks, O.D.K., et al., *Serine starvation induces stress and p53-dependent metabolic remodelling in cancer cells*. *Nature*, 2013. **493**(7433): p. 542-546.
256. Sullivan, M.R., et al., *Increased Serine Synthesis Provides an Advantage for Tumors Arising in Tissues Where Serine Levels Are Limiting*. *Cell Metabolism*, 2019. **29**(6): p. 1410-1421.e4.
257. Maddocks, O.D.K., et al., *Modulating the therapeutic response of tumours to dietary serine and glycine starvation*. *Nature*, 2017. **544**(7650): p. 372-376.
258. Cojocaru, E., et al., *Is the IDH Mutation a Good Target for Chondrosarcoma Treatment?* *Current Molecular Biology Reports*, 2020. **6**(1): p. 1-9.
259. Turcan, S., et al., *Mutant-IDH1-dependent chromatin state reprogramming, reversibility, and persistence*. *Nature Genetics*, 2018. **50**(1): p. 62-72.
260. Norsworthy, K.J., et al., *FDA Approval Summary: Ivosidenib for Relapsed or Refractory Acute Myeloid Leukemia with an Isocitrate Dehydrogenase-1 Mutation*. *Clin Cancer Res*, 2019.

261. Lin, T.L., et al., *Clonal leukemic evolution in myelodysplastic syndromes with TET2 and IDH1/2 mutations*. *Haematologica*, 2014. **99**(1): p. 28-36.

Biography

Hongyuan Zhang attended the University of Hong Kong for her undergraduate degree in Biochemistry and graduated with first-class honors in 2015. At the University of Hong Kong, Hongyuan studied cancer metabolism and planarian regeneration under the guidance of Dr. Nai Sum Wong and Dr. Danny Chan. After graduation, she joined Duke University through the Developmental and Stem Cell Biology program and later got affiliated with the Department of Cell Biology.

Hongyuan joined the lab of Dr. Benjamin Alman to study the cartilage tumors enchondroma and chondrosarcoma. Hongyuan published a co-first author research article “Intracellular cholesterol biosynthesis in enchondroma and chondrosarcoma” in *JCI Insight*. Hongyuan also published a review article “Enchondromatosis and Growth Plate Development” with Dr. Benjamin Alman in *Current Osteoporosis Reports*. In addition, Hongyuan is a co-author of several articles in *Development*, *Cell Metabolism*, *Scientific Reports*, *Cell Reports*, *Nature Cell Biology*, and *Cancer and Metabolism*.

Hongyuan is a recipient of Best Poster Award from Gordon Research Seminar (2017), Duke Graduate School Conference Travel Award (2018, 2019), Regeneration Next Initiative Travel Grant (2018). Hongyuan served as the Chair for Gordon Research Seminar – Bone and Teeth in 2020. Hongyuan presented her work at multiple national and international conferences including Gordon Research Conferences, ORS Annual Meetings, ASBMR Annual Meeting, and CTOS Annual Meeting, etc.